Indoor Environmental Control with a Direct Expansion (DX) Air conditioning (A/C) Unit in Residences in the Subtropics

Li Zheng

A thesis submitted in partial fulfillment of the requirements

for the Degree of Doctor of Philosophy

Department of Building Services Engineering

The Hong Kong Polytechnic University

March, 2006

Certificate of Originality

I hereby declare that this thesis is my own work and that, to the best of my knowledge and belief, it reproduces no material previously published or written, nor material that has been accepted for the award of any other degree or diploma, except where due acknowledgement has been made in the text.

Li Zheng

Department of Building Services Engineering

The Hong Kong Polytechnic University

Hong Kong SAR, China

March, 2006

Abstract

Direct expansion (DX) air conditioning (A/C) units are commonly used in residential buildings in the subtropics. They are normally equipped with single-speed compressors and supply fans, relying on on-off cycling compressors to maintain only indoor air dry-bulb temperature. This results in an uncontrolled equilibrium indoor humidity, leading to a reduced level of occupants' thermal comfort, poor indoor air quality (IAQ), and low energy efficiency.

The thesis reports on, first of all, a simulation study on the characteristics of space cooling loads and indoor environmental control in residences in the subtropics, using a building energy simulation program, EnergyPlus. Both the weather conditions and the typical arrangements of high-rise residential blocks in subtropical Hong Kong were used in the simulation study. The simulation results on both the space cooling loads characteristics and the hourly application sensible heat ratio (SHR) in the living/dining room and the master bedroom in a selected west-facing apartment under different operating modes of DX A/C units in the summer design day are presented. The problem of indoor environmental control, based on an on-off cycling compressor to maintain indoor air dry-bulb temperature only, due to the mismatch between the output latent cooling capacity from a DX A/C unit and the space latent cooling load in the two rooms both in the summer design day and during part load conditions was quantitatively investigated. In addition, the influences of indoor furnishings acting as moisture capacitors on indoor relative humidity (RH) levels were also quantitatively studied.

Secondly, the thesis presents an experimental study to investigate the inherent operational characteristics of a DX A/C unit at a fixed inlet air state of 24ºC and 50% RH when the speeds of both its compressor and supply fan were varied. The measured results suggested that varying both compressor and supply fan speeds can lead to varying equipment SHR, or the varying ability to dehumidify of the unit, and may therefore be preferably adopted for indoor environmental control in places subjected to variable latent cooling loads. Generally, lowering supply fan speed was more effective in enhancing the ability to dehumidify than increasing compressor speed. However, varying both speeds would also impact on both the total output cooling capacity and the operating efficiency of a DX A/C unit.

Thirdly, this thesis reports on an experimental study on indoor thermal comfort characteristics under the control of a DX A/C unit having variable-speed compressor and supply fan at a fixed space cooling load condition. The results of study suggested that under a given indoor total cooling load with a fixed application SHR, varying both speeds of compressor and supply fan in the DX A/C unit would not only result in different indoor temperatures and RH levels but also impact indoor air velocity and mean radiant temperature (MRT), influencing indoor thermal comfort. Therefore ANSI/ASHRAE Thermal Comfort Standard (55-2004) has been used to evaluate indoor thermal comfort characteristics under the control of a DX A/C unit having variable-speed compressor and supply fan. Experimental results showed that appropriate indoor thermal comfort levels may be attained at different speed combinations, but with varying operating efficiencies.

Finally, the thesis presents the development of a novel direct digital control (DDC)-based capacity controller for a DX A/C unit to regulate indoor temperature and RH by simultaneously varying the speeds of both its compressor and supply fan. The capacity controller consisted of a numerical control algorithm (NCA), using a number of real-time measured operating parameters and based on the energy balance between the air side and refrigerant side to determine both speeds. The results of controllability tests of the capacity controller suggested that the controller developed was operational, with an acceptable control accuracy but rooms for improvement with respect to control sensitivity. Therefore attempts to improve control sensitivity were made by incorporating a traditional Proportional-integral (PI) controller using the deviation between the actual RH and its setpoint as a control signal into the DDC-based capacity controller. The results of the controllability tests for the improved controller showed that it can achieve both a control accuracy and a reasonable control sensitivity.

Acknowledgements

I must express my grateful thanks to my Chief Supervisor, Dr. Deng Shiming, Associate Professor from the Department of Building Services Engineering (BSE), The Hong Kong Polytechnic University, for his readily available supervision, valuable suggestions, patient guidance, continuous help and encouragement throughout the course of the work.

My special thanks go to The Hong Kong Polytechnic University for financially supporting this project. I would like to also thank Dr. Lin Zhongping and Dr. Chen Wu for their assistances in my simulation and experimental works. In addition, I wish to express my gratitude to the technicians in the HVAC Laboratory of BSE Department for their supports during my experimental work.

Finally, I would like to express my deepest appreciation to my family members: He Dengfeng - my husband, my parents, my parents-in-law, my elder brother and his wife. I could not have finished my work without their on going patience, supports and understandings.

Table of Contents

List of Figures

List of Tables

Nomenclature

Variable	Description	Unit
C_{pa}	Air specific heat at constant pressure	kJ/kg·°C
COP	Coefficient of Performance	ND
d_a	Air moisture content	g/kg dry air
d_{sa}	Air saturated moisture content	g/kg dry air
D	Globe diameter	m
f_{cl}	Clothing area factor	ND
h_a	Air enthalpy	kJ/kg
h_c	Convective heat transfer coefficient	$W/m^2 \cdot K$
h_r	Refrigerant enthalpy	kJ/kg
I_{cl}	Clothing insulation value	clo
l	Stroke of cylinder	m
L	Thermal load on the human body	$met(W/m^2)$
m_a	Air mass flow rate	kg/s
m_r	Refrigerant mass flow rate	kg/s
M	Actively level	$met(W/m^2)$
n	Speed	rps
p_{asw}	Saturated water vapor pressure	kPa
p_{av}	Water vapor pressure	kPa
P_r	Refrigerant absolute pressure	Pa
PMV	Predicted Mean Vote	ND
PPD	Predicted Percentage Dissatisfied	%
q_{rt}	Specific total output cooling capacity from the DX A/C unit	kJ/kg
Q_{as}	Space sensible cooling load	kW
Q_{at}	Space total cooling load	kW
Q_{es}	Space sensible heat removed by the DX A/C unit	kW
Q_{et}	Space total heat removed by the DX A/C unit	kW
Q_{fgh}	Supply fan heat gain	kW

Q_{rt}	Total output cooling capacity from the DX A/C unit	kW
r	Radius of rotor	m
R_{cl}	Thermal resistance of clothing	$m^2 \cdot K/W$
RH	Air relative humidity level	%
SHR	Sensible heat ratio	ND
t_{adb}	Air dry-bulb temperature	°C
t_{awb}	Air wet-bulb temperature	°C
t_{cl}	Clothing temperature	°C
t_g	Globe temperature	°C
$\bar{t}_r$	Mean radiant temperature	°C
T_{awb}	Air wet-bulb absolute temperature	K
T_r	Refrigerant absolute temperature	K
v_r	Refrigerant specific volume	m^3/kg
V	Air velocity (for Chapter 7)	m/s
V	Swept volume of the rotor compressor (for Chapter 8)	m^3
W	Input power(for Chapter 6)	kW
W	External work done by muscles (for Chapter 7)	met(W/m^2)

Greek symbols

β	Compression index	ND
ε	Globe emissivity (for Chapter 7)	ND
ε	Rotor relative eccentricity (for Chapter 8)	ND
λ	Overall displacement coefficient of compressor	ND
λ_l	Compressor leakage coefficient	ND
λ_T	Compressor temperature coefficient	ND
λ_p	Compressor pressure coefficient	ND
λ_v	Compressor volumetric coefficient	ND

Note: ND = No Dimensions

Subscripts

0	State before the introduction of space cooling load step-changes
1	State after the introduction of space cooling load step-changes
2	State after the activation of the DDC-based capacity controller
ap	Application
c	Condenser exit
com	Compressor
comd	Compressor discharge
coms	Compressor suction
db	Dry-bulb
eq	Equipment
fan	Supply fan
fi	Supply fan inlet
fo	Supply fan outlet
i	Evaporator inlet
o	Evaporator outlet
r	Indoor air; Refrigerant
s	Supply air
sh	Superheat
t	Total

Chapter 1

Introduction

The development of air conditioning (A/C) technology is a natural consequence of both pursuing high quality living and working environment, and at the same time addressing the issue of sustainability. For residential buildings, currently the most commonly used A/C systems are of direct expansion (DX) type. DX A/C units have a number of advantages when compared to larger central chilled water-based A/C installations. These include higher energy efficiency, simpler system configuration and costing less to own and maintain. However, most DX A/C units are equipped with single-speed compressors and supply fans, relying on on-off cycling compressors as a low-cost approach to maintain only indoor air dry-bulb temperature, resulting in either space overcooling or an uncontrolled equilibrium indoor relative humidity (RH) level. Very often, the resultant indoor RH level would be out of the comfort range of 30% to 60% RH in summer as specified in the established thermal comfort standards. On-off cycling compressor based on indoor air dry-bulb temperature leads to a reduced level of thermal comfort for occupants, in addition to poor indoor air quality (IAQ) and low energy efficiency. For an on-off thermostat controlled DX A/C unit, very often dehumidification becomes a by-product of a cooling process, resulting in a relatively higher indoor RH level. Therefore, it has been a challenge to provide effective indoor environment control with DX A/C units.

With the advancement of A/C technology and the wider application of variable-speed drive (VSD) technology, it becomes possible for a DX A/C unit to have the speeds of its compressor and supply fan varied. Therefore, when there are changes in

both sensible and latent cooling load in an air conditioned space served by a DX A/C unit, it becomes possible to simultaneously vary the speeds of its compressor and supply fan, for simultaneous indoor temperature and humidity control.

The thesis begins with an extensive literature review on indoor environment control, with an emphasis on controlling indoor humidity, using DX A/C units in residences in the subtropics. The fundamental issues related to indoor environmental control, such as the suitable range of indoor RH for thermal comfort, the effects of RH level on human thermal comfort and building materials, the sources of indoor moisture, and the related problems of indoor environmental control using DX A/C units have been reviewed. A brief review of the established strategies currently used in controlling both indoor air temperature and humidity is also included. A number of important issues where further in-depth research work in achieving appropriate indoor environment control with DX A/C units is required have been identified. These are the expected targets of investigation in the project reported in this thesis.

The research proposal covering the aims and objectives, the project title and the methodologies adopted in this project is presented in Chapter 3.

Chapter 4 reports on a simulation study where the characteristics of residential space cooling loads and the issues related to indoor environmental control using DX A/C units were investigated and analyzed, using a building energy simulation program currently available in the public domain, EnergyPlus. The weather conditions of, and the typical arrangements of high-rise residential blocks in the subtropical Hong Kong were used in the simulation study. Both the detailed analysis of hourly space cooling

load characteristics and the hourly application sensible heat ratios (SHRs) in both the living/dinning room in a selected apartment at daytime and the master bedroom of the apartment at nighttime, respectively, in the summer design day, are presented. With on-off cycling compressor operation, the problem of indoor humidity control due to the mismatch between the output latent cooling capacity from a DX A/C unit and the space latent cooling load in the two rooms both in the summer design day and during part load conditions was quantitatively investigated. The influences of indoor furnishings acting as moisture capacitors on indoor RH levels were also quantitatively studied.

Chapter 5 describes an experimental DX A/C station available to facilitate the research work reported in this thesis. Detailed descriptions of the experimental station and its major components are firstly given. This is followed by describing the computerized measuring devices and a data acquisition system (DAS). A computer supervisory program used to operate and control the experimental station is also detailed. The availability of the experimental DX A/C station has been expected to be helpful in successfully carrying out the research work proposed in Chapter 3.

Chapter 6 reports on an experimental study to investigate the inherent operational characteristics of a DX A/C unit at fixed inlet air temperature and humidity to the DX A/C unit when the speeds of both its compressor and supply fan were varied, using the experimental DX A/C station described in Chapter 5. The characteristics included equipment SHRs and Coefficient of Performances (COPs) at various speed combinations, over the entire operational ranges of both speeds. Firstly, the experimental conditions and assumptions at which the study was undertaken are

presented. This is followed by reporting the experimental results, such as equipment SHRs, output sensible and latent cooling capacities, and COP, etc. Finally, a number of issues regarding the practical applications of the inherent operational characteristics and their possible constraints were discussed.

The experimental study presented in Chapter 7 investigated the indoor thermal comfort characteristics under the control of a DX A/C unit having variable-speed compressor and supply fan at a fixed space cooling load condition. The well-known Fanger's Predicted Mean Vote (PMV) and Predicted Percentage Dissatisfied (PPD) thermal comfort model is briefly introduced and simplified for the current experimental investigation. This is followed by reporting the experimental results of indoor thermal comfort characteristics under the control of a DX A/C unit at a given total space cooling load with a fixed application SHR. The potential of using thermal comfort indexes for indoor environmental control purpose was also discussed.

Chapter 8 reports on the development of a novel direct digital control (DDC)-based capacity controller for a DX A/C unit having variable-speed compressor and supply fan to simultaneously control indoor air temperature and RH in a conditioned space served by the DX A/C unit, using SHR as a control variable. Firstly, the core element of the capacity controller, a numerical calculation algorithm (NCA) based on a number of real-time measured operating parameters and the energy balance between the air side and the refrigerant side of the DX A/C unit to determine the speeds of both compressor and supply fan is described in detail. This is followed by reporting the results of controllability tests of the DDC-based capacity controller at various testing conditions. The results of controllability tests for the DDC-based capacity

controller suggested that the controller developed was operational, with an acceptable control accuracy but rooms for improvement with respect to control sensitivity. Therefore, attempts to improve control sensitivity were made by incorporating traditional Proportional-Integral (PI) control algorithms using the deviation between the actual indoor RH and its setpoint as a control signal into the DDC-based capacity controller. The results of the controllability tests showed that such an integrated controller could achieve both a control accuracy and a reasonable control sensitivity.

The conclusions of the thesis and the proposed future work are presented in the final Chapter.

Chapter 2

Literature Review

2.1 Introduction

Although the development of heating, ventilation, and air conditioning (HAVC) technology began at more than 100 years ago, only the last 50-60 years saw the extensive use of mechanical-cooling based air conditioning (A/C). To a layman, A/C simply means “the cooling of air”. This simple understanding of A/C is neither sufficiently useful nor accurate. A/C is in fact a process of treating air in an internal environment to establish and maintain the required air states in terms of temperature, humidity, cleanliness, and motion [Edward 1989]. This clearly demonstrates that these are the four basic parameters an A/C system will have to deal with.

Currently, A/C systems have been widely used in almost all types of buildings, such as industrial, commercial and residential buildings for different purposes. For residential buildings, the most commonly used A/C systems are of DX type. In USA, according to Department of Energy, packaged rooftop DX A/C units consume approximately 60% of the total energy used for cooling [Bordick and Gilbride 2002]. In Hong Kong, the annual total sale of DX residential air conditioners was round 400,000 units in 1999 and 2000, respectively [Zhang 2002]. A DX A/C unit is normally a piece of single packaged equipment that provides the basic functions of air distribution, outdoor air induction and filtration, and cooling/ heating. This type of A/C systems has a number of advantages when compared to large central chilled water-based A/C installations, such as, simpler configuration, more energy efficient

and generally costing less to own and maintain. However, most DX A/C units are currently equipped with single-speed compressors and fans, relying on on-off cycling compressors to maintain only indoor air dry-bulb temperature, resulting in either space overcooling or an uncontrolled equilibrium indoor RH level. Therefore, such a control strategy for DX A/C units often leads to a reduced level of occupants' thermal comfort, in addition to poor IAQ, and low energy efficiency [Fanger 2001, Brandemuehl and Katejanekarn 2004]. For many years, it has been a challenge to provide cost effective humidity control, because more attention has been paid to air temperature control only [Harriman III et al. 2000]. In addition, generally, occupants are as comfortable when a thermostat is set higher at a low RH level as it is set lower at a high RH level. For the latter, an air conditioner consumes additional energy [Kuwahara 1985, Henderson et al. 1992].

Residential buildings located in hot and humid subtropics experience more serious indoor environmental control problems often in the form of relatively higher indoor RH level than those in other regions. Hong Kong, for example, is a typical subtropical city, and residential buildings using DX A/C units in Hong Kong would also face similar indoor environmental control problems. The summer in Hong Kong is hot and humid from May through September, and most of the rainfall comes in this period. On the other hand, Hong Kong is also one of the most densely populated places in the world. Over 90% residential buildings are high-rise blocks, usually of 10 to 30 stories. Currently, with the increased household income and consequently the increased living standard, people would view A/C as an essential provision to maintain a thermally appropriate environment in residences. Split-type, window-type and packaged-type DX A/C units are commonly used in residential buildings.

Consequently, the energy use by DX A/C units dominates the total residential energy consumption, at one third of the total electricity use, in residential buildings in recent years [Lam 1996, Lam 2000].

In order to improve the indoor thermal comfort in residential buildings in particular those located in hot and humid climates served by DX A/C units, , it is therefore necessary to improve indoor air temperature and humidity control. Over the years, there have been increased interests in studying how to maintain appropriate indoor comfort level and acceptable IAQ, while minimizing energy use. The proper selection, sizing and operation of residential DX A/C units are the keys to improve the control of both indoor air temperature and humidity.

This Chapter firstly reviews the fundamental issues related to the control of indoor environment, with an emphasis on controlling indoor humidity. These issues include the suitable range of indoor RH for thermal comfort, the effects of RH level on human thermal comfort and building materials, the sources of indoor moisture and the related problems of indoor environmental control using DX A/C units. This is followed by reviewing the established strategies currently used in controlling both indoor air temperature and humidity. Finally, a number of important issues where further extensive research work is required are identified in order to achieve appropriate indoor environmental control using residential DX A/C units.

2.2 Fundamental issues of indoor environmental control with an emphasis on controlling indoor humidity

2.2.1 Suitable range of indoor RH for thermal comfort

When indoor humidity control is addressed, the value of moisture content is less important than that of RH, because practically the latter is more convenient to be measured. In summer, according to ASHRAE Handbook of Fundamentals 2001, the temperature range for comfort falls between 23°C and 26°C [ASHRAE 2001]. Similarly, a suitable indoor RH range is also required for assessing IAQ and human thermal comfort.

Although the temperature dimension for measuring comfort has been well defined and supported by laboratory and field observations, the RH limits are less certain, particularly for the upper limit. At lower RH levels, thermal sensation is a good indicator of overall thermal comfort and acceptability. However, at high RH levels, it has been found that thermal sensation alone is not a reliable predictor of thermal comfort [Tanabe et al. 1987]. In addition, the upper limit of RH affects the design and operation of A/C units, as this determines the amount of dehumidification, influencing energy use, peak power demand, design and operation of both buildings and their engineering systems. In addition, the upper limit of RH determines the range of climatic conditions under which ventilative and direct evaporative cooling are available alternatives to conventional cooling [Fountain et al. 1999].

The upper limit of RH in the comfort zone is controversial and not clearly defined, as evidenced by the evolution of indoor humidity standards, which has begun from the turn of last century [Olesen and Brager 2004]. Prior to 1915, documentation from the American Society of Heating and Ventilating Engineers (ASHVE) focused almost exclusively on the ventilation rates for different classes of buildings, with indoor RH rarely mentioned. In 1915, ASHVE introduced an upper RH limit of 50% as being desirable but not mandatory. In 1920, ASHVE adopted a "Synthetic Air Chart" with an air wet-bulb temperature limit of 17.8°C. For the next 75 years since the use of the Chart, the upper RH limit had changed between 60% and 100%. In 1932, ASHVE Ventilation Standard extended the Chart's upper RH limit to 70% across all temperatures. In 1938, ASHVE specified 75% as an upper limit and this value stayed over the next 20 years. In 1966, with the introduction of the ANSI/ASHRAE Standard 55, this upper limit of 75% was lowered to 60%. In 1974, the upper RH limit was set at a moisture content of 12 g/kg dry air (65% RH at 24°C dry-bulb temperature or at 16.8°C dew point temperature), which was still valid in 1981 Edition of ANSI/ASHRAE Standard 55 [Fountain et al. 1999]. In 1985, Theodore Sterling Ltd. and Simon Fraser University in British Columbia, Canada, finished a research project and established a widely accepted chart showing the optimum RH range between 30% and 60% [Sterling et al. 1985] (see Fig. 2.1). In its 1989 and 1992 Editions, ANSI/ASHRAE Standard 55 specified the upper RH limit at 60%, based primarily on the considerations of mold growth. For ANSI/ASHRAE Standard 55, in its 1992R and 2004 Editions, the recommended upper humidity limit was reversed to 12 g/kg dry air moisture content, which did not concern the condensation on building surfaces and contamination and damage to building components, and there were no established lower humidity limits for thermal

comfort [ANSI/ASHRAE 2004]. In addition, in ASHRAE Handbook of Fundamentals 2001, the ASHRAE summer comfort zone was confirmed as an area on a psychrometric chart between 23°C and 26°C dry-bulb effective temperature (ET), and between 2°C dew point temperature and 20°C wet-bulb temperature [ASHRAE 2001]. Furthermore, in ASHRAE Handbook of HVAC Systems and Equipment 2000, the range of acceptable RH was narrowed to between 30% and 60% at normal room temperature in order to minimize both the growth of bacteria and biological organisms and the speed at which chemical interactions occur [ASHRAE 2000]. Finally both ANSI/ASHRAE Standard 62-2001 Ventilation for Acceptable Indoor Quality and the United States Environmental Protection Agency (EPA) recommend that indoor RH should be maintained between 30% and 60% to minimize the growth of allergenic or pathogenic organisms [ANSI/ASHRAE 2001]. Therefore, for residential buildings, the upper limit should be set at 60% RH and the suitable range for indoor RH between 30% and 60% RH, while that for indoor air dry-bulb temperature should be between 23°C and 26°C.

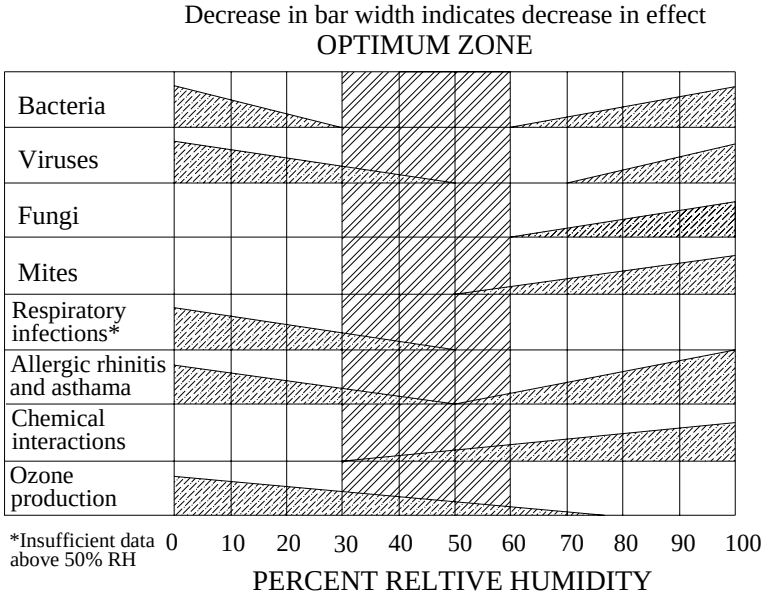

Fig. 2.1 Optimum humidity range for human comfort and health
(Adapted from Sterling et al. 1985)

2.2.2 The effects of RH level on human thermal comfort and building materials

2.2.2.1 RH level and its impacts on thermal comfort and health of occupants

Previous studies on the levels of RH affecting IAQ and human thermal comfort have been performed [de Dear et al. 1989, Tanabe and Kimura 1994, Armstrong and Liaw 2002, Miro 2005]. Indoor air RH levels affect occupants' thermal comfort in a number of ways both directly and indirectly. From the viewpoint of IAQ, decreasing air RH level results in an improved perception of IAQ; air is fresher, less stale and more acceptable. Therefore, within the comfort zone, it is recommended to keep moderately low levels of temperature and RH to improve the perceived air quality. This may even help decrease the amount of ventilation required for acceptable perceived air quality. It has been shown that people would perceive the indoor air quality better at 20°C and 40% RH at a small ventilation rate of 3.5 L/s/person than at 23°C and 50% RH at a ventilation rate of 10 L/s/person [Fanger 2001]. Furthermore, from the viewpoint of human perception, at a given temperature setpoint, decreased RH level results in occupants feeling cooler, drier and more comfortable. Also, at lower RH levels, fabrics, clothing and textures would appear more smooth and pleasant.

High levels of indoor air RH may cause health problems for occupants in spite of thermal neutrality due to the growth on surfaces of contaminated aerosols produced by spray humidification systems [Arens and Baughman 1996]. In general, health-related agents in connection with indoor RH level include dust mites, fungi, bacteria, viruses, and nonbiological pollutants. It has been shown that an indoor RH level

above 50% would help increase dust mite population. An indoor RH level above 70% would provide an excellent environment for the growth of fungi. Fungi and dust mites found inside residences have been identified as the main causes of asthma and hay fever [Arens and Baughman 1996]. All the agents affect human health, primarily through their inhalation of indoor air, although some of them have lesser effects through the skin. The discomfort caused by the uncomfortably high levels of insufficient cooling of the mucous membranes in upper respiratory tract by inhalation of humid and warm air, and skin humidity would increase the risk of individuals with allergies [Toftum and Fanger 1999]. In addition, a number of chemicals found indoors interact with water vapor to form respiratory and dermal irritants. Effects of high RH levels on chemical substances include increased off-gassing of formaldehyde from building and furnishing materials; combination with sulphur dioxide to form aerosols, salts, and acids including sulphuric acid and sulphate salts; and increased irritative effects of odor, particles, and vapors such as acrolein [Sterling 1985].

While a high RH level is problematic, a low RH level would also have comfort and health impact. Firstly, a low RH level can lead to the drying of skin and mucous surfaces, promoting the accumulation of electrostatic charges in fabric and others materials in buildings. On respiratory surfaces, drying can concentrate mucous to the extent that ciliary clearance and phagocytic activities will be reduced. Therefore, comfort complaints about dry nose, throat, eyes and skin often occur in low RH conditions, typically when the dew point is less than 0°C. A low RH level can also increase the susceptibility to respiratory disease as well as discomfort, such as asthmatics. Individuals with allergies, newborns and elderly are more susceptible to

respiratory infections [Green 1982, Berglund 1998]. Secondly, a low RH level enhances the formation of ozone indoors. Very high ozone levels, in combination with poorly ventilated equipment, will also produce an irritation effect on the mucous membrane of eyes, nose, throat and respiratory tract. Thirdly, low RH levels are well known as a general catalyst of chemical interactions resulting in a large variety of irritants and toxic substances commonly referred to as “smog”. Indoor smog could well be responsible for a large proportion of similar symptoms of ozone. The smog is commonly associated with tight building syndrome occurring in office and commercial buildings [Sterling 1985].

2.2.2.2 RH level and its impacts on building materials

Building materials may better be protected under a moderate level of RH. The dew point temperature of outdoor air is often higher than the temperature of interior wall surface; therefore, water vapor that infiltrates or permeates through building envelope may condense. The disorders caused are generally the deteriorations of interior coatings with yellowish, black spots, the breakdown of gypsum drywall or other similar building materials, and separation of vinyl material and its surfaces. Phenomena of corrosion of metal structure can appear in the event of cracks in the coating [Trowbridge et al. 1994, Shakun 1992, Gatley 1992, Lstiburek 2001, Lucas and Miranville 2004]. For the problem of thrive growth of mold and fungus on duct, floor or wall covering, four key ingredients are present: (1) Spores, the seed or start of mildew growth, are airborne and everywhere; (2) Temperature, spores grow under the same temperature range as that for human comfort; (3) Food, spores feed on a variety of building materials, including cellulose, vinyl, adhesives for wall covering;

(4) Water, spores thrive in 70% to 93% RH. Below a RH level of 60%, the growth of mildew is greatly retarded. Water is the only element that can be controlled effectively to slow down the growth. Therefore indoor RH level should be below 60% as the ANSI/ASHRAE Standard 62-2001 recommends [Shakun 1992, McGahey 1998]. On the other hand, if RH level is controlled to substantially below 30%, damage to furniture and building structure may also occur as a result of dryness due to the shrinking of wood and destruction of glued joints because of expansion and contraction [Pasch et al. 1996]. All these problems lead to an increase of maintenance costs for any buildings.

2.2.3 Sources of indoor moisture

When the issue of indoor environmental control is addressed, it is important to look at the sources of indoor moisture, as the amount of moisture removal must be equal to the amount being introduced into, both externally and internally.

2.2.3.1 External sources

Fundamentally, the external source for indoor moisture is the water vapor carried by outdoor air. It may be classified into three types. The first is by water vapor diffusion through building envelope from outdoors. Moisture migrates from a place of high vapor concentration to a place of lower vapor concentration by diffusion through materials. The moisture flowing as a result of diffusion is a function of the difference in vapor pressure between the two sides of a supporting wall in a building, the

permeability of construction materials, and the exposed surface area [Shakun 1992]. However, this type of moisture gains cannot be easily determined [Barringer and McGugan 1989]. The second is through the infiltration of outdoor air. The amount of moisture accumulated inside a conditioned space as a result of air infiltration is a function of infiltrated air mass flow rate, moisture content difference between incoming air and indoor air. Although the infiltration through a building enclosure is intermittent and unintentional, it has been emphasized that its effects on indoor RH level cannot be overlooked [Kohloss 1981, Fairey and Keresteciogl u 1985, Straube 2002]. Henderson et al. [1992] concluded that infiltration would have a great impact on space latent cooling load by simulating a typical building in both Miami and Atlanta. At constant indoor air dry-bulb temperature of 25.5°C, the space latent cooling load would increase from at 11% of the total space cooling at an average infiltration rate of 0.54 air change per hour (ACH) to at 17% of the total at that of 1.08 ACH. In general, air infiltration impacts more than vapor diffusion on indoor RH levels, producing 10 to 200 times more water vapor than vapor diffusion [Shakun 1992, Harriman Ⅲ et al. 2001]. The third and the most important is the outdoor air ventilated through A/C systems. In ASHRAE Standard 62.2P, Ventilation and Acceptable IAQ in Low-rise Residential Buildings, there is a special consideration that the moisture from outdoor air is of particular concern in hot and humid climates [Sherman 1999]. For a conditioned space, it is obvious that the latent cooling load from ventilation air is greater than all other latent cooling loads combined [Brandemuehl and Katejanekarn 2004]. Most residential buildings require the ASHRAE-recommended minimum ventilation rate to ensure IAQ and occupants' thermal comfort [McGahey 1998]. During occupied hours, both sensible and latent cooling loads from ventilation air are continuous. Furthermore, if the latent cooling

load from ventilation air is allowed to blend into that of return air stream, a simple, constant-air volume DX A/C unit would have a very difficult time to remove it [Kohloss 1981, Berbari 1998, Harriman III and Judge 2002]. In particular during part load conditions in hot and humid subtropics, the latent cooling load from ventilation air would have greater influences on indoor humidity than that at full load condition, and therefore should receive more attentions. Assuming that the minimum outdoor air intake at all time is 20% of the supply airflow rate at design/full load, at half load operation, the ratio of outdoor air would change to 40% of the supply airflow rate. In other words, ventilation requirement dictates the increased portion of outdoor air during part load operation. At the same time, outdoor air dry-bulb temperature is lower, close to indoor air dry-bulb temperature, but its dew point temperature is higher than that at design condition. Therefore, space sensible cooling load is reduced but space latent cooling load is increased [Shaw and Luxton 1988]. For example, according to the study by Lstiburek [2002], based on ASHRAE Standard 62.2P, for a single detached house (three bedrooms, 186 m^2), the desired controlled ventilation is quantified at 24 L/s, or between 0.15 and 0.2 ACH, based on typical house volume (ceiling height ranging between 2.4 m and 3 m). At part load conditions, the space latent cooling load is effectively doubled in this typical house when the required ventilation rate remains unchanged. The higher the moisture content of outdoor air, the higher the space latent cooling load a DX A/C unit would have to deal with.

2.2.3.2 Internal sources

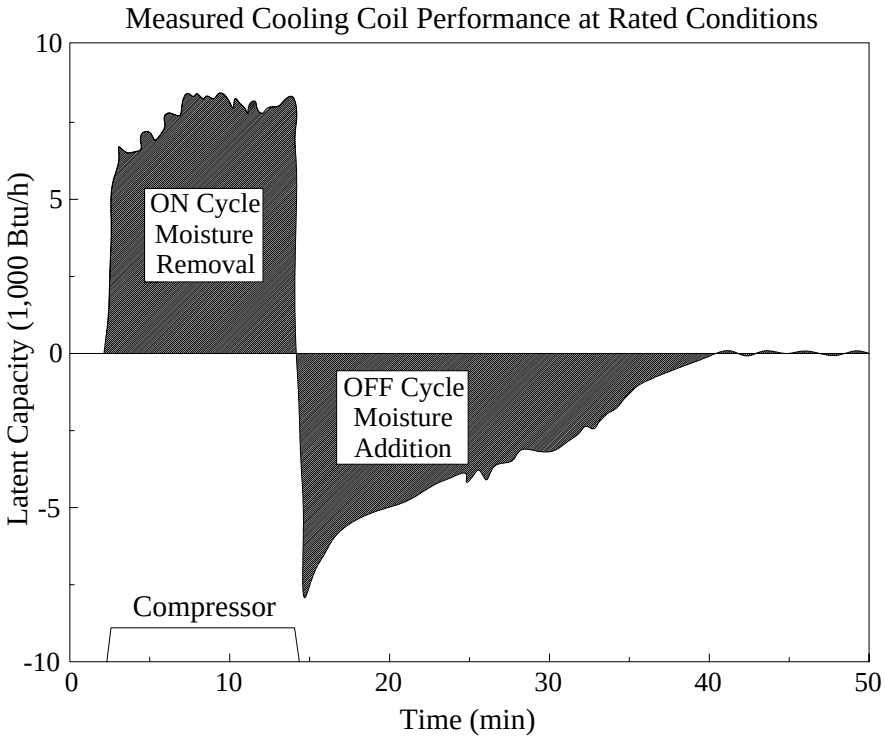

Fig. 2.2 Dehumidification and re-evaporation for an on-off cyclic operation air conditioner [Henderson 1998]

There are two internal sources for indoor moisture load. The first includes the moisture gains from occupants and other indoor activities, such as washing, cooking etc. The second is however related to the operation of a DX A/C unit. As in most residential buildings, a supply fan in a DX A/C unit is usually operated continuously regardless of its compressor status. When the compressor is on, moisture is condensed over cooling coil surface and collects in a drain pan. However, if the supply fan is on when the compressor cycles off, moisture from the wet cooling coil and drain pan may be reintroduced into supply air stream due to constant air circulation, raising the RH level in a conditioned space [Khattar et al. 1987, Shirey 1993, Arens and Baughman 1996, Kosar et al.1998, Amrane et al. 2003, Shirey and

Henderson 2004]. Fig. 2.2 shows this dehumidification and re-evaporation phenomenon of an air conditioner for an on-off cyclic operation at its rated condition [Henderson 1998]. The amount of moisture re-evaporated depends on physical characteristics of the evaporator coil and drain pan, for instant, fin spacing, pan slope etc., the thermostat cycling rate and the time constant of air conditioner latent performance at compressor start-up [Henderson and Rengarajan 1996].

Part of the moisture from the internal moisture sources becomes directly part of space latent cooling load, while others would be absorbed by internal building envelope and indoor furnishings, which may be regarded as “moisture capacitors”, such as wall paper, furniture and carpet etc., before a dynamic equilibrium of moisture transfer is achieved between indoor air and these capacitors [Rode and Mendes 2004]. The issues related to “moisture capacitors” will be discussed in Section 2.2.3.3.

For the moisture load which directly becomes part of space latent cooling load, such as those from occupants, indoor activities and reintroduced from a cooling coil, a parameter defined as indoor moisture generation rate (IMGR) can be used. IMGR is essential to studying the effects on the indoor moisture level and to accurately predicting heat and moisture transfer for system design. Using a heat and moisture transfer model and the actual measuring results for a test building, Lu [2003] compared the calculated indoor moisture content and RH by using the model and the measured values. When IMGR was assumed to be zero, both the calculated indoor moisture content and RH were lower than that measured. Therefore IMGR must be taken into account [Henderson 1992, Trowbridge et al. 1994, Doty 2001]. ASHRAE

Handbook of HVAC Systems and Equipment 2000 correctly points out that the moisture load contributed by human occupancy depends on the number of occupants and the level of their physical activity, and recommends an average rate of moisture generation of 320 g/h for a family of four [ASHRAE 2000]. However, TenWolde pointed out that IMGR had no clear relationship with the number of occupants; other factors like domestic cleaning and plants may also contribute. Very often, IMGR value may have to be experimentally determined [TenWolde 1994]. Therefore, moisture production rates in residences would vary widely.

2.2.3.3 Moisture capacitors

There have been a number of previous studies on the moisture from internal and external sources absorbed by indoor "moisture capacitors". It has been estimated that as much as one third of the moisture generated in a room could be absorbed by its surfaces [Kusuda 1983]. It was further indicated that the interaction between moisture storing and releasing can have impacts on indoor RH level. According to a research program carried out in Florida Solar Energy Center, if a building was cooled at nighttime with humid outdoor air, the building's internal surfaces would absorb moisture from outdoor air. If A/C was used during the forthcoming day to cool the building, it experienced an additional space latent cooling load as the moisture absorbed was released from internal surfaces of envelope and indoor furnishings [Fairey et al. 1986]. This type of space latent cooling load also contributed to the starting load of an A/C unit [Bailey et al. 1996]. On the other hand, a larger number of methods have been developed to deal with the dynamic behavior of the moisture exchange between indoor air and the internal surfaces of

building envelope. For example, Miller [1984] theoretically suggested using a simple resistor-capacitor electrical circuit to describe the dynamic behavior. Kusuda and Miki [1985] investigated the response of moisture storage of internal surfaces to a step increase in indoor RH with an infrared reflectance technique called the "Quadra-Beam" method. Plots of moisture content against time indicated that absorption rate appeared to follow an exponential decay. A finite element model and an implicit finite difference model were developed to evaluate moisture absorption and desorption of building materials by Fairey and Kerestecioglu [1985], Thomas and Burch [1990], respectively. In other studies, the lumped parameter analysis was used and the effective penetration depth theory was established [Kerestecioglue et al. 1990]. More recently, Biot number was used to classify the building materials into three main categories, and then the governing equation would be established and solved by analytic-numeric method or transfer function method [El Diasty et al. 1993, Chen and Chen 1998]. All of these methods have their own advantages, but they also have some limitations and are impractical to a certain extent.

Although the dynamic behavior of moisture storage for some building materials, such as concrete, gypsum plaster, plywood, timber, etc., and their effects on indoor RH level, have been extensively studied, the issue of moisture absorbed by indoor furnishings has been rarely addressed [Miller 1984, Isetti et al. 1988, Barringer and McGugan 1989, Wong and Wang 1990, Karagiozis and Salonvaara 2001, Lucas et al. 2002, Rode and Grau 2003, Rode et al. 2004, Gawin et al. 2004, Holm et al. 2004, Lucas and Miranville 2004]. There are two reasons for this. The first is that for a conditioned space, the interactions between building envelope materials and indoor air are more important than that between such indoor furnishings as furniture, quilt,

clothes and indoor air. The second is that after a building is occupied, while the format and material for building envelope would remain unchanged for a considerable period of time, indoor furnishings would for many reasons not.

Based on the discussions in this Section, it can be therefore observed that during part load conditions in hot and humid subtropical regions, for an A/C unit, its sensible load is reduced or may actually become negative. However, the mass transfer from both external and internal sources, which occurs in parallel with the heat transfer, will usually make the space latent cooling load to remain unchanged or even to increase, and therefore, lead to the problem of out of control for indoor humidity [Shaw and Luxton 1988, Brandemuehl and Katejanekarn 2004].

2.2.4 Indoor environmental control with an emphasis on humidity control with DX A/C units

For residential buildings, especially those located in hot and humid climates, the provisions of A/C installations have become indispensable. Much research work has been undertaken, focusing on temperature control using DX A/C units in residences in the subtropics. For the design and application of residential DX A/C units, indoor humidity control still remains problematic.

When the issue of indoor humidity control is addressed, it is worthy mentioning both sensible load which is temperature related and latent load which is moisture related, as well as the SHR defined as a ratio of sensible load to the total load. An equipment

SHR for an A/C unit occurs at a cooling coil, but an application SHR occurs in a conditioned space. An equipment SHR is largely a function of a cooling coil's dew point, the larger the temperature difference between the coil surface temperature and the entering air wet-bulb temperature, the greater the ability the coil has to remove excess moisture. How A/C units are designed, operated, and controlled would govern the coil surface temperature. On the other hand, an application SHR depends largely on the latent cooling load generated within a building, infiltrated through envelope or introduced as ventilation requirement. Part load operation can affect an equipment SHR, as well as an application SHR [Amrane et al. 2003].

The main problem for indoor environmental control with a DX A/C unit stems from the unit's inherent characteristics. A DX A/C unit removes moisture as a by-product of a cooling process. The current trend in designing an A/C unit is to have a smaller moisture removal capacity, in an attempt to boost energy-efficiency ratings (EER) and Coefficient of Performance (COP) [Kittler 1996]. The method used to improve efficiency is to increase the heat exchanger surface area. Such a strategy allows an A/C unit to run at a higher refrigerant temperature in its evaporator and a lower refrigerant temperature in its condenser, resulting in a lower latent capacity of the unit.

As a result, the equipment SHR of standard residential DX A/C units has been designed at between 0.7 and 0.8 at the Standard ARI rating conditions (the dry-bulb and wet-bulb temperatures for the air entering the cooling coil are 26.7°C and 19.4°C, respectively, and the dry-bulb outdoor air temperature is 35°C) [Henderson et al. 1992, Shirey 1993, Kittler 1996, Lstiburek 2002, Amrane et al. 2003, Westphalen

2004]. However, for many residential buildings experiencing higher ratios of space latent cooling load at between 40% and 50% of the total, the corresponding application SHRs are too low. It is therefore not possible for standard DX A/C units to deal with such large space latent cooling load, even though the total output cooling capacity from a DX A/C unit equals to the total space cooling load. Therefore, potentially an A/C unit will provide a desired temperature control but not a desired humidity control [McGahey 1998, Murphy 2002, Westphalen 2004, Brandemuehl and Katejanekarn 2004, Westphalen et al. 2004]. This inadequacy was demonstrated in the study of Kohloss [1981] and was confirmed by Katipamula et al. [1988]. In hot and humid subtropics, such as in Houston, Texas, USA, where an A/C unit with its equipment SHR greater than 0.8 failed to maintain indoor conditions within ASHRAE comfort zone (ASHREA 1981a) for as much as 30% of the operating time.

The second problem for indoor environmental control using DX A/C units is oversizing. A DX A/C unit is usually sized for full load with safety margins and, therefore, is oversized for part load operating hours [Khattar et al. 1987]. When a DX A/C unit in residence is suitable for full load operation, it would be a final insult to the building and its occupants during part load conditions with relatively low sensible heat factors accompanied by a further requirement on indoor humidity control. Although at a steady-state operational condition, the numerical values of both equipment SHR and application SHR are equal to each other, the total output cooling capacity may be larger than the reduced total space cooling load; there can be either surplus or deficit of both sensible and latent components in the total output cooling capacity. Therefore, the air conditioned space may be overcooled or indoor

RH would rise to above the design level [Shirey 1993, Berbari 1998, Lstiburek 2002, Murphy 2002, Harriman III and Judge 2002, Amrane et al. 2003, Hourahan 2004, Shirey and Henderson 2004]. Under the part load conditions, A/C units oversized by 20% might achieve space latent cooling load removal of approximately 15% of the total, whereas, correctly sized A/C units would achieve moisture removal of up to approximately 30%. Even with correctly sized standard systems, the part load problem associated with latent load remains, albeit not to the same extent [Lstiburek 2002]. Furthermore, when a DX A/C unit is operated at part load conditions, indoor humidity control problem would become worse with on-off cycling its compressor. The compressor will remove the sensible load with very little run-time to easily satisfy the thermostat setpoint and cycle off long before moisture removal can be affected [Jalalzadeh-Azar et al. 1998, Hourahan 2004].

The third problem is related to energy consumption. Usually, overcooling occurs as air has to be cooled to a suitable low dew point temperature to remove the space latent cooling load, but reheating is required to avoid overcooling a space. The challenge is that the limited natural resources cannot keep pace with this wasteful method for dehumidification [Coad 2000]. Recognizing the need for a revised energy standard, ASHRAE has eliminated the use of additional energy for reheating for constant-air-volume (CAV) systems with their design cooling capacities exceeding 40000 Btu/h (11724 W) [Hickey 2001]. On the other hand, after being more informed and aware of the importance of energy conservation and high energy cost, occupants have raised their thermostat setpoints in summer to avoid overcooling. As a result, some residences suffer from bad IAQ problems such as high indoor RH level and mold growth [Kurtz 2003]. These situations could well be exacerbated

when a low ventilation rate is used for energy conservation and when there is inadequate exhaust of indoor moisture sources [Arens and Baughman 1996].

2.3 Strategies to control indoor environment with an emphasis on controlling indoor humidity

In hot and humid climates, indoor environmental control using A/C installations is essential to provide building occupants with a suitable indoor thermal environment. While indoor air temperature control can be easily to achieve, even with DX A/C units, indoor humidity control remains more problematic on a relatively scale. However, indoor humidity control is important in determining occupants' thermal comfort, IAQ and energy efficiency. In this section, all strategies currently available to control indoor humidity are reviewed.

2.3.1 The strategies related to eliminating moisture sources

2.3.1.1 Applying vapor retarders

In order to reduce the space latent cooling load from water vapor migrating through building envelope, vapor retarders can be used. The building materials that are generally classed as impermeable vapor retarders include rubber membranes, polyethylene film, glass and aluminum foil etc. [Lstiburek 2002, Lstiburek 2004]. Trowbridge et al. [1994] studied a typical residential building in Austin, Texas, USA,

by simulation. The mass transfer coefficients at the outside of external walls were set to zero to become a moisture impermeable envelope. Comparing the result of simulation with that of experiment, the vapor retarders were inconsequential in reducing interior moisture levels in either April or August. The typical difference in RH level between the permeable and impermeable envelope for these months was shown to be on the order of 1%. This finding suggested that moisture transport through the external envelope was a negligible contributor to indoor moisture content and indoor humidity control for hot and humid climates. This was also further confirmed by Fairey and Keresteciogl u [1985] and Harriman III et al. [2001].

2.3.1.2 Reducing outdoor air infiltration

Infiltration of outdoor air was found to be one of the greatest single influences on indoor RH level [Kohloss 1981, Straube 2002]. Measures such as applying air barriers, e.g., rubber and bitumen-based membranes, can be used to resist the infiltration. The position to place air barriers is critical. In hot and humid climates, air barriers should be located external to a thermal insulation layer, where moisture would condense. In addition, all barriers must be kept continuum to ensure efficiency, all seams and joints must be sealed with tape, overlapping is not adequate [Harriman III et al. 2001, Lstiburek 2005]. However, provided there is no moisture removal when an A/C unit operates, even a building experiencing no infiltration will eventually have a high RH level by internal moisture sources. With moisture removal, indoor RH steadily decreases from initial conditions, approaching a lower limit depending on the A/C's supply air dew point and its run time. A zero infiltration strategy is, of course, unrealistic as well as undesirable, considering the

need to provide sufficient outdoor air to maintain good IAQ [Trowbridge et al. 1994], especially for split-type DX A/C units which do not have the provisions of providing outdoor air to conditioned spaces themselves.

2.3.1.3 Reducing ventilation air rate

Since the majority of space latent cooling load results from humid outdoor ventilation air, reducing the ventilation rate can help lower indoor RH level. In fact, although this strategy can slightly lower the indoor RH level, it may not adequately solve the problem of high indoor RH level associated with CAV systems that are controlled based on space air dry-bulb temperature alone. More importantly, it results in underventilated spaces, possibly leading to other IAQ problems [Murephy 2002].

2.3.1.4 Increasing moisture capacitance

One of the indoor RH control strategies is increasing moisture capacitance of the materials used in building envelope and other internal materials. This can help dampen the fluctuation of indoor RH level. Such a damping effect was theoretically predicted by Isetti et al. [1988] and experimentally demonstrated by Cummings and Kamel [1988]. Other studies suggested that moisture storage in building envelope helped reduce required output cooling capacity and energy use of an A/C unit, in order to maintain a desired indoor RH level. However, building envelope and internal materials would eventually become moisture saturated. Clearly, increasing

moisture capacitance without a means for drying structural mass would provide little relief of high indoor RH problem [Trowbridge et al. 1994].

2.3.2 Pre-conditioning outdoor air

Using a separate A/C unit to condition outdoor air and an air handing unit (AHU) to condition recirculated indoor air is a feasible way to control indoor humidity [Lstiburek 2002]. This approach, which is similar to the idea presented by Kohloss [1981], is to introduce pre-conditioned outdoor air into a conditioned space at the dew point temperature of indoor air, which is sufficient to deal with entire space latent cooling load. At the same time, operating a conventional AHU with its equipment SHR of 1.0 is to meet any remaining space sensible cooling load. The key concept embodied in this strategy is that the ventilation air enters a conditioned space at a rate sufficient to overcome all infiltration, such that the conditioned space is pressurized. Because the outdoor air after a separate A/C unit's treatment is direr than the air that enters the space directly, a reduction of indoor RH level is expected [Trowbridge et al. 1994, Mazzei et al. 2005].

2.3.3 Alternatives for traditional mechanical-cooling dehumidification

2.3.3.1 Heat pipe heat exchanger (HPHE) technology

Traditionally, the principal method for indoor humidity control currently used is to overcool air to extract more moisture and then reheat it to a suit able supply temperature. This strategy is inherently costly and inefficient since it uses a great deal of energy to overcool air and then more energy to reheat it. Consequently, reheating is uncommon in residential A/C units and is virtually unknown in single-family residences [McFarland et al. 1996]. The key exceptions are to use energy recovered from an exhaust air stream or the heat rejected from a condenser. This offers multiple design alternatives, for example, HPHE technology [Yau 2001, Lin 2001, Hickey 2001, Soylemez 2003]. HPHE is an alternative for reheating, making a conventional DX A/C unit a more effective dehumidifier.

The early form of HPHE is a sensible heat exchanger (SHE), which was first developed in the 1950s [McFarland et al. 1996]. It can be used to transfer thermal energy from return air stream to supply air stream without requiring auxiliary power input. Compared to an ordinary air reheating process, this transfer of energy precools return air, thereby increasing the latent capacity of an evaporator, and reducing the required A/C unit size, energy consumption and peak demand. After being cooled and dehumidified by an evaporator, the very cold supply air is reheated by a SHE to a proper temperature for delivery to a space. Early methods of SHE included direct air-to-air heat exchanger or pumped fluid systems utilizing water, brine, or volatile

refrigerant. Although these methods were more efficient than air reheating method, they have their own disadvantages [Shirey 1993].

HPHE technology was firstly developed at Los Alamos Scientific Laboratory for spacecraft application in 1968. Khattar [1985] and Dinh [1986] had respectively applied this technology to increasing the cost-effectiveness and efficiency of sensible heat exchange between supply and return airstreams. HPHE technology used in A/C systems is efficient to enhance dehumidification. This type of equipment consists of sealed tubes partially filled with volatile working fluid, typically a refrigerant for A/C systems. When one end of a HPHE is placed in warm return air stream, HPHE refrigerant absorbs heat from air and evaporates. The vapor travels to the other end of the pipe, located in cold supply air stream, due to pressure force. Heat is transferred from HPHE refrigerant to cold supply air, causing the refrigerant vapor to condense and return to the other side of the heat pipe via gravity or capillary force. The advantages of HPHE over early sensible heat transfer method include lower first cost, higher effectiveness per square foot of heat exchanger surface area; lower air side pressure drop, fewer heat exchanger rows; reduced maintenance, no moving parts; and reduced operating costs, no pump power [Shirey 1993]. Despite these merits, the use of HPHE would however incur an increased air pressure loss, higher manufacturing cost, and the increased overall size of A/C systems. Till now, HPHE has been applied successfully in various types of buildings, such as supermarket, art museum. All of these have demonstrated the effectiveness of HPHE as a method for dehumidification [Shirey 1993, Hill and Jeter 1994, McFarland et al. 1996, Xiao et al. 1997].

Currently, other alternatives which provide similar functions to HPHE have also been used, such as spiral coil heat exchangers (SCHE), plate type heat exchangers (PTHE), heat recovery wheels in conjunction with cooling coils and run-around loops, etc. SCHE is an improved cooling and dehumidifying unit. An advantage a SCHE has over conventional heat exchanger systems is its ability to accommodate differential thermal expansion. Moreover, it is a more compact system with spiral coil arrangement; for the same heat transfer surface, it has a volume of 15% smaller than that of a crossflow heat exchanger. Spiral layers may be readily removed for cleaning of the fouled heat transfer surface, which is particularly desirable in A/C systems where clean air is important [Ho and Wijeysundera 1999]. PTHE provides the same function as a HPHE. Although with a lower efficiency than that of a HPHE and without flexibility in designing ductwork, a PTHE is usually less expensive and can be made more easily by more manufacturers [Harriman III et al. 2001].

2.3.3.2 Other related alternatives

Besides the HPHE technology, there are two other alternatives currently used to replace the traditional mechanical-cooling dehumidification strategy. One is hot gas reheat, and the other hot liquid reheat, both using the recovered heat energy from a refrigeration process.

Hot gas reheat allows the control of space humidity by using heat energy that would otherwise be rejected outdoors. When space humidity exceeds the desired limit, hot refrigerant gas leaving the compressor is redirected through a reheating coil downstream of a cooling coil. The compressor continues to operate, dehumidifying

the air, while reheat avoids overcooling the space. On the other hand, hot liquid reheat realizes a higher efficiency than hot gas reheat by extracting heat from the high-pressure liquid refrigerant. Whereas hot gas reheat reduces the condenser load, hot liquid reheat increases the specific enthalpy rise of the refrigerant passing through the evaporator. This minimizes the energy impact of reheating. However, hot liquid reheat has a lower reheat capacity than hot gas reheat, especially at moderate-temperature ambient conditions. Both of these two reheat methods are easier to control than using HPHE because they typically require single solenoid valve, while multiple valves should be provided for HPHE [Westphalia 2004, Westphalen et al. 2004, Taras 2004].

2.3.4 Evaporator bypass

Evaporator bypass is one of the approaches that can enhance dehumidification performance. It is used by unitary systems having two or more compressors with evaporators arranged with a top/bottom split of the compressor circuits. Further gains can be realized by allowing part of the supply air to bypass the evaporator through a modulating damper. Such a system must incorporate safety measures to prevent the evaporator from frosting under cooling and drying conditions [Westphalia 2004, Westphalen et al. 2004].

2.3.5 Standalone dehumidifiers with desiccant

Over the last 10 years, manufacturers have been actively developing new dehumidification equipment [Harriman III and Judge 2002]. Experiences with newly constructed buildings in hot and humid climates have led to a conclusion that supplemental dehumidification during part load periods is necessary, in particular in buildings with controlled ventilation [Lstiburek 2002]. A standalone dehumidifier with desiccant is an example of supplemental dehumidification equipment [Mazzei et al. 2005, Sand and Fischer 2005]. Two approaches are used when using a standalone dehumidifier. One is to directly introduce the dehumidified outdoor air into a space. With the advantage of maintaining constant ventilation and humidity control while allowing a lower A/C system's capacity, this approach is usually suitable for schools, hotels and supermarkets. The other is to pre-treat the outdoor air introduced to an A/C system. This approach is a good method for restaurants, movie theaters and office buildings; because it helps to reduce the size of conventional A/C systems and can provide independent control of indoor humidity [McGahey 1998, Fischer et al. 2002].

The drying agents used in a standalone dehumidifier are solid or liquid desiccants. Solid desiccant equipment may be classified into two types, "active" type and "passive" type. The equipment using heated reactivation air is called an "active" dehumidifier. The heat used for reactivation often comes from distributed power generation or natural gas, all of which are rather inexpensive during humid seasons. Unlike an "active" one, a "passive" dehumidifier uses a building's dry exhaust air instead of heated air for reactivation [Harriman III et al. 2001, Harriman III et al.

1999]. A solid-desiccant based dehumidifier is more compact but, presents a higher pressure drop for both the air to be dehumidified and the air for regeneration, therefore a higher fan power is required. The final temperature of the processed air is always high, leading to a decrease of the adsorption capacity of desiccant. In addition, heat generated by a solid desiccant dehumidifier affects thermal comfort [Andersson and Lindholm 2001, Capehart 2003, Subramanyam et al. 2004, Alpuche et al. 2005].

On the other hand, comparing to a solid desiccant-based system, a liquid desiccant-based system needs a lower fan power. The use of a liquid desiccant based system can help more easily to control the temperature during absorption, resulting in a lower temperature of the processed air. Another advantage of using liquid desiccant is air cleaning. It is believed that the liquid desiccant washing action in hospital environment would both reduce airborne bacteria and remove particulate matter [Marsala et al. 1989, Dai et al. 2001, Dieckmann et al. 2004, Rowland et al. 2005, Elsarrag et al. 2005]. Latent heat and sensible heat of water vapor extracted from the air are dumped into cooling water of the absorber, often, in order to keep a low dew point of the processed air. This operation is cooled by a chiller with further operating costs. Therefore the operating costs using desiccants are higher when compared to other indoor humidity control strategies [Scalabrin and Scaltriti 1985, Lstiburek 2002].

Although the operating cost of a standalone dehumidifier with desiccant is slightly high, it has its own advantages. Firstly, its initial cost is low, for example, only adding approximately US$300 for the equipment used in a typical house in the U.S.

Secondly, this strategy is simple to implement and typically compensates for oversized A/C units. Thirdly, such a dehumidifier can provide both appropriate sensible and latent cooling.

2.3.6 Varying the operation mode of supply fans

In most buildings where DX A/C units are used, their indoor supply fans are originally operated continuously regardless of compressor status based on the setpoint of a thermostat. During “on” mode, while moisture is condensed over cooling coil surface and collected in a drain pan, air movement is maintained. However, during “off” mode, moisture from wet cooling coil and drain pan may be reintroduced into supply air stream due to constant air circulation for ventilation, increasing indoor RH level (see Fig. 2.2). Therefore, the fluctuation in indoor RH has been observed [Khattar et al. 1985, Shirey 1993, Amrane et al. 2003]. Furthermore, during “on” mode, the fan motor consumes a significant amount of energy for air movement, typically raising moving air temperature by 1.1°C. Not only does this add heat to a conditioned space, but also a DX A/C unit must run longer to remove the added heat when a compressor turns on. In part load conditions or with oversized DX A/C units, where a compressor runs for a short time and turns off, this operation mode can adversely affect moisture removal and exacerbate high RH problem [Khattar et al. 1987, Shirey and Henderson 2004].

The supply fan control can be changed to “auto” mode, in which a fan cycled on and off in accordance with compressor operation. This mode is typically used for

residential A/C units, where the supply fan only runs when a compressor is on. When the compressor shuts off, the supply fan will also stop, allowing moisture to drain out of the A/C unit. In addition, with such an "auto" mode, improved energy efficiency is expected. For example, for temperature-controlled zones within a museum, such an auto fan mode stabilized and substantially reduced RH level while providing annual energy savings of 18% to 20% [Shirey 1993]. However, for this operating mode, pockets of warm air may develop and the thermostat may also sense false temperature due to this phenomenon. With respect to the fact that there is much concern over occupants' discomfort due to the lack of air motion or reduced ventilation, although this strategy provides improved indoor humidity control and energy saving, it does not meet ANSI/ASHARE Standard 62-1999 and is not recommended.

Other field and laboratory tests have shown that even when a supply fan is cycled on and off with a compressor, there is a degradation of latent capacity at part load conditions. It was observed that the equipment SHR for an A/C unit at its start-up state was not the same as that at its steady-state. This was caused by a lag or delay in latent capacity of a cooling coil at start-up in the range of 2 to 4 minutes [Henderson and Rengarajan 1996, Shirey and Henderson 2004]. Others found the delay ranging from 1 to 2.5 minutes, depending on the cycling rate of a compressor and the inlet air temperature and humidity at a coil. Latent capacity was actually negative for most of this initial period [Katipamula and O' Neal 1991].

2.3.7 The strategy for improved environmental control by a DX A/C unit

Various strategies discussed in Section 2.3.1 have their inherent weakness and, for practical applications will have minimal effect on indoor humidity control. Others discussed in Sections 2.3.2 to 2.3.5 are more applicable for large non-residential buildings. In residential buildings, it is normally impossible to add other equipment to an A/C unit, usually of DX type. The strategy discussed in Section 2.3.6 is effective for residential DX A/C unit, and therefore has been seen in practice; however, it is essentially for on-off cycling, but not continuous control for indoor humidity, assuming that indoor air temperature can well be controlled. For residential buildings, the key problem for indoor environmental control involving the use of DX A/C units is the mismatch between output sensible and latent cooling capacities from the DX A/C units and the corresponding space sensible and latent cooling loads.

The improvement of the control for DX A/C units can have a significant impact on environmental control and in particular dehumidification performance. To solve the contradiction of latent and sensible load removal, incorporating multi- or variable-speed drives instead of such other technology as pre-conditioning, is more effective [Lstiburek 2002, Kurt et al. 2004]. Theoretically, accurate control of both indoor temperature and humidity during a cooling and dehumidifying process may then be realized.

2.3.7.1 Lowering airflow rate using variable-speed supply fan

An experimental study by Chuah et al. [1998] concluded that for dehumidification control, airflow rate was of the prime concern. Previous field studies have demonstrated that lowering the airflow across a cooling coil and lowering evaporator coil refrigerant temperatures can enhance dehumidification efficiency [Khattar et al. 1987, Shaw and Luxton 1988, Yang and Lee 1991, Kittler 1996, Khattar and Henderson 1999, Kurtz 2003, Westphalen 2004, Shirey and Henderson 2004, Hourahan 2004]. Implementing this strategy would lower space humidity level by 10% to 15% RH. The reduction in energy costs associated with various type of A/C units used, would cover the full range of climates, but is most significant in humid and tropical climates [Shaw and Luxton 1988].

While much available open literature focused solely on reducing airflow rate with multi- or variable-speed supply fan, which itself is an improvement for A/C units, there has been relatively little research work looking into varying the speeds of both the supply fan and the compressor of a DX A/C unit for better indoor environmental control.

2.3.7.2 Applying variable-speed compressor and supply fan in a DX A/C unit

For a DX A/C unit, the sensible and latent components of its total output cooling capacity may be altered by varying its supply fan speed and compressor speed simultaneously. One available strategy is to control the space temperature by varying compressor speed and the space RH level by varying supply fan speed, separately.

Variation of the two speeds enables variation of the sensible and latent components of the total output cooling capacity of a DX A/C unit [Krakow et al. 1995].

An experimental verification for the feasibility of such a control strategy was carried out by Krakow et al. [1995]. The conditioned space was a 76.5 m^3 room on the ground floor of a large building in Canada. The experimental results illustrated that the space temperature and RH were maintained within ± 0.3°C and ± 2.5% RH, respectively, of their setpoint values. The sensible and latent components of the A/C unit's output cooling capacity appeared to respond to the variations of the applied and transmitted space cooling loads. The applied space cooling load on the A/C unit consisted of the heat output from electrical-resistance space heaters and a humidifier. The transmitted space cooling load consisted of indeterminate amounts of heat conducted through external and internal envelope, etc. A numerical simulation model incorporating Proportional-Integral-Differential (PID) control was also developed. The experimental and simulation results confirmed the feasibility of this control strategy. In this study, only simple comparisons and analysis were given. Detailed temperature and RH data and the related energy consumption were not indicated. Moreover, it was observed from the experimental results presented that the transient behaviors were poor, as it took approximately 2 hours after increasing the power input for the humidifier for indoor RH to return to its original level before the disturbance.

In addition, in the simulation study carried out by Andrade et al. [2002], a detailed, physically based A/C simulation model was augmented by adding load equations describing space sensible and latent cooling loads experience by a typical residential

building. The simulation results showed that the use of a variable-speed compressor and a variable-speed supply fan can help prevent short on-off cycling and improve indoor humidity control while possibly increasing system efficiency by having different combinations of compressor and fan speeds at the expanse of running a DX A/C unit longer. It may be seen, however, the strategy was verified only by simulation; no actual experimental validation has been carried out. Also this study was essentially for on-off cycling, not continuous control over the condensing unit in a DX A/C unit.

2.4 Conclusions

The development of air conditioning technology is a natural consequence of both pursuing high quality living and working environment and at the same time, addressing the issue of sustainability. For residential buildings, the most commonly used A/C systems are of DX type. DX A/C units have a number of advantages when compared to large central chilled water-based A/C installations. Currently, most DX A/C units are equipped with single-speed compressors and supply fans, relying on on-off cycling compressors to maintain only indoor dry-bulb temperature. For residential buildings located in hot and humid subtropics, such as Hong Kong, indoor environmental control, in particular indoor humidity control, with a DX A/C unit has always been a challenge.

Extensive related research work on indoor thermal comfort and moisture sources has been undertaken. Firstly, extensive research work on indoor thermal comfort has led

to the establishment of internationally accepted thermal comfort standards, such as ASNI/ASHRAE 55 and ISO Standard 7730. Suitable ranges for indoor environmental parameters, such as indoor air temperature and RH, have been specified. Secondly, a number of previous studies clearly indicated that indoor moisture comes from external and internal sources. However, little studies on how each of moisture sources, such as ventilation, would directly influence the space latent cooling load and the resultant application SHR. Thirdly, although the dynamic moisture storage behaviors of building envelope have been extensively studied, the influences of indoor furnishings acting as moisture capacitors on indoor RH level have been rarely addressed.

On the other hand, a number of problems for indoor environmental control using a DX A/C unit have been reported. The current trend in designing a DX A/C unit is to have a smaller moisture removal capacity, in an attempt to boost EER and COP. Therefore, the unit removes moisture as a by-product of a cooling process. Previous related studies also covered the methods used to improve efficiency of a DX A/C unit, and the optimization of evaporator structural parameters for better moisture removal, etc. However, no previous work on investigating the inherent operational characteristics of DX A/C units equipped with variable-speed compressors and supply fans with respect to the indoor environmental control can be identified.

With respect to the strategies currently used to control indoor humidity, the passive methods to eliminate moisture sources are not effective. Other strategies, such as pre-conditioning fresh air, HPHE technology, and standalone dehumidifiers with desiccant, etc., are more suitable for large non-residential buildings. For residential

buildings served by DX A/C units, with single-speed compressors and supply fans, often space overcooling or uncontrolled indoor RH have been experienced. However, the use of variable-speed compressor and supply fan in a DX A/C unit is expected to have a significant impact on solving the contradiction of latent and sensible load removal, therefore continuously and accurately regulating both the indoor air temperature and RH level become possible. Since there has been relatively little research work looking into this issue, with existing studies essentially focusing on on-off cycling with single-speed compressor and supply fan, further research work should be carried out on using a DX A/C unit with variable-speed compressor and supply fan for simultaneous indoor air temperature and RH control.

The literature review on indoor environmental control with an emphasis on simultaneously controlling indoor air temperature and humidity using DX A/C units in residences in the subtropics reported in this Chapter has identified a number of important areas where further in-depth research work is required. These are the expected targets of investigation reported in this thesis.

Chapter 3

Proposition

3.1 Background

It is evident from the literature review presented in Chapter 2 that the most commonly used A/C systems in residential buildings are of DX type. DX A/C units are currently equipped with single-speed compressors and fans, relying on on-off cycling compressors to maintain only indoor dry-bulb temperature, resulting in either space overcooling or an uncontrolled equilibrium indoor RH level. This is particular true for residential buildings located in hot and humid subtropics. Therefore, developing an appropriate indoor environmental control strategy using DX A/C units has always been a challenge for subtropical residential buildings.

No previous work on studying the inherent operational characteristics of DX A/C units when the speeds of compressors and supply fans were simultaneously varied may be identified. This suggested that there is a need to experimentally obtain the inherent operational characteristics of DX A/C units having variable-speed compressors and supply fans which would usefully facilitate the investigation of indoor environmental control using DX A/C units in residences. Furthermore, no previous research work on the impact of varying speeds of a DX A/C unit's compressor and supply fan on indoor thermal comfort level may be identified either. This implied that consideration should also be given to this particular issue.

With respect to the strategies currently used to control indoor environment in residences using DX A/C units, the use of variable-speed compressor and supply fan in a DX A/C unit is expected to have a significant impact on solving the contradiction of latent and sensible load removal, and to facilitate the continuously and accurately regulation of both the indoor air temperature and RH level. The previous limited reported research work warrants the need to develop novel control strategies for DX A/C units with variable-speed compressors and supply fans for simultaneous indoor air temperature and RH control.

3.2 Project title

This thesis focuses on the following four major issues related to indoor environmental control with a DX A/C unit having variable-speed compressor and supply fan in residences in the subtropics: 1) Studying the characteristics of space cooling loads by simulation; 2) Investigating the inherent operational characteristics of a DX A/C unit at fixed inlet air temperature and humidity; 3) Investigating the indoor thermal comfort characteristics under the control of a DX A/C unit under a fixed space cooling load condition; and 4) Developing a novel DDC-based capacity controller for simultaneously controlling indoor air temperature and humidity. The proposed research project is therefore entitled “Indoor environmental control with a direct expansion (DX) air conditioning (A/C) unit in residences in the subtropics”.

3.3 Aims and objectives

The objectives of the research project reported in this thesis are:

1) To carry out a simulation study on the characteristics of space cooling loads in residences in the subtropics, and to investigate both the indoor humidity control problem due to the mismatch between the output latent cooling capacity from a DX A/C unit and the space latent cooling load when the space sensible cooling load is satisfied by on-off cycling compressor, and the influences of indoor furnishings acting as moisture capacitors on indoor RH level;
2) To investigate the inherent operational characteristics of a DX A/C unit having variable-speed compressor and supply fan at fixed inlet air temperature and humidity;
3) To investigate the indoor thermal comfort characteristics under the control of a DX A/C unit having variable-speed compressor and supply fan at a fixed space cooling load condition;
4) To develop a novel DDC-based capacity controller of a DX A/C unit for simultaneous indoor air temperature and humidity control.

3.4 Research methodologies

The simulation study on the characteristics of space cooling loads in residences in the subtropics and the indoor humidity control problem due to the mismatch will be

investigated using a building energy simulation program – EnergyPlus, based on the typical layout of high-rise residential blocks and weather conditions in Hong Kong.

The experimental investigation on the inherent operational characteristics of a DX A/C unit having a variable-speed compressor and supply fan will be carried out using an experimental DX A/C station available in the HVAC laboratory in the Department of Building Services Engineering (BSE) in The Hong Kong Polytechnic University. The inlet air temperature and RH will be maintained constant to provide a reference for evaluating the inherent operational characteristics. Both compressor and supply fan speeds will be discretely varied between their maximums and minimums.

The experimental approach will also be applied to studying the indoor thermal comfort characteristics under the control of a DX A/C unit. All the experiments will be carried out under a given space total cooling load with a fixed application SHR at discretely varied experimental compressor and supply fan speeds.

Finally, in the development of a novel DDC-based capacity controller for indoor environmental control, the energy balance between the air side and refrigerant side of a DX A/C unit will be applied and a number of real-time measured operating parameters in the DX A/C unit will be used. The novel capacity controller to be developed will be implemented in the experimental DX A/C station, and controllability tests carried out to see whether the expected control sensitivity and accuracy may be achieved.

Chapter 4

The Simulated Characteristics of Space Cooling Loads and Indoor Environmental Control in Residences in the Subtropics

4.1 Introduction

For residential buildings located in the subtropics, because of hot and humid climatic conditions, air conditioning (A/C) is normally required for up to 7 to 8 months in a year [Lam 1993]. Unlike the A/C for commercial buildings, residential A/C is very often provided by the use of a discrete system, i.e., room air conditioners (RAC) which are generally of DX type. In hot and humid subtropics, A/C will have to deal with both sensible and latent loads in a space, and in many cases to deal with space latent cooling load using a DX A/C unit is more challenging and difficult.

On the other hand, sensible heat ratio (SHR) is an important parameter in studying both the characteristics of space cooling loads occurring in a conditioned space and the ability of cooling and dehumidification for the cooling coil of a DX A/C unit. The SHR for an air conditioned space is normally called an application SHR and that for an air conditioner an equipment SHR. An equipment SHR is largely a function of the design of a cooling coil while an application SHR depends however mainly on the characteristics of space sensible and latent cooling loads [Amrane et al. 2003].

Studies related to the space cooling loads in residential buildings located in hot and humid subtropics have been reported. These included the studies on the effect of thermal insulation of external wall or roof and the U-value of windows on space

cooling loads [Sullivan et al. 1994, Bojic et al. 2001, Shariah et al. 1997]. Furthermore, a number of reported studies discussed the control of indoor RH level under part load conditions, and briefly mentioned that the mismatches between the total output cooling capability and its sensible/latent components from DX A/C units and the total space cooling load and its sensible/latent components, respectively, can significantly influence the indoor environmental control in residences using DX A/C units [Lstiburek 2002, Murphy 2002, Hourahan 2004, Shirey and Henderson 2004, Harriman III and Judge 2002, Amrane et al. 2003, Shirey 1993, Andrade et al. 2002]. However, in all the previously reported studies, the characteristics of space cooling loads and the mismatches and their impacts on indoor environmental control were rarely studied.

On the other hand, dynamic behaviors of the moisture absorption and desorption between indoor air and the surfaces of indoor moisture capacitors including indoor furnishings were studied [Barringer and McGugan 1989, Bailey et al. 1996, Diasty et al. 1992, Trowbridge et al. 1994, Barringer and McGugan 1994]. The damping of the fluctuation of indoor RH level due to the presence of indoor furnishings was qualitatively predicted [Cummings and Kamel 1988, Trowbridge 1994]. However, in these previously reported studies, no quantitative assessments on how the presence of indoor furnishings would influence indoor RH level were given.

This Chapter reports on a simulation study where the characteristics of subtropical residential space cooling loads and the issues related to indoor environmental control using DX A/C units were investigated and analyzed, using a building energy simulation program currently available in the public domain, EnergyPlus [Website_1

2004]. The weather conditions of, and the typical arrangements of high-rise residential blocks in the subtropical Hong Kong were used in the simulation study. An introduction of the simulation program, EnergPlus, and the detailed descriptions of a typical apartment in a model high-rise residential block which was used as a platform to perform the simulation study, and a number of assumptions used in the simulation, are firstly presented. This is followed by reporting both the detailed analysis of hourly space cooling loads characteristics and the hourly application SHRs in both the living/dining room of the apartment at daytime and the master bedroom of the apartment at nighttime, respectively, in the summer design day. Thirdly, the problem of indoor environmental control, based on on-off cycling compressor to maintain only indoor air dry-bulb temperature, due to the mismatch between the output latent cooling capacity from a DX A/C unit and the space latent cooling load in the two rooms both in the summer design day and during part load conditions was quantitatively investigated. Finally, the influences of indoor furnishings acting as moisture capacitors on indoor RH levels were also quantitatively studied.

4.2 The simulation software - EnegyPlus

EnergyPlus, which was first released in April 2004 (Version 1.2.0), is a building energy simulation program for modeling building heating, cooling, lighting, ventilating, and other energy flows. Based on a user's description of a building from the perspective of the building's physical make-up, associated mechanical systems, etc., EnergyPlus calculates the heating and cooling loads necessary to maintain the

indoor thermal control setpoints, the conditions throughout a secondary HVAC system, the coil loads, and the energy consumption of primary plant equipment [EnergyPlus Archive 2004].

EnergyPlus has its roots in both Building Loads Analysis and System Thermodynamics (BLAST) and Department of Energy-2 (DOE-2) building energy simulation programs. It builds on the most popular features and capabilities of BLAST and DOE-2, but also includes many additional innovative simulation capabilities such as time steps of less than an hour, modular systems and plants integrated with heat balance-based zone simulation, multi-zone air flow, thermal comfort, and photovoltaic systems [Website_1 2004]. EnergyPlus allows users to calculate the impacts of different heating, cooling and ventilating equipment and various types of lighting installations and windows to maximize building energy use efficiency and occupant comfort. Users can simulate the effect of window blinds, electrochromic window glazings, and complex daylighting systems, which are the features not seen in earlier version of DOE software [Website_2 2004]. The current version of EnergyPlus (Version 1.2.2) provides an integrated, simultaneous solution where building responses and primary and secondary systems are tightly coupled (iteration performed when necessary). It employs the heat balance based solution technique for determining building thermal loads, allowing simultaneous calculations of radiant and convective effects at both the interior and exterior surfaces during each time step of simulation. It combines heat and mass transfer models that account for moisture adsorption/desorption either as a layer-by-layer integration into the conduction transfer functions or as an effective moisture penetration depth model. Furthermore, it links to other simulation environments such

as WINDOW5, COMIS (an air flow model), TRANSYS and SPARK to allow more detailed analysis of other components in building environmental systems.

The source code of EnergyPlus is currently available in public domain and open for public inspection, revision, etc. EnergyPlus has an improved structure to define a well organized modular concept that would facilitate adding features and links to other programs. The key benefit of modularity is that new modules can be developed concurrently without interfering with other modules under development and with only a limited knowledge of the entire program structure. FORTRAN90, which is a modern, modular language with good compilers on many platforms and allows C-like data structure and mixed language modules, has been used for the initial release of EnergyPlus.

However, EnergyPlus is a standalone simulation program without a 'user friendly' graphical interface. It reads input and writes output as simple ASCII text files. Furthermore, it is currently not a life cycle cost analysis tool.

4.3 Description of the apartment in a model building and the assumptions used in the simulation

A hypothetic 30-story residential block, which was modeled after those widely used in Hong Kong was used as the platform for performing the simulation study. This hypothetic block was used in a previous related simulation study, therefore detailed descriptions of the model block and all the assumptions used in the previous study

were previously given [Lin and Deng 2004]. However, for the completeness of this Chapter, these are repeated here. In addition, unlike in the previous related study, only the apartment facing west, one of a total of eight apartments in a floor, was used in this study. The floor plan of the selected west-facing apartment is shown in Fig. 4.1.

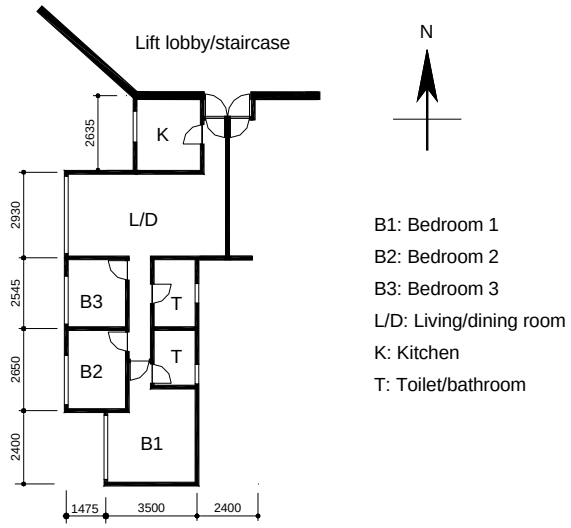

Fig. 4.1 Floor plan of a west-facing apartment under study in a hypothetic high-rise residential building

4.3.1 Occupancy pattern

In this apartment, there were three bedrooms, one living/dining room, one kitchen and two bathrooms. It was occupied by a four-person family consisting of two working adults and two school children. In this simulation study, it was assumed that the living/dining room was occupied by all family members at daytime; and the master bedroom (i.e., bedroom 1) by the two working adults and the other two smaller bedrooms, each by one of two school children respectively, at nighttime.

4.3.2 Building envelope

The construction details of this apartment were the required inputs to EnergyPlus. These are detailed in Tables 4.1a and 4.1b, respectively. In Table 4.1b, the details of indoor furnishings are given for the purpose of studying the influences of their presences on indoor RH levels. Table 4.2 lists the physical properties of the materials used in building elements. It was assumed that the apartment was not shaded by other buildings in its close vicinity.

Table 4.1a Details of building elements (1)

Building element	Layer 1 (facing outdoors)	Layer 2	Layer 3 (facing indoors)
External wall	13mm Cement/Sand Plaster	100mm Concrete	13mm Gypsum Plaster
Internal partitions	13mm Gypsum plaster	100mm Concrete	13mm Gypsum Plaster
Flooring	5 mm Vinyl Tiles	25mm Screed	100mm Concrete

Table 4.1b Details of building elements (2)

Building element	Description
Door (internal)	Each consisting of two sheets of 6 mm thick plywood, separated by a 38 mm air cavity.
Window	Each consisting of one sheet of 5 mm thick glass (i.e., single-layer window), a generic interior window shade and an external attached shading concrete slab of 500 mm wide.
Indoor furnishings	Living/dining room: Consisting one piece of wooden furniture made of 18mm thick wood sheet of a surface area of 15 m^2, one sheet of 6 mm thick wool carpet of a surface area of 8 m^2, and one sheet of 3 mm thick cotton of surface area 12 m^2. Master bedroom: Consisting one piece of wooden furniture made of 18mm thick wood sheet of a surface area of 10 m^2, one sheet of 6 mm thick wool carpet of a surface area of 6 m^2, and one sheet of 3 mm thick cotton of surface area 12 m^2.

Table 4.2 Physical properties of building elements

Materials	Specific heat capacity (J/kg·K)	Density (kg/m^3)	Thermal conductivity (W/K·m)
Concrete	653	2400	2.16
Cement/sand plaster	840	1860	0.72
Gypsum plaster	837	1120	0.38
Glass	-	-	0.9
Wood	2093	800	0.16
Wool	1380	145	0.05
Cotton	1300	80	0.06

4.3.3 Operating pattern of DX A/C units

In this apartment, the living/dining room and all the bedrooms were equipped with

window-type room air conditioners (WRACs), but no A/C was provided in the toilet/bathrooms and the kitchen. In order to better understand the space cooling loads characteristics and the application SHRs in both the living/dining room and the master bedroom, simulations were performed under two operating modes of DX A/C units. The first was daytime operating mode (DOM), where the DX A/C unit for the living/dining room operated daily from 7:00 to 21:00. The second was nighttime operating mode (NOM), where the DX A/C unit in the master bedroom operated daily from 22:00 to 6:00 in the following day.

During simulation, a DX A/C unit was set at "continuous fan cycling compressor", which meant that the fan in the DX A/C unit ran continuously while its compressor was on-off cycled to meet the space sensible cooling load.

4.3.4 Internal heat gains

The activity levels of occupants were assumed to be 60 W/(m^2 person) (1.0 met for resting) when they were awake in the living/dining room and 40 W/(m^2 person) (0.7 met for sleeping) when they were asleep in the master bedroom. Detailed internal heat gain from lights, electric appliances, and the activity level of occupants when they were in the living/dining room and in the master bedroom are given in Table 4.3 and 4.4, respectively.

Table 4.3 Hourly internal heat gains from lights, electric appliances and the activity level of the occupants in the living/dining room

	Lighting load* (W/m^2)	Electric appliance load* (W/m^2)	Activity level (W/person)
7:00-12:00	9.865	1.36	108
12:00-13:00	19.73	27.22	108
13:00-16:00	9.865	27.22	108
16:00-17:00	9.865	1.36	108
17:00-20:00	19.73	1.36	108
20:00-21:00	19.73	27.22	108
21:00-22:00	19.73	1.36	108

* From Bojic et al. [2002].

Table 4.4 Hourly internal heat gains from lights, electric appliances and the activity level of the occupants in the master bedroom

	Lighting load* (W/m^2)	Electric appliance load* (W/m^2)	Activity level (W/person)
22:00-23:00	16.33	23.53	72
23:00-24:00	16.33	0	72
0:00-6:30	0	0	72
6:30-7:00	8.165	23.53	72

* From Bojic et al. [2002].

4.3.5 Ventilation requirement

The ventilation rate for the living/dining room and the master bedroom was 7.5 L/s per person as required by ASHRAE Standard 62-2001 [ANSI/ASHRAE 2001] when the rooms were conditioned.

4.3.6 Indoor setpoints of air temperature and RH level, and meteorological data

ASHRAE [ANSI/ASHRAE 2004] recommends a comfort zone based on the 90% acceptance of thermal conditions or 10% Predicted Percentage Dissatisfaction (PPD) (Comfort class B). The operative temperature is around 25°C at a RH of 50% in this comfort zone. Since the operative temperature is approximately the mean value of air temperature and mean radiant temperature (MRT) in most practical cases and indoor air temperature is normally lower than MRT [Lin and Deng 2004], indoor air temperature should be kept below 25°C. In addition, Hong Kong Building Environmental Assessment Method (HK-BEAM) [HK-BEAM 2003] also recommends 50% as the design indoor RH level in residential buildings in Hong Kong. Therefore, 24°C and 50% were selected as the indoor dry-bulb air temperature and RH setpoints required by EnergyPlus.

Using the outdoor cooling design conditions corresponding to annual percentile value of 0.4, the maximum dry-bulb temperature, the maximum wet-bulb temperature and the daily temperature range in the summer design day for Hong Kong were 33.2°C, 28.2°C, and 4.5°C, respectively [Lam and Hui 1995]. EnergyPlus sinusoidally distributed the 4.5°C range over 24 hours in the design day, and outdoor air temperature at any hour in the design day may then be determined.

In addition to the parameters for the summer design day, a weather database has been compiled using the measured hourly data for dry-bulb air temperature, dew point temperature, solar radiation, wind speed and direction, cloud cover, etc., for the year 1989, which was considered as the typical reference year (TRY) for Hong Kong.

4.4 Simulation results

EnergyPlus has been used to perform the computation of space cooling loads in both the living/dining room and the master bedroom in the selected apartment at a time step of 10 minutes in the summer design day and during other air conditioning months from April to October to investigate their cooling loads characteristics under different operating modes, with a particular emphasis on the consequences of the mismatch between the output latent cooling capacity from a DX A/C unit and the space latent cooling load, given that space sensible cooling load is met by on-off cycling the DX A/C unit's compressor.

The total cooling load in a space consists of those from both external sources such as heat gains through building envelope or due to ventilation, and internal sources such as heat gains from occupancy, lights and electric appliances, etc. However, it can be reasonably assumed that the space latent cooling load due to outdoor humid air permeating through building envelope can be neglected, because it only accounts for less than 1% of the total space latent cooling load [Fairey and Keresteciogl u 1985, Harriman III et al. 2001]. For residential buildings located in hot and humid subtropics, Trowbridge et al. [1994] pointed out that the typical difference of indoor RH level between a permeable and an impermeable envelope was almost zero. These suggested that the impact of permeation of a building envelope was negligible, and therefore the contribution to the total space cooling load due to outdoor humid air permeating through building envelope was set to zero in EnergyPlus in this simulation study.

4.4.1 Space cooling loads characteristics in the living/dining room at DOM

Fig. 4.2 shows the profile of the hourly total space cooling load for the living/dining room at DOM in the summer design day. It could be observed that there were three distinct periods of load variation. Period 1 was in the morning between 7:00 and 11:00 when the room was not subjected to solar radiation and the total space cooling load stayed relatively low at between 165 and 180 W/m^2. However, when the DX A/C unit started operation at 7:00, the total space cooling load was 180 W/m^2, which was higher than that in other hours within this period. This relatively large starting cooling load resulted mainly from the heat or water vapor that was stored in or released from building envelope and indoor furnishings overnight. The second period covered the whole afternoon between 11:00 and 17:00 when the room under study was being subjected to solar radiation given its west-facing orientation. The total space cooling load demonstrated a going-up trend over the period, peaking at 17:00. During the third period between 17:00 and 21:00, the total space cooling load showed a decreasing trend from its peak at the start of the period as both the solar radiation was weakening and outdoor air temperature dropping, reaching just over 180 W/m^2 at the end of the period. It could also be seen that within each period, there were fluctuations of smaller amplitudes, due to the turning on-off of domestic lights and electric appliances.

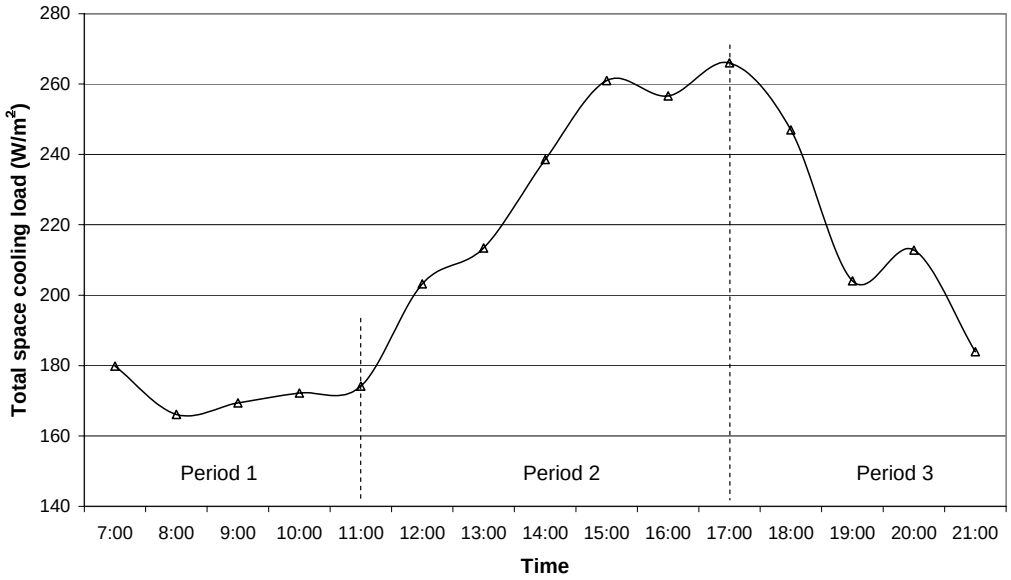

Fig. 4.2 Profile of the hourly total space cooling load for the living/dining room at DOM in the summer design day

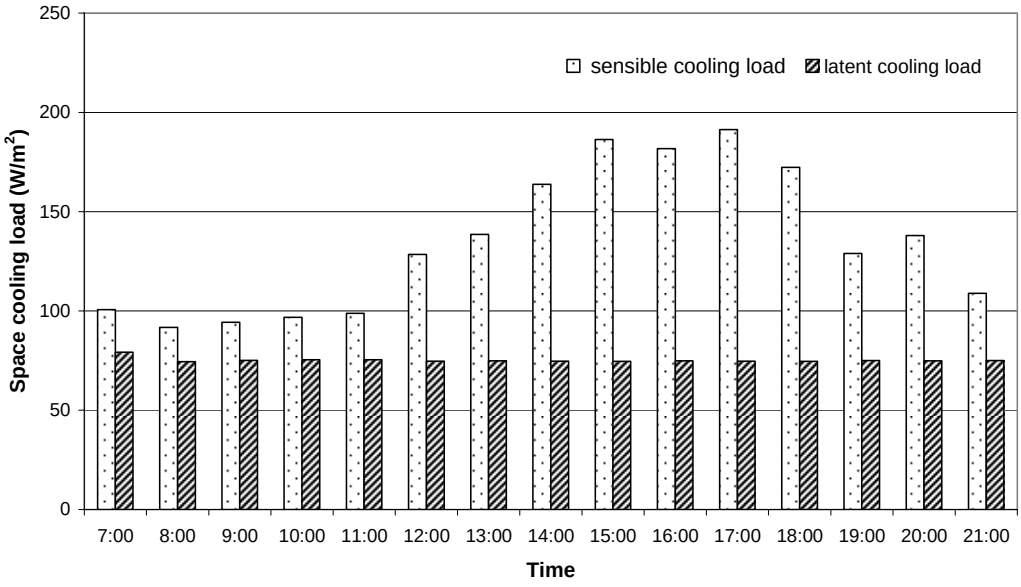

Fig. 4.3 Profiles of hourly space sensible and latent cooling loads for the living/dining room at DOM in the summer design day

Fig. 4.3 shows the profiles of hourly space sensible and latent cooling loads for the living/dining room at DOM in the summer design day. It could be seen that the space latent cooling load stayed constant except that in the first hour due to pull-down, as the space latent cooling load was only influenced by daytime ventilation, which was

dependent on the number of occupants. However, on the other hand, the variation pattern for the space sensible cooling load was similar to that of the total cooling load, peaking also at 17:00. With the availability of both the hourly sensible cooling loads and latent cooling loads, it was possible to calculate the hourly application SHRs at DOM in the summer design day. Over all the operating hours of the DX A/C unit, the hourly application SHRs ranged between 0.55 and 0.72, with an average being 0.63.

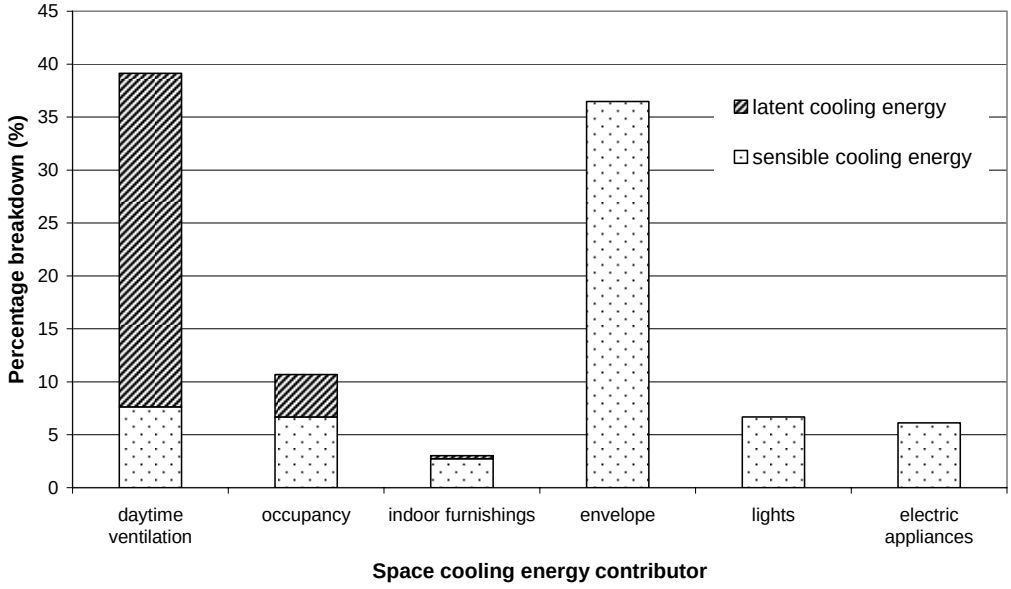

Fig. 4.4 Percentage breakdown of the daily total space cooling energy for the living/dining room at DOM in the summer design day

Fig. 4.4 shows the percentage breakdown of the daily total space cooling energy which was obtained by integrating the hourly total space cooling load over all the operating hours for the living/dining room at DOM in the summer design day. It could be seen that both daytime ventilation and the heat gain through building envelope were responsible for 39% and 36.5% of the daily total cooling energy, respectively. Furthermore, it could also be observed that the latent cooling energy

was dominated by daytime ventilation accounting for 88 % of the total latent cooling energy.

With the availability of space hourly cooling load profiles and the hourly application SHRs for the living/dining room in the summer design day, it was possible to use EnergyPlus to investigate both the indoor air temperature and RH level in the room should it be served by DX A/C units having on-off cycling compressors with fixed total output cooling capacities but different equipment SHRs to see how a DX A/C unit with different output latent cooling capacities would affect the indoor air temperature and humidity control.

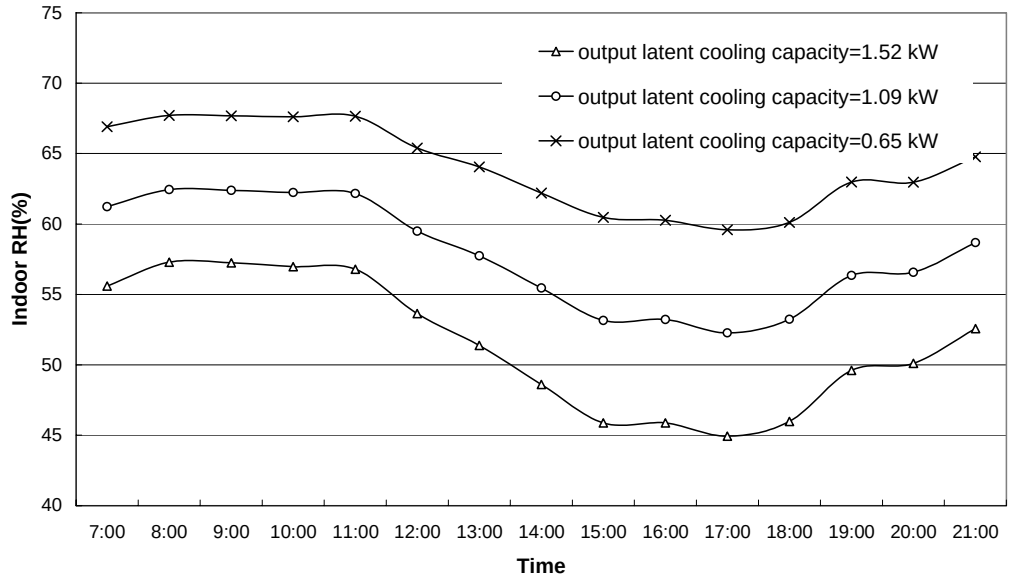

Fig. 4.5 Indoor RH levels at different DX A/C unit's output latent cooling capacities in the living/dining room at DOM in the summer design day

It was assumed that three different DX A/C units having the same total output cooling capacity of 4.35 kW, but with different equipment SHRs of 0.65, 0.75 and 0.85, respectively, were used in the living/dining room at DOM in the summer

design day. Their corresponding output latent cooling capacities were 1.52 kW, 1.09 kW and 0.65 kW, respectively. It should be pointed out that the total output cooling capacity and equipment SHR were necessary inputs for EnergyPlus, and their numeric values would stay unchanged through the simulation. The simulation results showed that when using DX A/C units having different output latent cooling capacities, although indoor air dry-bulb temperature could be maintained at its setpoint of 24ºC by matching the output sensible cooling capacity from the DX A/C unit and the space sensible cooling load through on-off cycling compressor, there were noticeable differences in the resulted indoor RH levels. Fig. 4.5 shows the simulated resulted indoor air RH levels at the three different output latent cooling capacities in the living/dining room following the hourly cooling load profile shown in Fig. 4.2 at DOM in the summer design day. It was understood that air conditioners with different equipment SHRs would have the different ability to handle space latent cooling load. The larger the output latent cooling capacity from a DX A/C unit, the larger its ability to deal with space latent cooling load. As seen from Fig. 4.5, when a DX A/C unit having its output latent cooling capacity of 1.52 kW was used to deal with the space cooling loads of the living/dining room as specified in Fig. 4.3, indoor RH setpoint of 50% could be acceptably maintained at a range between 45% and 57%. However, when a DX A/C unit having its output latent cooling capacity of 1.09 kW was used, indoor RH setpoint of 50% could be hardly maintained, with the actual resulted indoor RH levels ranging between 52% and 62%. When a DX A/C unit having an even poorer latent cooling removal ability (i.e., having a lower output latent cooling capacity of 0.65 kW) was used, the resulted indoor RH levels deviated significantly from the setpoint of 50%, with the lowest RH level being close to 60%. It can also be observed from Fig. 4.5 that under the three different output latent

cooling capacities from DX A/C units, indoor RH levels in the morning hours were higher than those in the afternoon hours, due mainly to the on-off cycling of compressor to meet space sensible cooling load. The higher the space sensible cooling load, the longer hours the compressor was operated. When the compressor was operated for longer hours, more output cooling capacity would be available for both sensible and latent loads, leading to a lower indoor RH level.

4.4.2 Space cooling loads characteristics in the master bedroom at NOM

The space cooling loads characteristics in the master bedroom at NOM were significantly different from that in the living/dining room at DOM. The analysis on the characteristics of cooling load in a bedroom served by a DX A/C unit has been previously investigated in a related study [Lin and Deng 2004]. However, this previous related study mainly focused on the characteristics of space sensible cooling load.

The profile of the hourly total space cooling load for the master bedroom at NOM in the summer design day is shown in Fig. 4.6. Such a profile was very much similar to that investigated and reported in the previous related study where nonetheless a different bedroom of smaller size and single occupancy was used [Lin and Deng 2004]. Fig. 4.7 shows the profile of both hourly space sensible and latent cooling load for the master bedroom at NOM in the summer design day. It could be seen that while the sensible cooling load varied significantly over the operating period with its peak occurring at the beginning of the NOM period, space latent cooling load stayed

relatively constant except for the first hour due to pull-down load at the beginning of NOM. On the other hand, at NOM, the hourly application SHRs for the bedroom ranged between 0.6 and 0.85, with an averaged application SHR being 0.69.

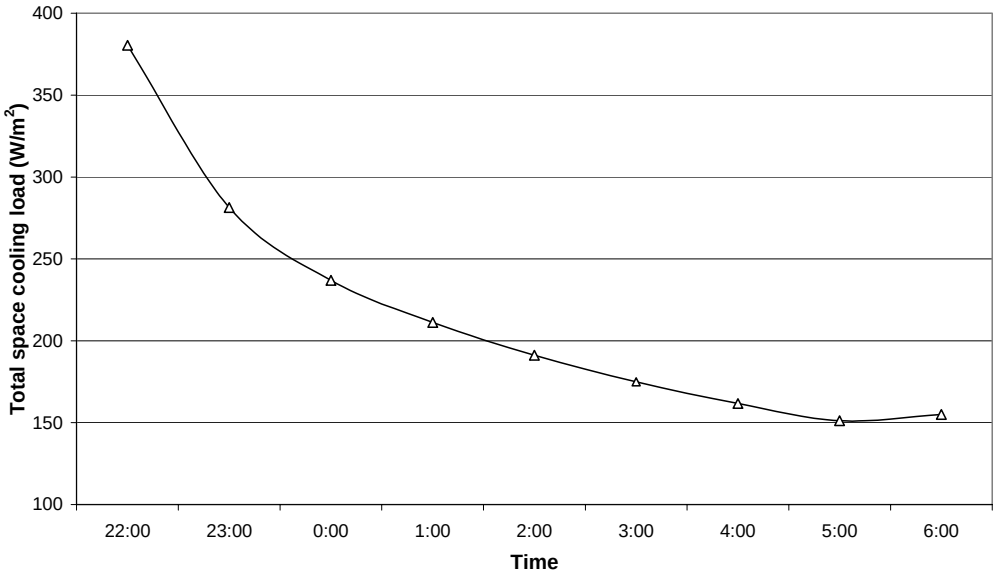

Fig. 4.6 Profile of the hourly total space cooling load for the master bedroom at NOM in the summer design day

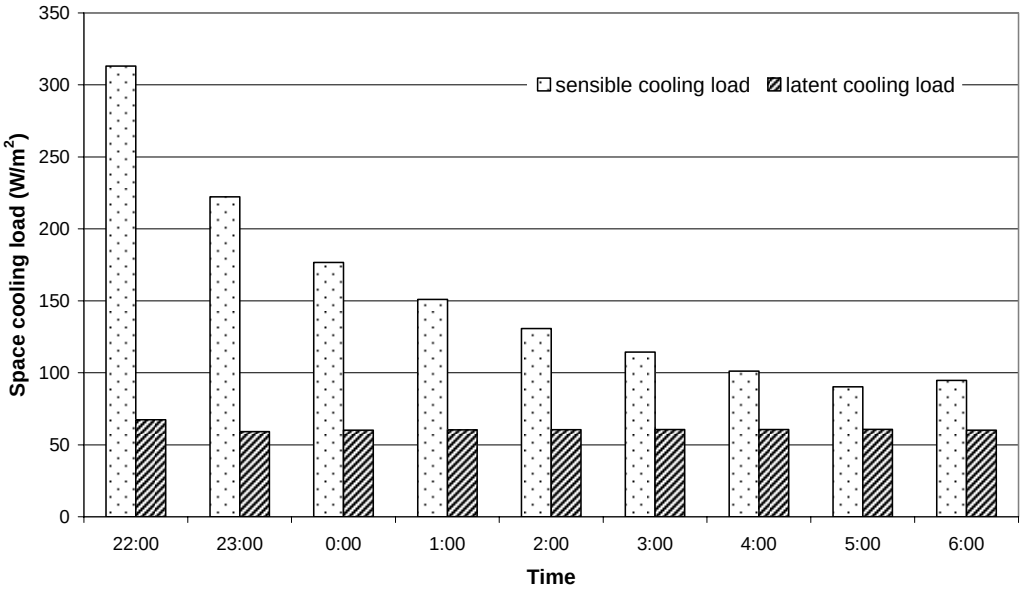

Fig. 4.7 Profile of the hourly space sensible and latent cooling loads for the master bedroom at NOM in the summer design day

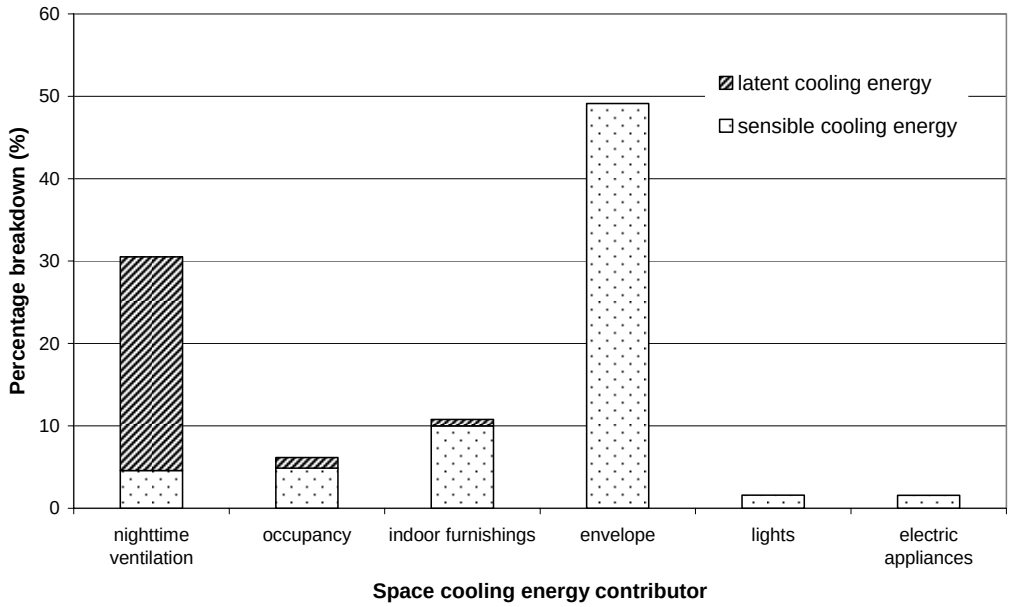

Fig. 4.8 Percentage breakdown of the daily total space cooling energy for the master bedroom at NOM in the summer design day

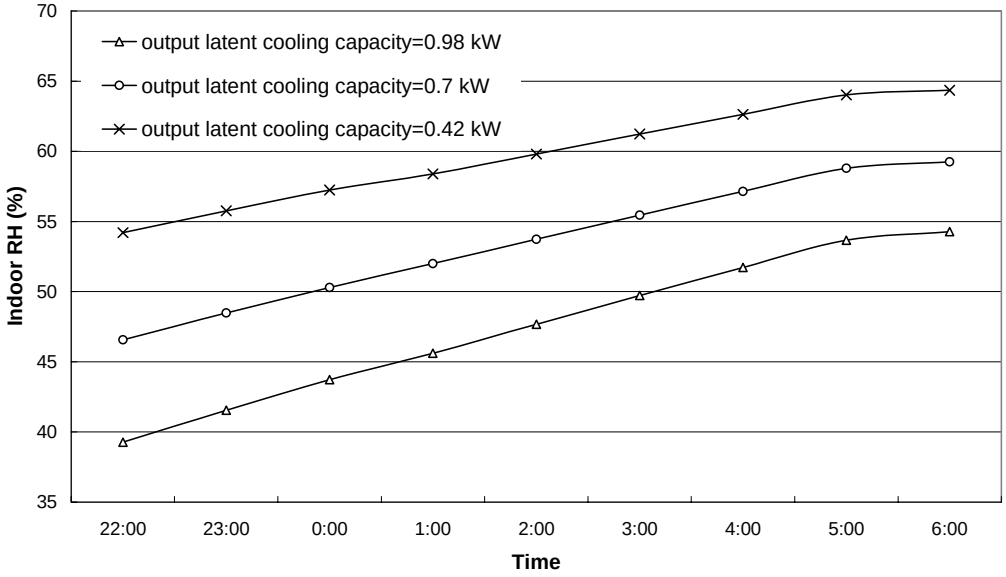

Fig. 4.9 Indoor RH levels at different DX A/C unit's output latent cooling capacities in the master bedroom at NOM in the summer design day

Fig. 4.8 shows percentage breakdown of the daily total space cooling energy for the master bedroom at NOM in the summer design day. Unlike the cooling load characteristics for the living/dining room at DOM, at NOM, the heat gain through

building envelope was responsible for nearly 50% of the total space cooling energy. On the other hand, nighttime ventilation was the second largest space cooling energy contributor, accounting for over 30% of the total. The remaining 20% of the total space cooling energy was due to the heat stored in indoor furnishings, occupancy, lights and electric appliances.

Similar to the situation for the living/dining room at DOM, EnergyPlus was also used to investigate both the indoor air temperature and RH level in the bedroom if it was served by DX A/C units having the same total output cooling capacity of 2.8 kW, but with different equipment SHRs of 0.65, 0.75 and 0.85, respectively. The corresponding output latent cooling capacities were 0.98 kW, 0.7 kW and 0.42 kW, respectively. Fig. 4.9 shows the indoor air RH levels at three different output latent cooling capacities in the master bedroom at NOM in the summer design day. While indoor air dry-bulb temperature was all maintained at 24ºC within the operating hours by on-off cycling compressor, there were also noticeable differences in the resulted indoor RH levels. The averaged indoor RH levels in the master bedroom were 60%, 54% and 48%, with their respective RH variation ranges being 54 to 64%, 47 to 59% and 39 to 54%, respectively, when the DX A/C units having their respective output latent cooling capacities of 0.42 kW, 0.7 kW and 0.98 kW were used to deal with the space cooling loads as specified in Fig. 4.7. The larger the difference between the output latent cooling capacity and the space latent cooling load, the greater the deviation of resulted indoor RH from its setpoint. On the other hand, it could be observed that with on-off cycling compressor for the DX A/C unit to maintain the indoor air dry-bulb temperature setpoint, the resulted indoor RH levels demonstrated an increasing trend over the operating hours at NOM. This was

considered due to the fact that, as illustrated in Fig. 4.7, space sensible cooling load significantly decreased over the operating time.

4.4.3 The application SHRs during part load operation

As discussed in Section 4.4.2, in the summer design day, the averaged application SHR for living/dining room at DOM and master bedroom at NOM ranged between 0.63 and 0.69, respectively. However, in the subtropical residences, air conditioning would normally be required from April to October [Lam 1993], and it was considered necessary to investigate the indoor environmental control under part load operation.

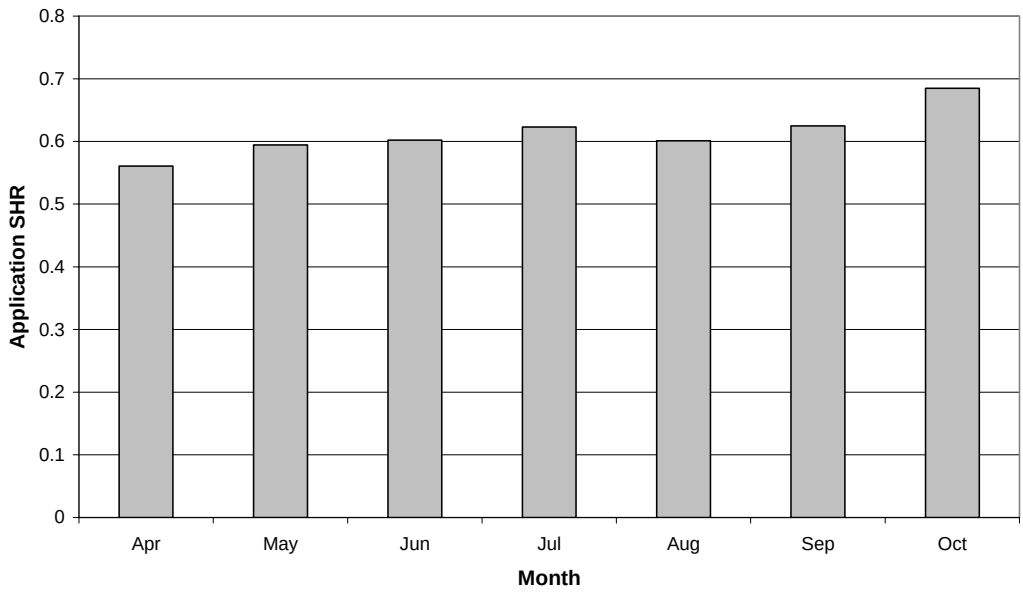

Fig. 4.10 Averaged monthly application SHRs during DX A/C units' operating months for the living/dining room at DOM

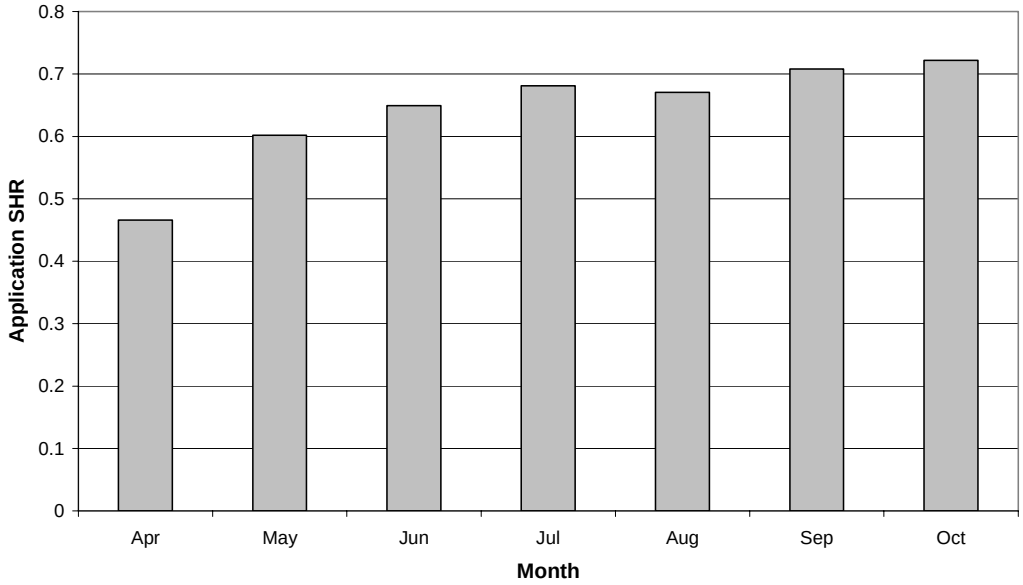

Fig. 4.11 Averaged monthly application SHRs during DX A/C units' operating months for the master bedroom at NOM

Fig. 4.10 and Fig. 4.11 show the averaged monthly application SHRs from April to October for the living/dining room at DOM and the master bedroom at NOM, respectively. From Fig. 4.10, it could be seen that for the living/dining room at DOM, the averaged monthly application SHRs for the months between May and September stayed around 0.6. In April which was normally a relatively wetter month in the subtropical Hong Kong, the average application SHR for the room was the lowest at 0.56. On the other hand, in October which was a relatively drier month, the average application SHR for the room was the highest at 0.68. Therefore, when an on-off controlled DX A/C unit having both a fixed total output cooling capacity and a fixed equipment SHR worked well in October, it would have a poor control of indoor RH in April. For the master bedroom at NOM, similar indoor environmental control problem may also occur.

4.4.4 The effects of indoor furnishings on indoor RH level

The indoor furnishings include internal furniture of wood nature, carpet, clothes, curtain, sofa, and the bedding of textile nature, etc. In this simulation study, the contribution to the total cooling load due to the presence of indoor furnishings and its effects on indoor RH level at DOM and NOM have been investigated.

All indoor furnishings were modeled by using three types of typical indoor materials, wood furniture, wool carpet and cotton, as listed in Table 4.1b. In addition, in order to evaluate the influence of indoor furnishings alone on both space cooling loads and indoor RH levels, it was assumed in this part of study that there was a vapor barrier covering the entire interior wall surface in the selected apartment and the mass transfer coefficients for the moisture movement between wall surfaces and the indoor air was set to zero, so that the moisture absorption and desorption by internal envelope surfaces could be ignored.

As illustrated in Fig. 4.4 and Fig. 4.8, indoor furnishings would be responsible for 3.0% of the total space cooling energy for the living/dining room at DOM, and 10.8% for the master bedroom at NOM, respectively, due to heat storage and moisture absorption and desorption. Their contributions to the total space latent cooling energy were 0.8% at DOM and 2.7% at NOM, respectively. Fig. 4.12 and Fig. 4.13 show the indoor RH levels with and without the presence of indoor furnishings, when DX A/C units having a total output cooling capacity of 4.35 kW and 2.8 kW with their equipment SHR of 0.75 (output latent cooling capacities were 1.09 kW and 0.7 kW, respectively) were used in the summer design day at DOM in

the living/dining room and at NOM in the master bedroom, respectively. It could be seen from both diagrams that with the presence of indoor furnishings, the resulted indoor RH level was slightly lower than that without. The averaged decrease in RH level was 0.6% at DOM and 1.8% at NOM, respectively. This was due to the fact that these indoor furnishings were able to store a certain amount of moisture, as determined by their physical properties. The differences between indoor RH levels with and without the presence of indoor furnishings were relatively large during the earlier hours of, but gradually diminished towards the end of the operating period, at both DOM and NOM, when a dynamic equilibrium of moisture transfer between the indoor air and these materials was established. Nonetheless, the impact of indoor furnishings on indoor RH level was negligibly small at less than 2% RH, especially at the DOM condition, and could therefore be neglected for practical calculations in residential buildings.

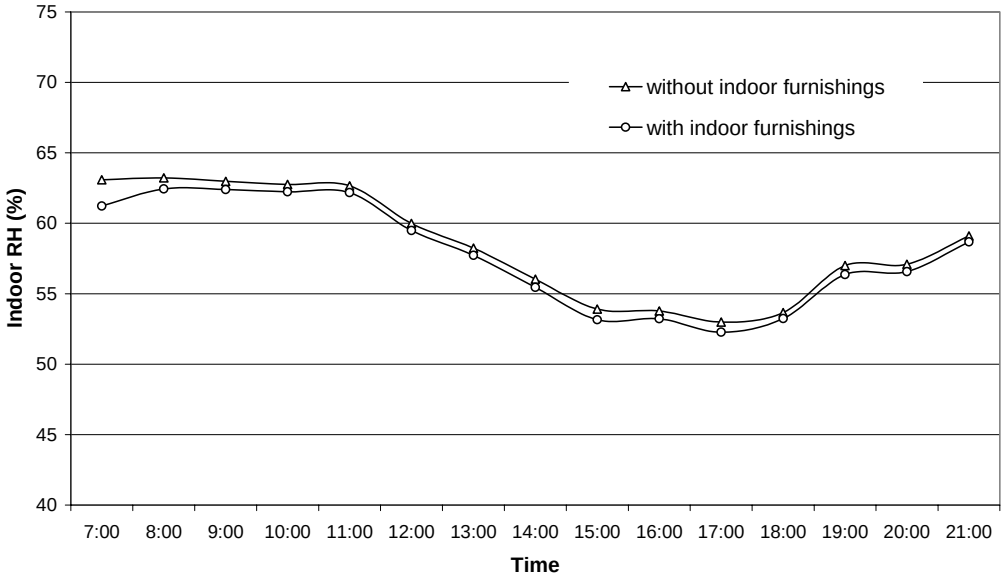

Fig. 4.12 Indoor RH levels with and without the presence of indoor furnishings in the living/dining room served by a DX A/C unit at DOM in the summer design day

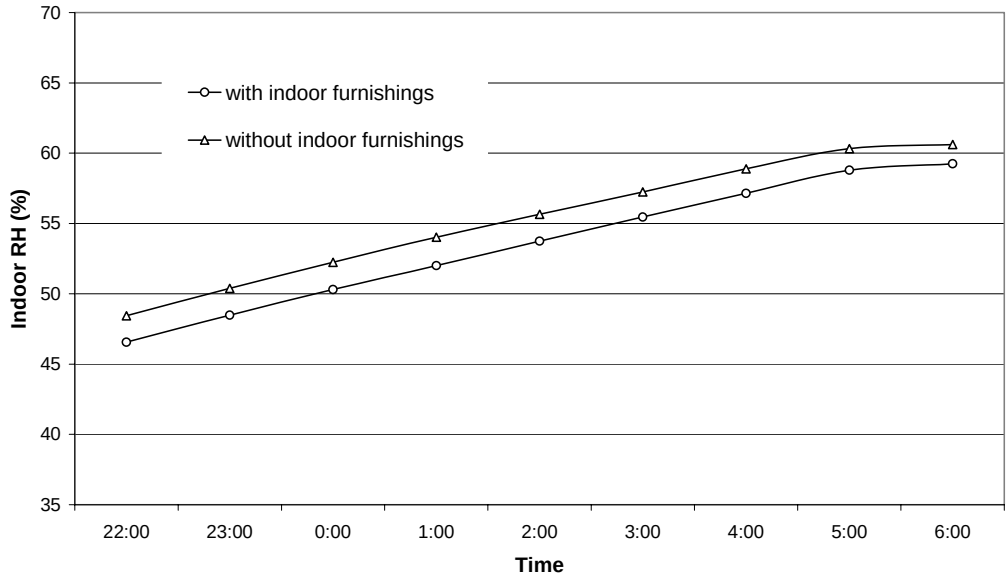

Fig. 4.13 Indoor RH levels with and without the presence of indoor furnishings in the master bedroom served by a DX A/C unit at NOM in the summer design day

4.5 Discussions

The simulation results showed that residential space latent cooling load was basically due to ventilation and occupancy, and therefore stayed relatively steady at both DOM and NOM in the summer design day. However, at DOM, residential space sensible cooling load was significantly affected by solar heat gains and indoor-outdoor air temperature difference; both varying significantly over the time. This resulted in a significant variation of space sensible cooling load at DOM. On the other hand, at NOM, the space sensible cooling load was affected by both the heat stored in building envelope and accumulated over the non-air conditioning period, and the indoor-outdoor air temperature difference. Significant variation of space sensible cooling load was also resulted in at NOM. Consequently, in the summer design day the resulted hourly application SHRs were also varied, at the range between 0.55 and 0.72 with a mean of 0.63 at DOM, and between 0.6 and 0.85 with

a mean of 0.69 at NOM, respectively.

The results of the simulation study also quantitatively indicated that the consequences of the mismatch between the output latent cooling capacity from a DX A/C unit and the space latent cooling load: while indoor air dry-bulb temperature setpoint may be maintained by on-off cycling the DX A/C unit's compressor, there would be deviations in indoor RH level of varied magnitudes, depending on the magnitudes of mismatch, as reported in Section 4.4.1. This demonstrated that for residential buildings located in the subtropics, given their space cooling loads characteristics, i.e., smaller application SHRs due to hot and humid climates, with on-off compressor cycling, if there is a mismatch between the output latent cooling capacity from a DX A/C unit and the space latent cooling load, although indoor air dry-bulb temperature may be controlled, indoor RH may well be out of control.

Furthermore, as seen in both Fig. 4.10 and Fig. 4.11, the monthly averaged application SHRs ranged between 0.57 and 0.68 for the living/dining room at DOM and between 0.47 and 0.72 for the master bedroom at NOM. For both operating modes, the indoor humidity control would become much more deteriorated in April when the averaged monthly application SHRs were 0.57 for the living/dining room and 0.47 for the master bedroom, respectively, noting that April was normally a relatively wetter month in the subtropical Hong Kong, if a DX A/C worked reasonably well in drier months such as October.

Although it was previously pointed out by others that the presence of indoor furnishings would act as indoor moisture capacitors to influence indoor RH level, no

detailed quantitative estimations were given. This simulation study has however given a quantitative assessment of the influences on indoor RH level due to the presence of indoor furnishings, which was negligibly small at less than 2% RH and may therefore be neglected for practical calculation.

4.6 Conclusions

The space cooling loads characteristics in the living/dining room at DOM and in the master bedroom at NOM using the weather data and typical high-rise residential layouts in the subtropical Hong Kong, and the problem of indoor humidity control due to the mismatch between the output latent cooling capacity from a DX A/C unit and the space latent cooling load have been investigated using EnergyPlus.

Application SHRs for residential buildings located in the hot and humid subtropics normally ranged between 0.6 and 0.7. On the other hand, the problem of the mismatch between the output latent cooling capacity from a DX A/C unit and the space latent cooling load would lead to indoor RH levels deviating from its setpoint. Furthermore, the presence of indoor furnishings would not significantly affect the indoor RH level.

Although the simulation study was based on the weather conditions and the typical arrangements of high-rise residential blocks in Hong Kong, it is expected the results obtained can be indicative for applications to other tropical and subtropical regions.

Chapter 5

The Experimental DX A/C Station

5.1 Introduction

An experimental DX A/C station is available in the Heating, Ventilation and Air Conditioning (HVAC) Laboratory of Department of BSE in The Hong Kong Polytechnic University. The primary purpose of having the experimental station is to facilitate carrying out the research work related to DX A/C technology.

The experimental station resembles a typical DX A/C unit. Advanced technologies such as variable-speed compressor and supply fan, and electronic expansion valve (EEV), as well as a computerized data measuring, logging and control system, have been incorporated into the experimental station.

This Chapter presents firstly detailed descriptions of the experimental station and its major components. This is followed by describing the computerized instrumentation and a data acquisition system (DAS). Finally, the computer supervisory program used to operate and control the experimental station is detailed.

5.2 Detailed descriptions of the experimental station and its major components

The experimental DX A/C station is mainly composed of two parts, i.e., a DX refrigeration plant (refrigerant side) and an air-distribution sub-system (air side). The

schematic diagrams of both the complete experimental station and the DX refrigeration plant are shown in Fig. 5.1 and Fig. 5.2, respectively.

5.2.1 The DX refrigeration plant

As shown in Fig. 5.2, the major components in the DX refrigeration plant include a variable-speed rotor compressor, an EEV, a high-efficiency tube-louver-finned DX evaporator and an air-cooled tube-plate-finned condenser. The evaporator is placed inside the supply air duct to work as a DX air cooling coil. The design air face velocity for the DX cooling coil is 2.5 m/s. The nominal output cooling capacity from the DX refrigeration plant is 9.9 kW (~2.8 RT). The actual output cooling capacity from the DX refrigeration plant can however be modulated from 15% to 110% of the nominal capacity. Other details of the compressor can be found in Table 5.1. The compressor is driven by a variable-speed drive (VSD). The EEV includes a throttling needle valve, a step motor and a pulse generator. It is used to maintain the degree of refrigerant superheat at the evaporator exit. The working fluid of the plant is refrigerant R22, with a total charge of 5.3 kg.

In addition, two three-way connectors and two flexible joints, whose locations are indicated in Fig. 5.2, are reserved in the refrigerant pipeline for the purpose of possibly modifying the station for other related studies. A condenser air duct, which is not normally required in real applications, is used to duct the condenser cooling air carrying the rejected heat from the condenser away to outside Laboratory. The condenser fan, housed inside the condenser air duct, can also be variable-speed

operated. An electrical heater controlled by Solid State Relay (SSR) is used to adjust the temperature of the cooling air entering the condenser for various experimental purposes. A refrigerant mass flow meter is installed upstream of the EEV. Other necessary accessories and control devices, such as an oil separator, a refrigerant receiver, a sight glass and safety devices, are provided in the refrigeration plant to ensure its normal and safe operation.

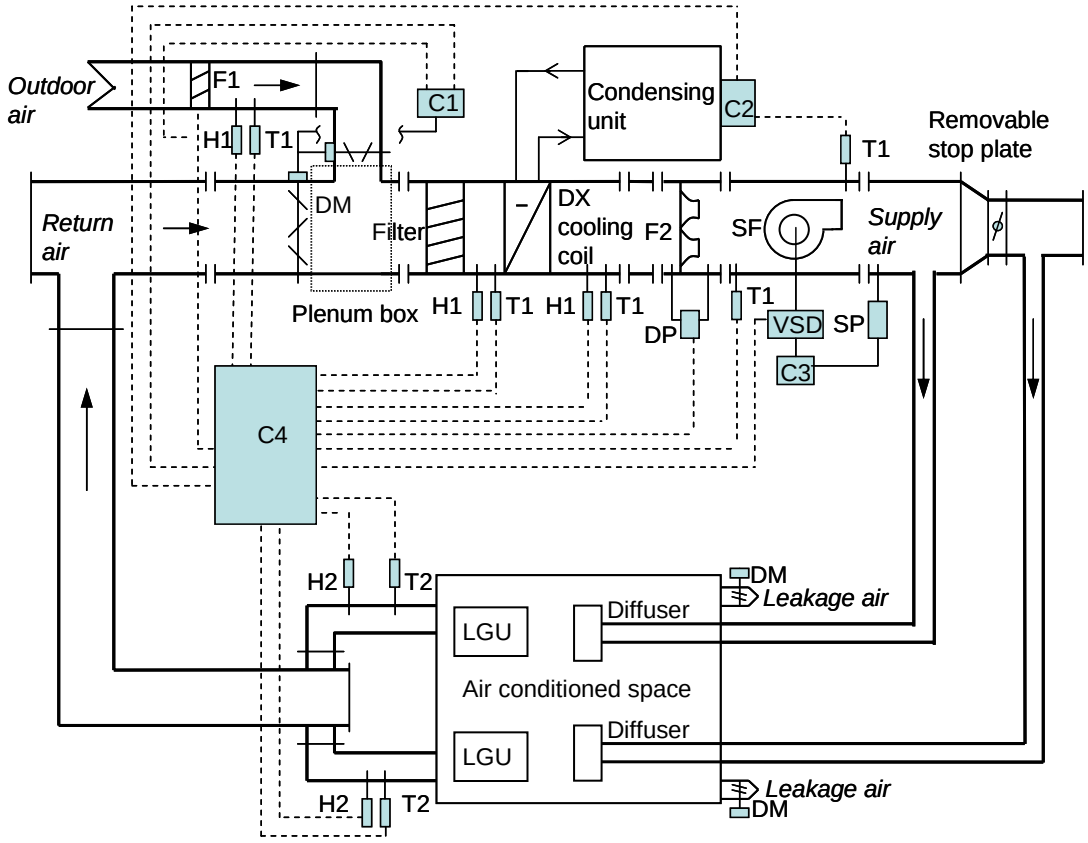

C1-controller of outdoor/return air damper	C2-controller of condensing unit	C3-controller of supply fan
C4-data acquisition and control unit	DM-damper	DP-differential pressure transducer
F1-hot film anemometer	F2-supply airflow rate measuring apparatus	H1-air wet-bulb temperature sensor
H2-air humidity meter	LGU-load generating unit	SF-supply fan with motor outside duct
SP-static pressure measuring device	T1,T2-air dry-bulb temperature sensor	VSD-variable speed drives

Fig. 5.1 The schematic diagram of the complete experimental DX A/C station

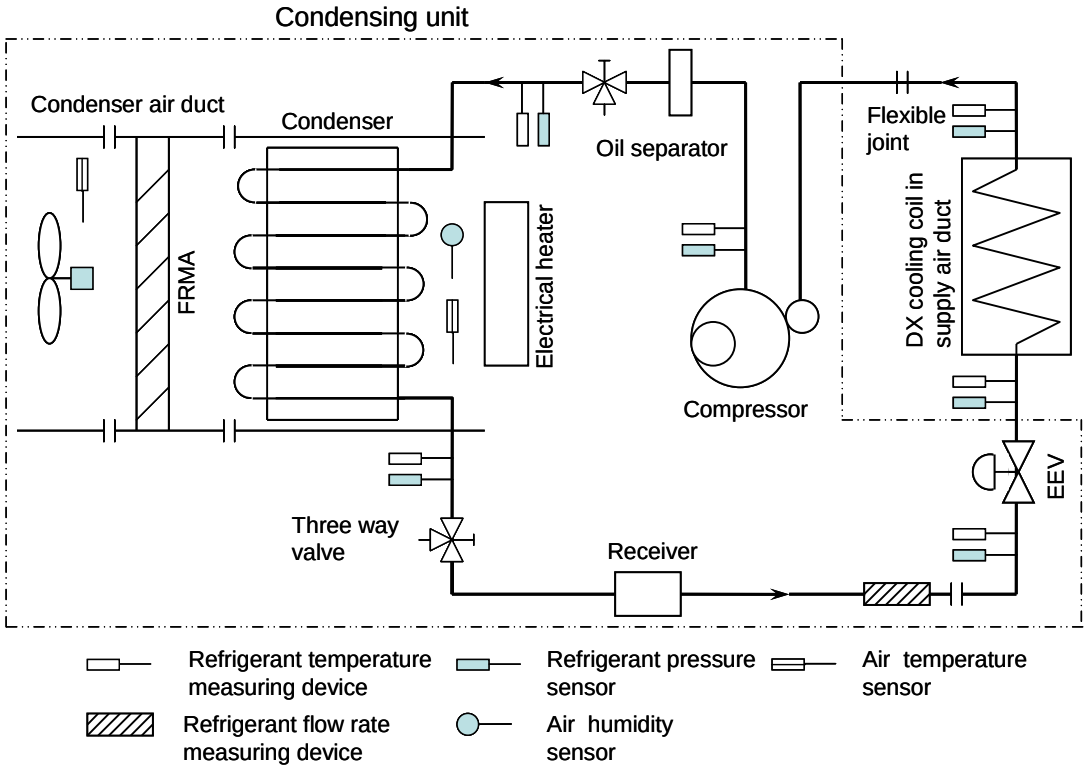

Fig. 5.2 The schematic diagram of the DX refrigeration plant

Table 5.1 Details of the variable-speed compressor

Model	HITACHI THS20MC6-Y
Allowable Frequency range	15~110 Hz
Rated Capacity	9900 W at 90 Hz
Displacement	3.04 ml/rev

5.2.2 Air-distribution sub-system

The air-distribution sub-system in the experimental DX A/C station is schematically shown in Fig. 5.1. It includes an air-distribution ductwork with return and outdoor air dampers, a variable-speed centrifugal supply fan with its motor placed outside the duct, and a conditioned space. The supply fan is driven by a VSD. The details of the supply fan are given in Table 5.2.

The size of the air conditioned space is 7.6 m (L)×3.8 m (W)×2.8 m (H). Inside the space, there are sensible heat and moisture load generating units (LGU). The units are intended to simulate the cooling load in the conditioned space. Its heat and moisture generation rate as regulated by SSR may be varied manually or automatically with a pre-set pattern through operator's programming. In addition, leakage outlets with residual-pressure relief dampers are installed in the space so that a positive internal pressure of not more than 20 Pa can be maintained at all time. In the air-distribution sub-system of the experimental DX A/C station, return air from the space mixes with outdoor air in a plenum box upstream of an air filter. The mixed air is filtrated and then cooled and dehumidified by the DX cooling coil. Afterwards, the cooled and dehumidified air passes through the supply fan, to be supplied to the space to deal with the cooling load from LGUs.

Table 5.2 Details of the variable-speed supply fan

Model	KRUGER BSB 31
Nominal flow rate	1700 m^3/h (0.47 m^3/s)
Total pressure head	1100 Pa

5.3 Computerized instrumentation and data acquisition system (DAS)

The computerized instrumentation for the experimental DX A/C station is also shown in both Fig. 5.1 and Fig. 5.2. The station is fully instrumented for measuring all of its operating parameters, which may be classified into three types, i.e., temperature, pressure and flow rate. Since all measurements are computerized, all sensors and measuring devices are able to output direct current (DC) signal of 4-20 *mA* or 1-5 *V*, which are transferred to a DAS for logging and recording.

5.3.1 Sensors/measuring devices for temperatures, pressures and flow rates

Eleven sets of air temperature and humidity measuring sensors are located in the air-distribution sub-system of the experimental station. Air RH is indirectly measured via measuring air dry-bulb and wet-bulb temperatures. On the other hand, as shown in Fig. 5.2, there are five temperature sensors for measuring refrigerant temperatures in the DX refrigeration plant. To ensure fast response of the sensors for facilitating the study of transient behaviors of the DX refrigeration plant, these temperature sensors are inserted into the refrigerant circuit, and are thus in direct contact with the refrigerant. The temperature sensors for air and refrigerant are of platinum Resistance Temperature Device (RTDs) type, using three-wire Wheatstone bridge connection and with a pre-calibrated accuracy of ±0.1℃. The specifications of the RTDs are: CHINO Pt100/0℃-3W, Class A, SUSΦ3.2-150L.

Refrigerant pressures in various locations in the DX refrigeration plant are measured using pressure transmitters with an accuracy of ±0.13% of full scale reading (Model: SETRA C206). The atmospheric pressure is measured with a barometer having an accuracy of ±0.05kPa (Model: VAISALA PTB-101B).

There are two sets of air flow rate measuring apparatus (FRMA) in the air-distribution system. One set of FRMA is used to measure the total supply airflow rate, i.e., the airflow rate passing through the DX cooling coil. The other is for measuring the airflow rate passing through the condenser. The two sets of FRMA are constructed in accordance with ANSI/ASHRAE Standards 41.2, consisting of nozzles of different sizes, diffusion baffles and a manometer with a measuring

accuracy of ±0.1% of full scale reading (Model: ROSEMOUNT 3051). The number of nozzles in operation can be altered automatically.

On the other hand, outdoor airflow rate is measured using a hot-film anemometer with a reported accuracy of ±0.1 m/s (Model: E+E 70-VT62B5). The anemometer is installed 500 mm, which is longer than the recommended length of entrance of 200 mm by its manufacturer, downstream of the outdoor air inlet, to ensure the measuring accuracy of outdoor airflow rate. The power consumption of the variable-speed compressor is measured using a pulse-width-modulation (PWM) digital power meter with a reported uncertainty of ±2% of reading (Model: EVERFINE PF9833). The refrigerant mass flow rate passing through the EEV is measured by a Coriolis mass flow meter with a reported accuracy of ±0.25% of full scale reading (Model: KROHNE MFM1081K+F). The supply air static pressure is measured using a manometer with a reported accuracy of ±0.1% of full scale reading (Model: ROSEMOUNT 3051).

In order to ensure the measuring accuracy for the temperatures of the air flowing inside air duct, standardized air sampling devices recommended by the ISO Standard 5151 are used in the experimental station.

5.3.2 The DAS

A data acquisition unit (Model: AGLIENT 34970A/34902A) is used in this experimental station. It provides up to 48 channels for monitoring various types of

system parameters. The DC signal from various measuring devices/sensors can be scaled into their real physical values of the measured parameters using a logging & control (L&C) supervisory program which is developed using LabVIEW programming platform. The minimum data sampling interval is one second. It should be noted that the flow rates of both supply air and condenser cooling air are calculated using the air static pressure drops across their respective nozzles. The outdoor airflow rate is evaluated by multiplying the measured air velocity with the sectional area of the outdoor air duct. The output cooling capacity from the DX A/C unit is calculated based on the enthalpy-difference of air across the DX cooling coil.

5.4 LabVIEW logging & control (L&C) supervisory program

A computer supervisory program which is capable of performing simultaneously data-logging and parameter-controlling is necessary. It needs to communicate with not only the data acquisition unit, but also conventional standalone digital programmable PI controllers which are to be detailed in Section 5.5. A commercially available programming package, LabVIEW, provides a powerful programming and graphical platform for data acquisition and analysis, as well as for control application.

A data L&C supervisory program has been developed using LabVIEW, with all measured parameters real-time monitored, curve-data displayed, recorded and processed. The program can also perform the retrieval, query and trend-log graphing of historical data for measured parameters. The program runs on a personal computer

(PC).

On the other hand, the LabVIEW-based L&C supervisory program enables the PC to act as a central supervisory control unit for different low-level control loops, which will be discussed in Section 5.5, in the experimental station. The PC can therefore not only modify the control settings of those standalone microprocessor-based PI controllers, but also deactivate any of these controllers. The LabVIEW-based L&C supervisory program also provides an independent self-programming module (SPM) by which new control algorithms may be easily implemented through programming. A SPM performs in a similar manner to a central processing unit of a physical digital controller. The variables available from all measured parameters can be input to, and processed according to a specified control algorithm in a SPM to produce required control outputs. Once a SPM is initiated to replace a given standalone controller, the controller must be deactivated, but works as a digital-analog converter to receive the control output from the SPM. An analogue control signal is then produced by the controller to initiate the related actuator for necessary control action.

5.5 Conventional control loops in the experimental station

Totally, there are ten conventional control loops in this experimental station. These loops either are activated using the LabVIEW-based supervisory program or use PI controllers which are of digital programmable type with RS-485 communication port (Model: YOKOGAWA UT350-1). The controller’s proportional band, integral times, and setpoints are all allowed to be reset.

Among the ten control loops, four are for varying heat and moisture generation rate of the LGUs located in the space. Electrical power input to the LGU is regulated using SSR according to the instructions from their respective control loops, to simulate the space cooling load. In addition, there is one control loop for maintaining the condenser inlet air temperature at its setting through regulating electrical power input by SSR.

The remaining five conventional PI control loops are as follows: supply air temperature by regulating the compressor speed; supply air static pressure by regulating the supply fan speed; condensing pressure by regulating the condenser fan speed; refrigerant superheat by regulating EEV opening; outdoor airflow rate by jointly regulating both outdoor and return air dampers' openings. These five control loops can be activated by using either the conventional physical digital PI controller available in the experimental station or a SPM specifically for any new control algorithm to be developed.

The control of supply air temperature is used as an example for illustration. When the conventional PI controller is enabled, the controller measures the supply air temperature using the temperature sensor and then compares the measured with its setpoint. A deviation is processed in the controller according to a pre-set PI control algorithm and an analogue control signal of 4~20 *mA* is produced and sent by the PI controller to the VSD for compressor motor to regulate its speed. On the other hand, such a conventional PI controller may be replaced by a SPM to be specifically developed based on a new control algorithm for compressor speed control. The SPM may take the advantages of using simultaneously multiple input variables, e.g.,

supply air temperature and its setpoint, evaporating and condensing pressure, degree of refrigerant superheat, etc. Control outputs can then be created using the SPM according to the new control strategy and algorithm, and communicated to the physical digital PI controller which now works only as a digital-analog converter. An analog control signal is then generated and sent to the VSD of compressor for its speed control.

5.6 Conclusion

An experimental DX A/C station is available for carrying out the proposed project. The station consists of two parts: a DX refrigeration plant having a variable-speed compressor and EEV; and an air-distribution sub-system.

The experimental DX A/C station has been fully instrumented using high quality sensors/measuring devices. Totally forty-three operating parameters in the station can be measured and monitored simultaneously and ten conventional PI feedback control loops are provided. Two sets of airflow rate measuring apparatus are constructed in accordance with ANSI/ASHRAE 41.2. Sensors for measuring refrigerant properties are in direct contact with refrigerant, and a Corioli mass flow meter is used for measuring the refstationerant flow rate passing through the EEV.

A L&C supervisory program has been developed specifically for this experimental station using LabVIEW programming platform. All parameters can be real-time measured, monitored, curve-data displayed, recorded and processed by the L&C

program. The LabVIEW-based L&C program provides an independent SPM by which any new control algorithms to be developed may be implemented.

The availability of such an experimental DX A/C station is expected to be extremely useful in investigating both the inherent operational characteristics of a DX A/C unit, and indoor thermal comfort characteristics under the control of a DX A/C unit having variable-speed compressor and supply fan. On the other hand, a novel DDC-based capacity controller could be developed through simultaneously varying compressor and supply fan speeds to achieve simultaneous indoor temperature and humidity control, and the controllability tests for the capacity controller carried out using the experimental station.

Chapter 6

Experimental Study I: Inherent Operational Characteristics of a DX A/C Unit with Variable-speed Compressor and Supply Fan at Fixed Inlet Air Temperature and Humidity

6.1 Introduction

In buildings, appropriately controlling indoor thermal environment is important since this directly affects building occupants' thermal comfort, IAQ and the operating efficiency of building A/C installations. It has been pointed out in Chapter 4 that for residential buildings located in hot and humid subtropical regions, since DX A/C units normally rely on on-off cycling compressors to maintain only indoor air dry-bulb temperature, the mismatch between the output latent cooling capacity from a DX A/C unit and the space latent cooling load would lead to indoor RH level deviating from its setpoint.

Based on the previous studies by Andrade et al. [2002] and Krakow et al. [1995], it can be seen that for a DX A/C unit, varying its compressor speed and supply fan speed can effectively help improve environmental control. With the wider application of variable-speed drive (VSD) technology, it becomes possible for all DX A/C units to have the speeds of their compressors and supply fans varied, that their total output cooling capacities and equipment SHRs can be varied to match varying space sensible and latent cooling loads for better indoor environment control. On the other hand, varying the speeds of both compressor and supply fan in a DX

A/C unit would also impact its operational energy efficiency expressed in terms of COP, as different combinations of both speeds may result in different COPs, constrained by the required total output cooling capacity from the DX A/C unit. However, there has been no previously reported research work on systematically studying the inherent operational characteristics of a DX A/C unit having variable-speed compressor and supply fan in terms of its equipment SHR and COP over its entire range of speed variation. Such operational characteristics are expected to be extremely useful in the design and operation of buildings, in particular in those located in the subtropics, using DX A/C installations for environmental control.

This Chapter reports on an experimental study to investigate the inherent operational characteristics of a DX A/C unit when the speeds of both its compressor and supply fan are varied, using the experimental station described in Chapter 5. These characteristics include equipment SHRs and COPs at various speed combinations, over the entire operational ranges of both speeds. Firstly, the experimental conditions and assumptions at which the study was undertaken are presented. This is followed by reporting the experimental results, such as equipment SHR, output sensible and latent cooling capacities, and COP. Finally, a number of issues regarding the practical applications of the inherent operational characteristics and their possible constraints are discussed.

6.2 Experimental conditions and assumptions

The experimental work has been carried out using the experimental DX A/C station whose schematic diagrams are shown in Chapter 5. Since the main purpose of the experimental work was to obtain the inherent operational characteristics of a DX A/C unit when the speeds of its compressor and supply fan were varied, the approach used in the experimental work was to use fixed air state parameters (i.e., air dry-bulb temperature and web-bulb temperature) upstream of the DX cooling coil in the DX A/C unit, as reference, for all speed combinations. Therefore, by measuring the state parameters of air downstream of the DX cooling coil at various combinations of both compressor speed and supply fan speed, the inherent operational characteristics of the DX A/C unit, such as equipment SHRs and COPs based on the specific fixed inlet air temperature and humidity, may then be obtained or calculated. On the other hand, in order to simplify the experimental procedure, no fresh air was introduced by fully closing the fresh air damper in the experimental station as its thermal load may be fully represented by using the load generating units (LGUs).

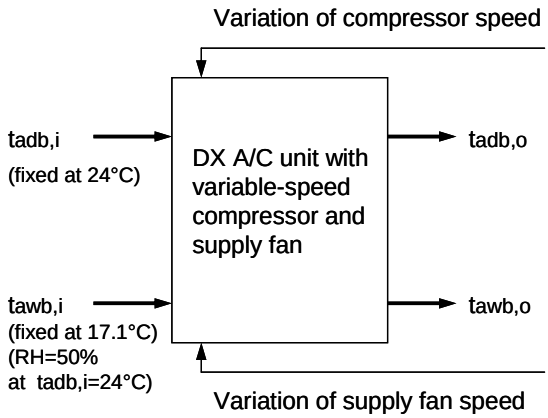

Fig. 6.1 Schematics of the experimental approach

Fig. 6.1 illustrates the approach used in the experiments to obtain the inherent operational characteristics. In Fig. 6.1, $t_{adb,i}$ and $t_{awb,i}$ are the dry-bulb and wet-bulb temperature of inlet air to, and $t_{adb,o}$ and $t_{awb,o}$ the dry-bulb and wet-bulb temperature of outlet air of the DX A/C unit, respectively. While $t_{adb,i}$ and $t_{awb,i}$ were to be maintained at their respective fixed values, $t_{adb,o}$ and $t_{awb,o}$ were variable when both compressor speed and supply fan speed were varied. Consequently, the outputs from the LGUs that were PID controlled must be varied in response to the changes of output cooling capacity from the DX A/C unit. This was to establish various application SHRs in the room to create various steady-state experimental conditions so that fixed inlet air parameters to the DX A/C unit, or simply the indoor air setpoints were maintained. Essentially, application SHRs were equal to equipment SHRs at steady-state conditions at all speed combinations. Fig. 6.2 illustrates an example where SHRs for both equipment and application are 0.75, at the fixed inlet air temperature and RH of 24°C and 50%, respectively.

To be consistent with the indoor air setpoints used in Chapter 4, in the experimental work reported in this Chapter, inlet air parameters to the DX A/C unit, or equivalently the air parameters inside the conditioned room in the experimental station, were fixed at 24°C and 50% RH, respectively.

Since the speeds of both compressor and supply fan may be continuously varied, therefore theoretically, there existed an infinite number of speed combinations. To carry out experimental work under all possible speed combinations was neither practical nor necessary; therefore the following representative discrete experimental compressor and supply fan speeds, which would be used as a vehicle to

experimentally obtain the curves representing inherent operational characteristics of the DX A/C unit, were selected. They are shown in Tables 6.1 and 6.2, respectively.

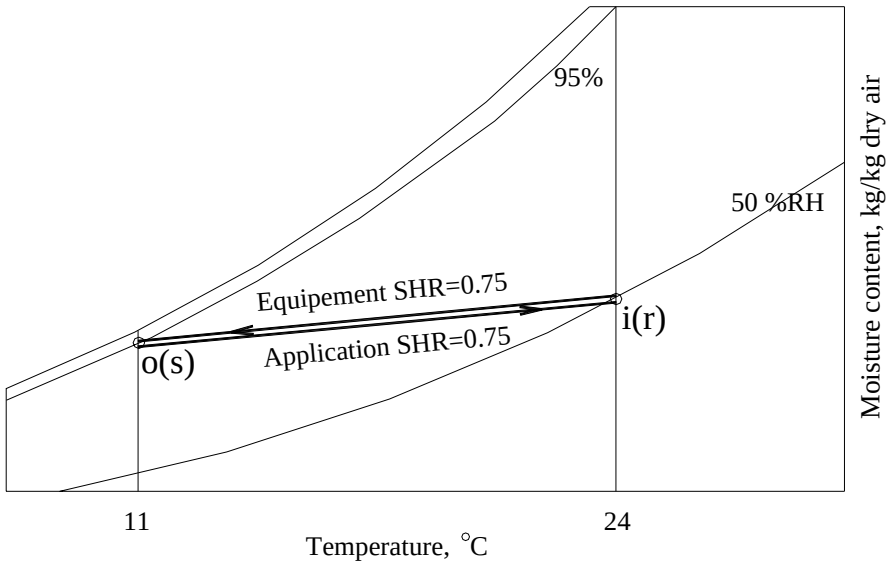

Fig. 6.2 SHRs for both equipment and application are 0.75
at fixed 24°C and 50% inlet air state

Table 6.1 Selected experimental compressor speed

	1	2	3	4	5	6	7
VSD Frequency (Hz)	48	57	66	75	84	92	101
Rotational speed (rpm)	2904	3432	3960	4488	5016	5544	6072
% of maximum speed	30	40	50	60	70	80	90

Table 6.2 Selected experimental supply fan speed or airflow rate

	A	B	C	D	E	F	G
VSD Frequency (Hz)	26	31	36	41	46	50	55
Rotational speed (rpm)	1584	1872	2160	2448	2736	3024	3312
Supply airflow rate (m^3/h)	790	950	1110	1270	1420	1570	1700
% of maximum speed	30	40	50	60	70	80	90

During all experiments, condenser cooling airflow rate was maintained constant at 3100 m^3/h, with a fixed condenser cooling air inlet temperature of 35ºC, using the

existing PID controller in the DX A/C unit. On the other hand, refrigerant degree of superheat was also maintained constant at 6ºC by using the EEV and its associated PID controller in the experimental station.

6.3 Calculation procedures based on experimental data

As seen in Fig. 6.1, using the experimental station, both dry-bulb and wet-bulb air temperatures at both the inlet and outlet of the DX cooling coil may be directly measured. Also being measured directly was the air mass flow rate, m_a, which depended on the rotational speed of the supply fan.

The sensible heat removed by the DX A/C unit may be expressed by:

$$Q_{es} = m_a C_{pa} \left(t_{adb,i} - t_{adb,o} \right) \tag{6.1}$$

The total heat removed by the DX A/C unit is:

$$Q_{et} = m_a \left(h_{a,i} - h_{a,o} \right) \tag{6.2}$$

and equipment SHR is defined as:

$$\text{Equipment SHR} = \frac{Q_{es}}{Q_{et}} = \frac{C_{pa} \left(t_{adb,i} - t_{adb,o} \right)}{\left(h_{a,i} - h_{a,o} \right)} \tag{6.3}$$

where the inlet and outlet air enthalpies are respectively evaluated by:

$$h_{a,i} = 1.005t_{adb,i} + 0.001d_{a,i}(2500 + 1.84t_{adb,i}) \tag{6.4}$$

$$h_{a,o} = 1.005t_{adb,o} + 0.001d_{a,o}(2500 + 1.84t_{adb,o}) \tag{6.5}$$

In Equations (6.4) and (6.5), $d_{a,i}$ and $d_{a,o}$ are the moisture contents of air entering and exiting the DX A/C unit, respectively, and may be evaluated by:

$$d_{a,i} = \frac{(2500 - 1.347t_{awb,i})d_{sa,i} - 1010(t_{adb,i} - t_{awb,i})}{2500 + 1.84t_{adb,i} - 4.187t_{awb,i}} \tag{6.6}$$

$$d_{a,o} = \frac{(2500 - 1.347t_{awb,o})d_{sa,o} - 1010(t_{adb,o} - t_{awb,o})}{2500 + 1.84t_{adb,o} - 4.187t_{awb,o}} \tag{6.7}$$

In Equations (6.6) and (6.7), $t_{awb,i}$ and $t_{awb,o}$ are the wet-bulb temperatures of air entering and exiting the DX A/C unit, respectively; $d_{sa,i}$ and $d_{sa,o}$ the saturated moisture contents of air entering and exiting the DX A/C unit, respectively, and can be evaluated based on:

$$d_{sa} = 622\,p_{asw}/(101.325 - p_{asw}) \tag{6.8}$$

where p_{asw} is the saturated water vapor pressure as a function of t_{awb}, and can be estimated by the following equation when t_{awb} is between 0 and 200ºC:

$$p_{asw} = \frac{e^{-5.800\times10^{3}T_{awb}^{-1}+1.391-0.0486T_{awb}+0.418\times10^{-4}T_{awb}^{2}-0.145\times10^{-7}T_{awb}^{3}+6.546\times\ln(T_{awb})}}{1000} \tag{6.9}$$

where T_{awb} is the absolute air wet-bulb temperature, and evaluated by:

$$T_{awb} = 273 + t_{awb} \tag{6.10}$$

On the other hand, an application SHR for the A/C process shown in Fig. 6.2 can be evaluated by:

$$\text{Application SHR} = \frac{C_{pa}\left(t_{adb,s} - t_{adb,r}\right)}{\left(h_{a,s} - h_{a,r}\right)} \tag{6.11}$$

At steady-state operation, points *s* and *o*, and *r* and *i* overlap, as shown in Fig. 6.2. Therefore, numerically, the values of an application SHR and an equipment SHR are equal to each other at steady-state operation.

6.4 Experimental Results

The inherent operational characteristics of the experimental DX A/C unit when the speeds of its compressor and supply fan were varied, at fixed inlet air temperature and RH of 24ºC and 50%, were obtained. The obtained inherent operational characteristics related to equipment SHR and the operating efficiency of the DX A/C unit are separately presented in this Section.

6.4.1 Operational characteristics related to equipment SHR

Fig. 6.3 and Fig. 6.4 show the outlet air dry-bulb and wet-bulb temperatures from the DX A/C unit at different compressor speed and supply fan speed combinations at fixed 24ºC and 50% RH inlet air state. It can be seen from both diagrams that similar variation trends for both dry-bulb and wet-bulb air temperatures were exhibited. Taking dry-bulb air temperature as an example, it can be seen that under a fixed supply fan speed, running compressor at a lower speed would result in a higher outlet air dry-bulb temperature. This was understandable because a lower compressor speed would imply a lower output cooling capacity, leading to a higher outlet air temperature. On the other hand, given a fixed compressor speed, lowering supply fan speed would lead to a lower outlet air temperature, due to that less airflow rate would result in a lower refrigerant evaporating temperature, hence a lower cooling coil surface temperature. This was clearly desirable for achieving better dehumidification.

Fig. 6.5 shows equipment SHRs which were calculated using Equations (6.1) to (6.10). It may be observed that, at a fixed compressor speed, running supply fan at a lower speed would enable the DX A/C unit to have a lower equipment SHR, which was beneficial to dehumidification. Also as seen in Fig. 6.5, at a fixed supply fan speed, running compressor at a higher speed would also result in a lower equipment SHR, when there was more output cooling capacity from the DX A/C unit, leading to a lower cooling coil surface temperature. It can be further interestingly observed that the curves for higher compressor speeds were closer to each other, compared to that the curves for lower compressor speeds were more apart from each other. The

observation suggested that at higher compressor speeds, increasing compressor speed would impact less on equipment SHR than at lower compressor speeds. This may be explained by the fact that the saturation curve of air on a psychrometric chart, i.e., 95% RH line, is relatively steeper at higher air temperatures, and more gradual at lower air temperatures. Therefore, at higher compressor speeds, more output cooling capacity would result in lower outlet air temperatures, and the lines representing air handling processes are more inclined to be close to each other, suggesting less deviation in the resultant equipment SHR. This is illustrated in Fig. 6.6 where the air handling process represented by o_1-i is at the highest compressor speed, while o_6-i the lowest compressor speed.

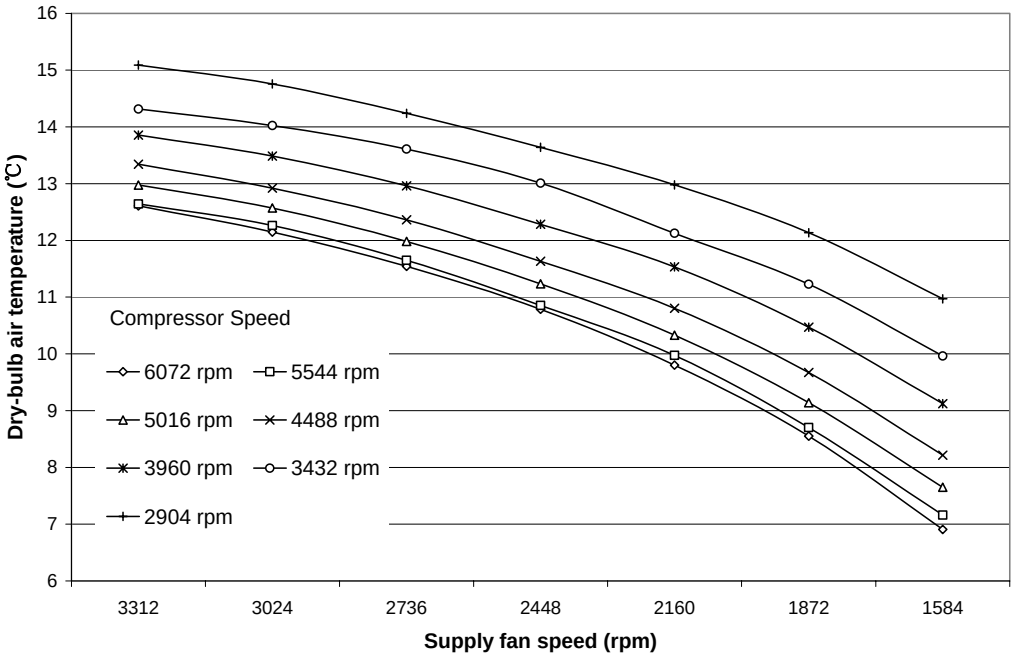

Fig. 6.3 Outlet air dry-bulb temperature at different compressor speed and supply fan speed combinations at fixed 24ºC and 50% RH inlet air state

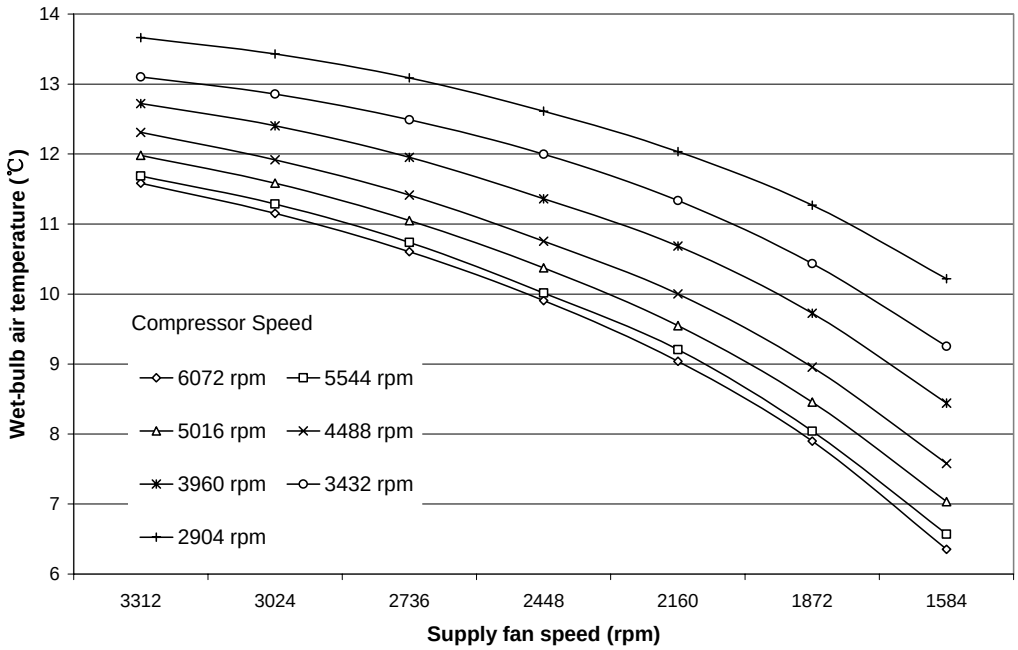

Fig. 6.4 Outlet air wet-bulb temperature at different compressor speed and supply fan speed combinations at fixed 24ºC and 50% RH inlet air state

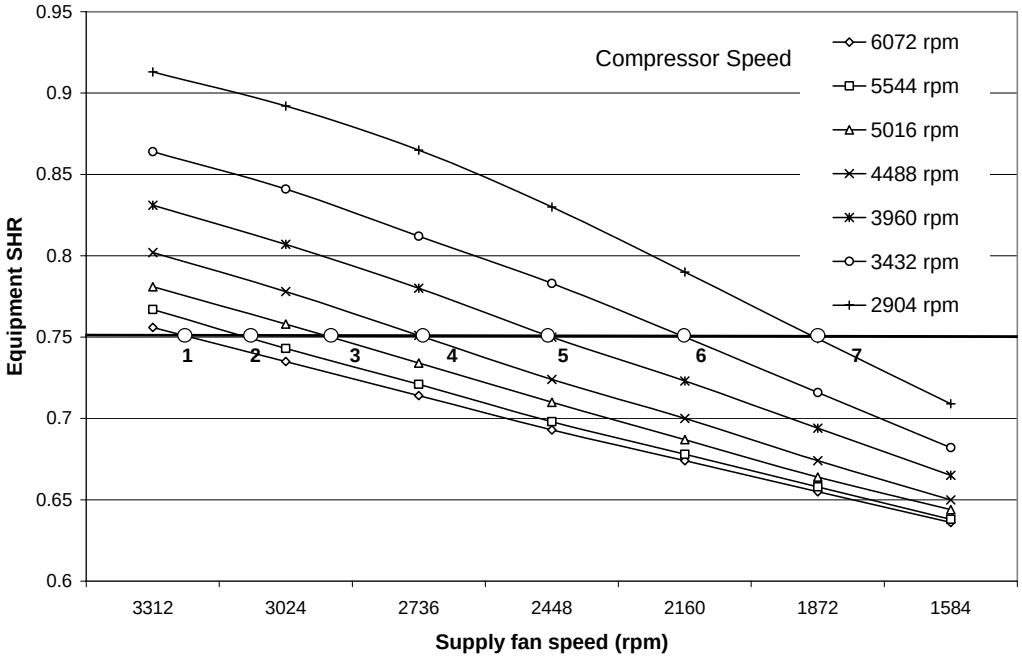

Fig. 6.5 Equipment SHR at different compressor speed and supply fan speed combinations at fixed 24ºC and 50% RH inlet air state

On the other hand, the characteristics shown in Fig. 6.6 are also attributed to the fact that at higher compressor speeds, further increasing compressor speed would not

significantly increase the output cooling capacity of the DX A/C unit, as compared to the increases observed at the lower compressor speeds, as depicted in Fig. 6.7. From the diagram, it is clear that the output cooling capacity from the DX A/C unit was predominately affected by changing compressor speed, although at a given fixed compressor speed, reducing supply fan speed would also reduce, but less significantly, the output cooling capacity.

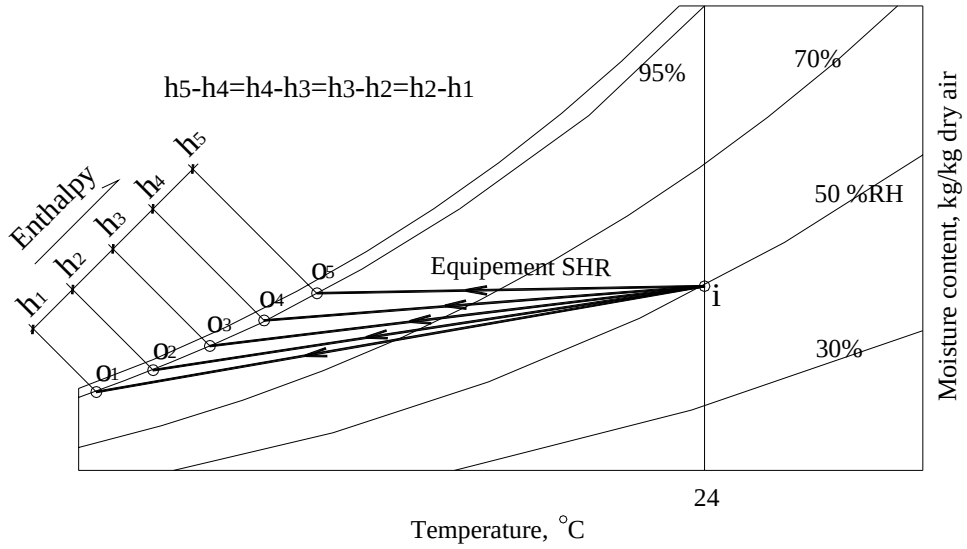

Fig. 6.6 Air handling processes and equipment SHRs at different compressor speeds at a fixed supply fan speed

Fig. 6.8 illustrates the output sensible cooling capacity at different compressor speed and supply fan speed combinations at fixed 24ºC and 50% RH inlet air state. Comparing to that for the total output cooling capacity shown in Fig. 6.7, at a fixed compressor speed, the rate of decrease for sensible component was more noticeable when the supply fan speed was reduced. This is largely because the latent component of the total output cooling capacity for the DX A/C unit was, on the contrary, actually increased at lower supply fan speeds, as illustrated in Fig. 6.9. This was in agreement with the findings in a number of previous studies [MacArthur and Grald

1988, Chuah et al. 1998, Khattar et al. 1987, Khattar and Henderson 1999, Kurtz 2003, Hourahan 2004], which suggested that running a supply fan at a lower speed could result in improved dehumidification.

From Figs. 6.7 to 6.9, it can be seen that at a given compressor speed, although there were not significant changes in the total output cooling capacity with varying supply fan speed (Fig. 6.7), there were significant changes in the ratio between the sensible and latent components of the total output cooling capacity (Fig. 6.8 and Fig. 6.9), with a lower supply fan speed or smaller airflow rate leading to a larger latent heat removal, thus a lower equipment SHR. This was considered to be mainly caused by a lower cooling coil surface temperature at a lower supply fan speed, or a larger latent heat transfer potential.

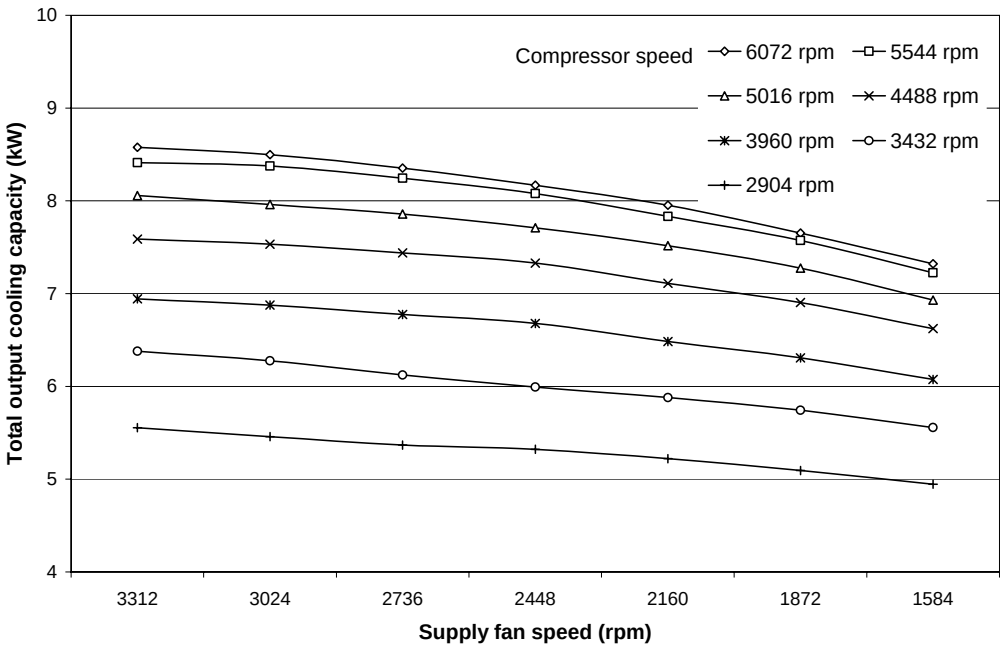

Fig. 6.7 Total output cooling capacity at different compressor speed and supply fan speed combinations at fixed 24ºC and 50% RH inlet air state

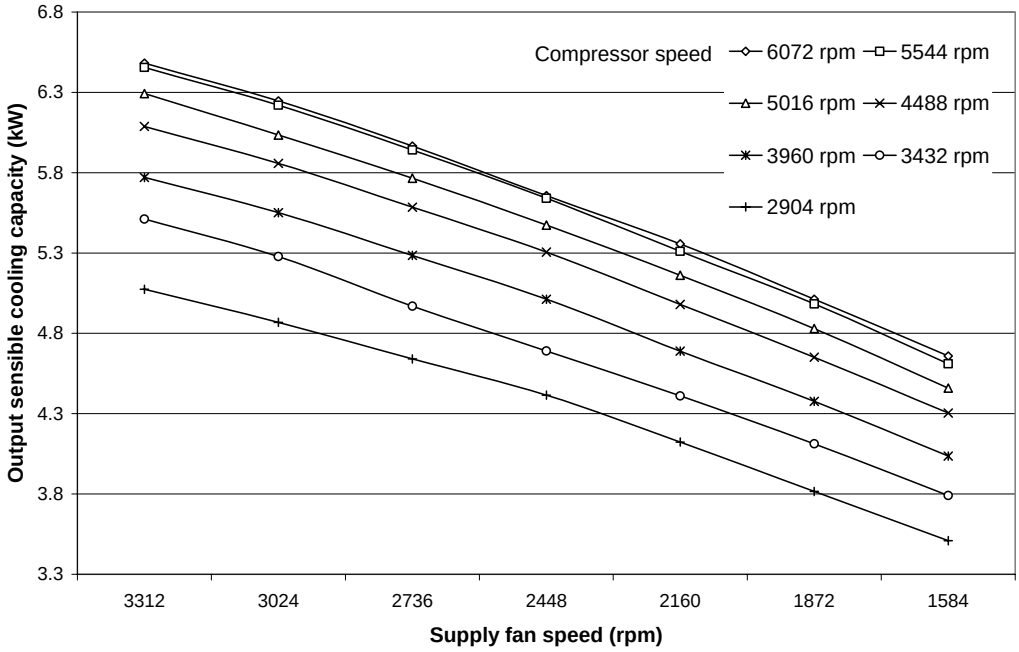

Fig. 6.8 Output sensible cooling capacity at different compressor speed and supply fan speed combinations at fixed 24ºC and 50% RH inlet air state

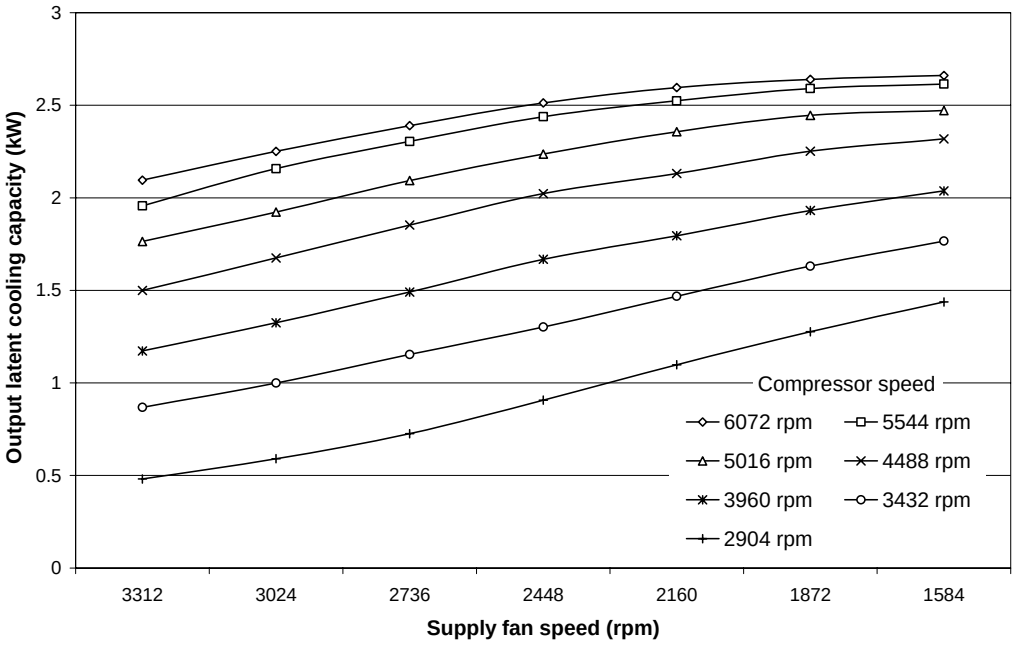

Fig. 6.9 Output latent cooling capacity at different compressor speed and supply fan speed combinations at fixed 24ºC and 50% RH inlet air state

6.4.2 Operational characteristics related to operating efficiency

As seen in Section 6.4.1, it was possible to vary the speeds of both compressor and supply fan in a DX A/C unit in order to achieve varying output cooling capacity, varying ratios of its sensible and latent components, and consequently, varying equipment SHRs. These inherent operational characteristics were, on one hand, important in practical application, and on the other hand, constrained by the operational efficiency of a DX A/C unit, as varying speeds would change the power inputs to both compressor and supply fan in the unit. This Section presents the measured operational characteristics relating to operating efficiency including power inputs to compressor and COP, under various speed combinations at the fixed 24ºC and 50% RH inlet air state.

Since the power inputs to both compressor and supply fan were considered, two types of COP were defined as follows.

Coefficient of Performance based on compressor input power, which was normally used for ordinary refrigeration systems:

$$COP_{com} = Q_{et} / W_{com} \tag{6.12}$$

where Q_{et} is the total output cooling capacity and W_{com} the power input to compressor.

Coefficient of Performance based on the power inputs to both compressor and supply fan in a DX A/C unit:

$$COP_{com+fan} = Q_{et} / \left(W_{com} + W_{fan} \right) \tag{6.13}$$

Where W_{fan} is the power input to supply fan.

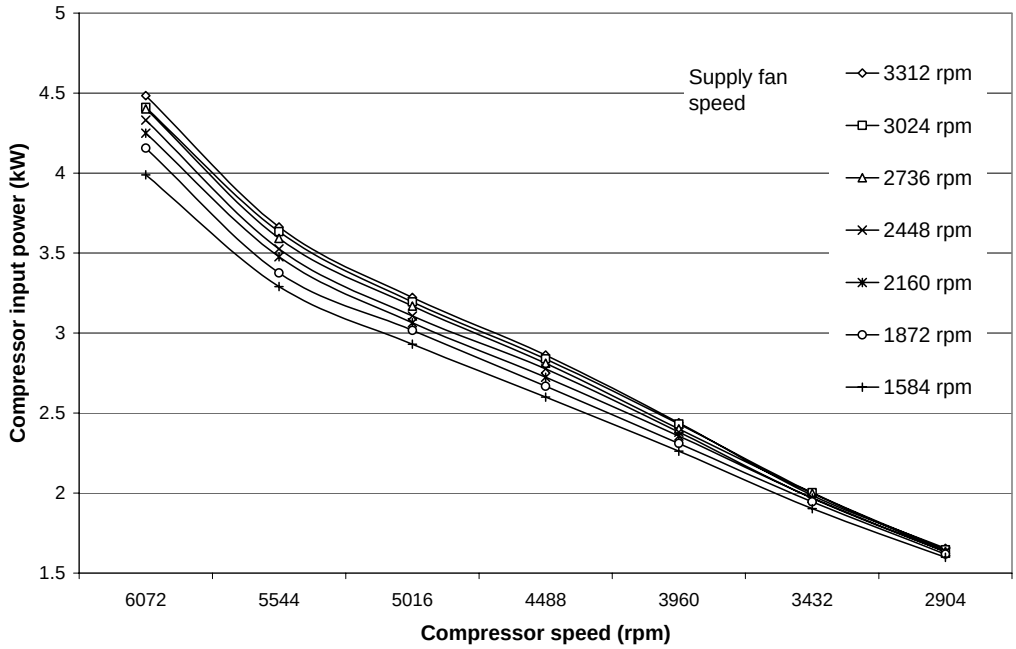

Fig. 6.10 Compressor input power at different compressor speed and supply fan speed combinations at fixed 24ºC and 50% RH inlet air state

Fig. 6.10 shows the measured input power to compressor at different compressor speed and supply fan speed combinations at fixed 24ºC and 50% RH inlet air state to the DX A/C unit. It was obvious that varying compressor speed would significantly change the power input to compressor. However, it can be noted that varying supply fan speed would also, although not to the same extent, influence compressor power input, which was particularly noticeable at higher compressor speeds. This was

because the change of the cooling load imposed on the DX cooling coil due to changing supply fan speed would alter both the refrigerant mass flow rate passing through the DX evaporator (Fig. 6.11) and the condensing and evaporating pressures.

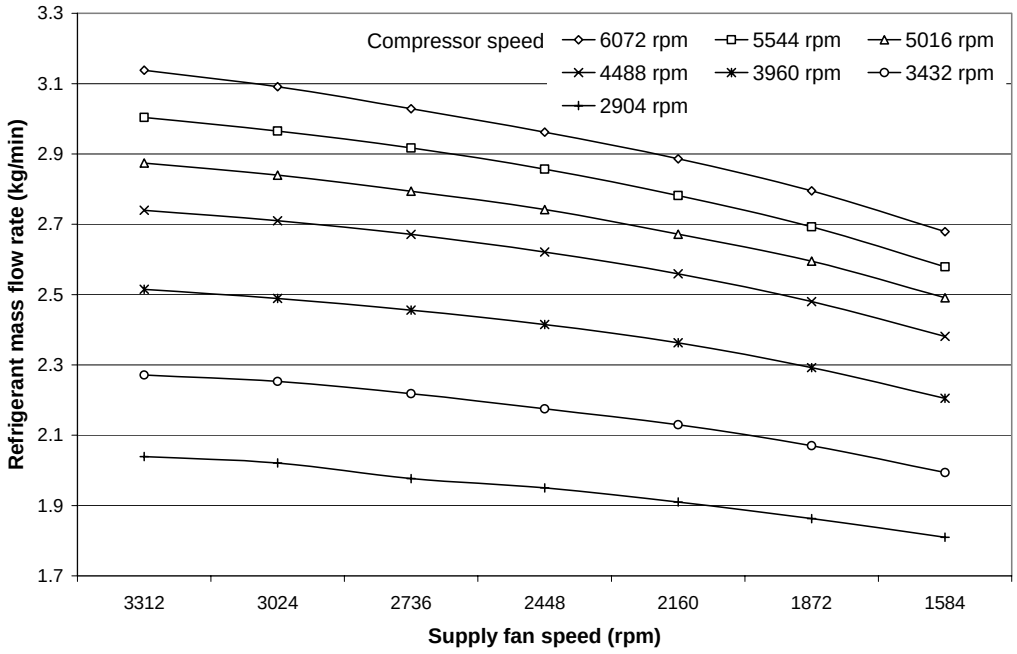

Fig. 6.11 Refrigerant mass flow rates at different compressor and supply fan speed combinations at fixed 24ºC and 50% RH inlet air state

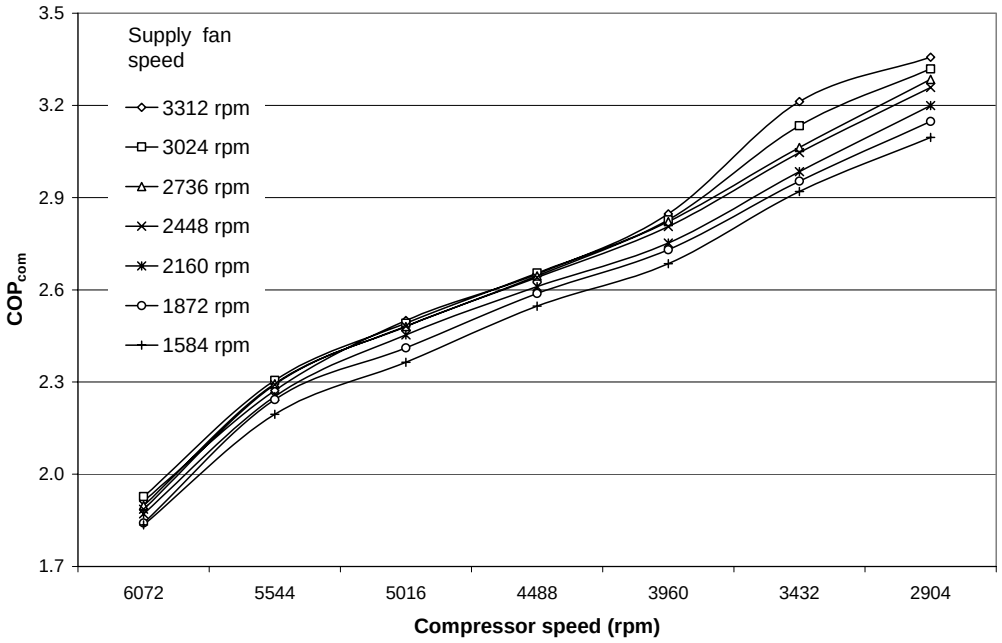

Fig. 6.12 COP_{com} at different compressor and supply fan speed combinations at fixed 24ºC and 50% RH inlet air state

It was also interesting to note from Fig. 6.10 that at the lowest compressor speed, i.e., 2904 rpm, the changes in compressor power input due to varying supply fan speed became less noticeable, when the compressor may be operating already at its minimum output condition, and therefore, changing supply fan speed did not greatly affect the power input to compressor.

Fig. 6.12 shows the values of COP_{com} (i.e., based on only the power input to compressor) at different compressor speed and supply fan speed combinations at fixed 24ºC and 50% RH inlet air state. It can be seen that there were significant variations for COP_{com}, which were dominated by the variation of compressor speed. Generally speaking, a lower compressor speed would lead to a higher COP_{com} and vice-verse. Under a given compressor speed, a higher supply fan speed would also lead to a higher COP_{com}, although this became less noticeable with the increase of compressor speed. It must, however, be pointed out that both situations mentioned above resulted in a higher COP_{com} because the DX A/C unit was operated with a higher evaporating temperature, and consequently, its output cooling capacity may not be adequate for certain applications.

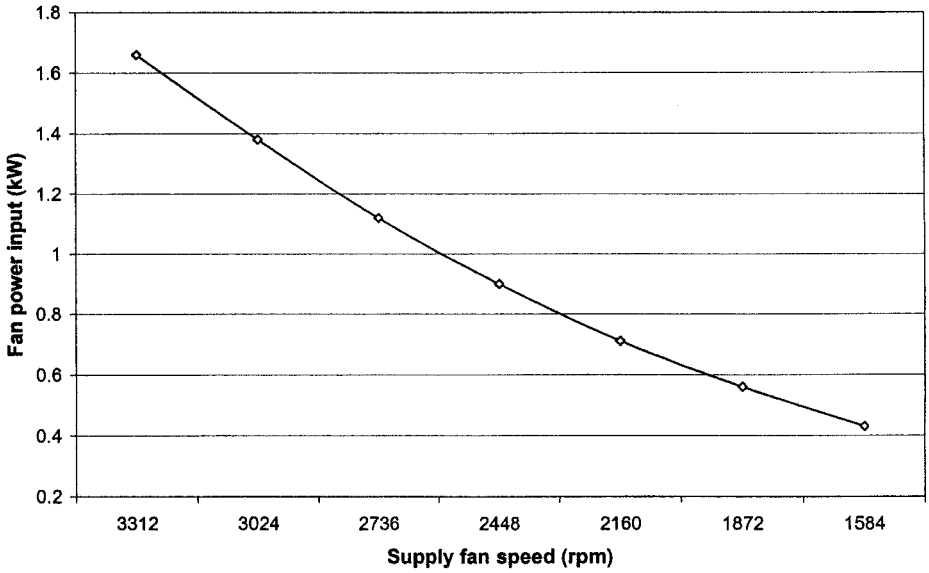

Fig. 6.13 Measured supply fan power input at different supply fan speed

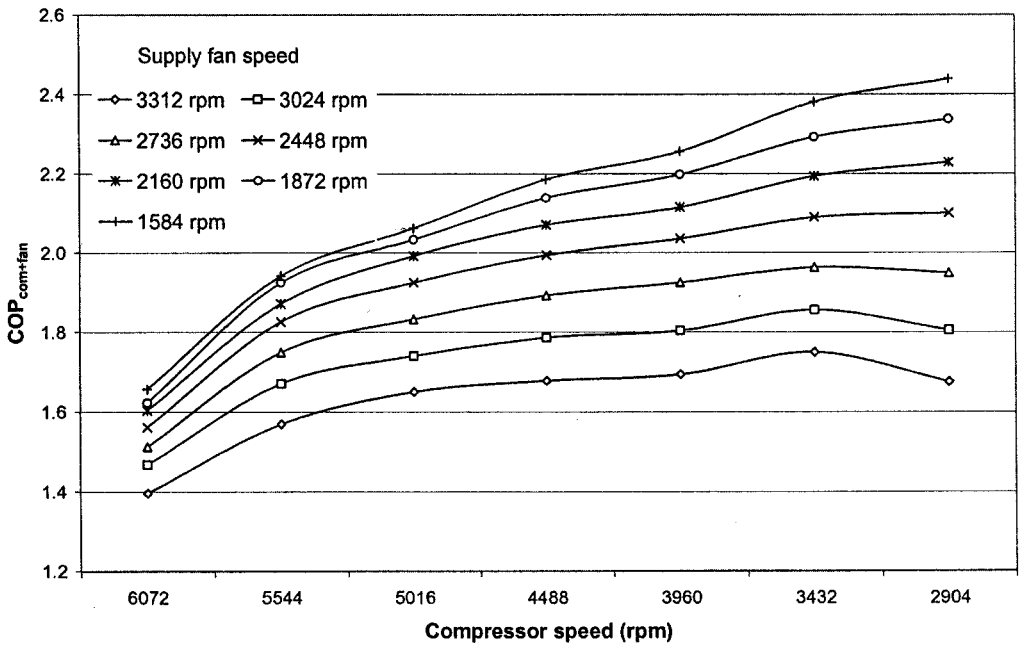

Fig. 6.14 $COP_{com+fan}$ at different compressor and supply fan speed combinations at fixed 24°C and 50% RH inlet air state

On the other hand, the measured supply fan power input appeared independent of the variation of compressor speed, and was only affected by fan speed. Fig. 6.13 shows the supply fan power input at different fan speeds. It is seen that a higher fan speed would call for a larger power input.

Fig. 6.14 shows the coefficient of performance based on the power inputs to both compressor and supply fan, $COP_{com+fan}$, at different compressor speed and supply fan speed combinations at fixed 24 ºC and 50% RH inlet air state. Since the power input to supply fan was also included, the actual values of $COP_{com+fan}$, under the same compressor speed, were lower than that of COP_{com}. It may be observed that when compared to COP_{com} values shown in Fig. 6.12, the values of $COP_{com+fan}$ were dependent upon the changes of both compressor speed and supply fan speed. Generally, lowering the speeds of both compressor and supply fan would result in higher $COP_{com+fan}$ values, at the expense of reduced output cooling capacity from the DX A/C unit.

6.5 Discussions

The measured inherent operational characteristics for the DX A/C unit having variable-speed compressor and supply fan presented in Section 6.4 were based on the fixed inlet state of 24ºC air dry-bulb temperature and 50% RH. This air state was chosen because it was representative and typically recommended by various design standards [ANSI/ASHRAE 2004, HK-BEAM 2003, Lin and Deng 2004]. It should be pointed out that with different inlet air states; there would be deviations of varying degrees from what have been presented. Nonetheless, the characteristics presented in Section 6.4 were typical and representative, and therefore were significant in discussing the inherent operational characteristics for DX A/C units having variable-speed compressor and supply fan.

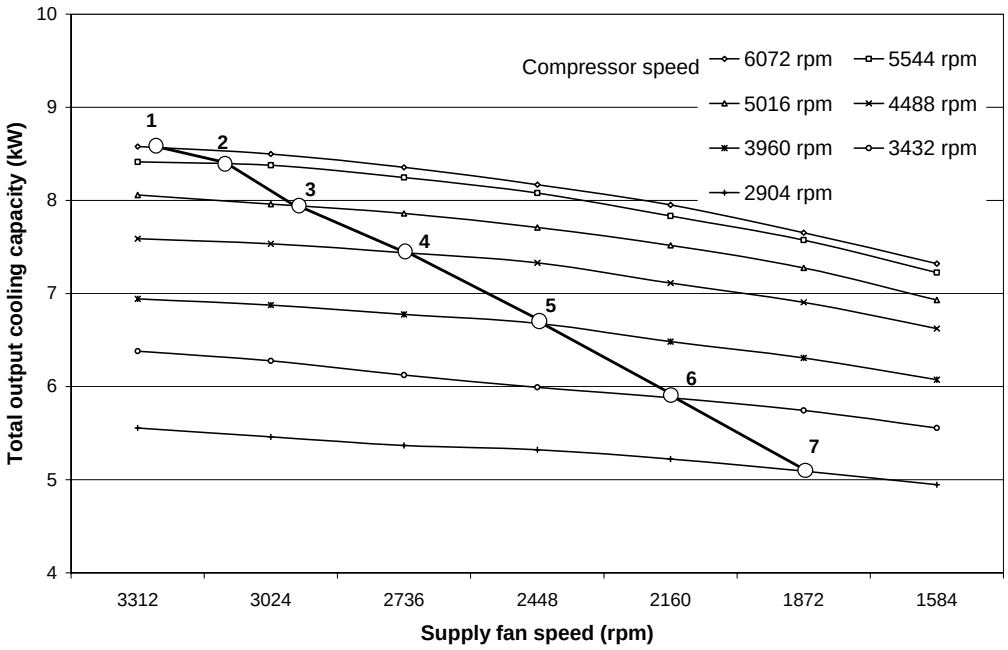

Fig. 6.15 Total output cooling capacity with equipment SHR being 0.75 at different compressor and supply fan speed combinations at fixed 24ºC and 50% RH inlet air state

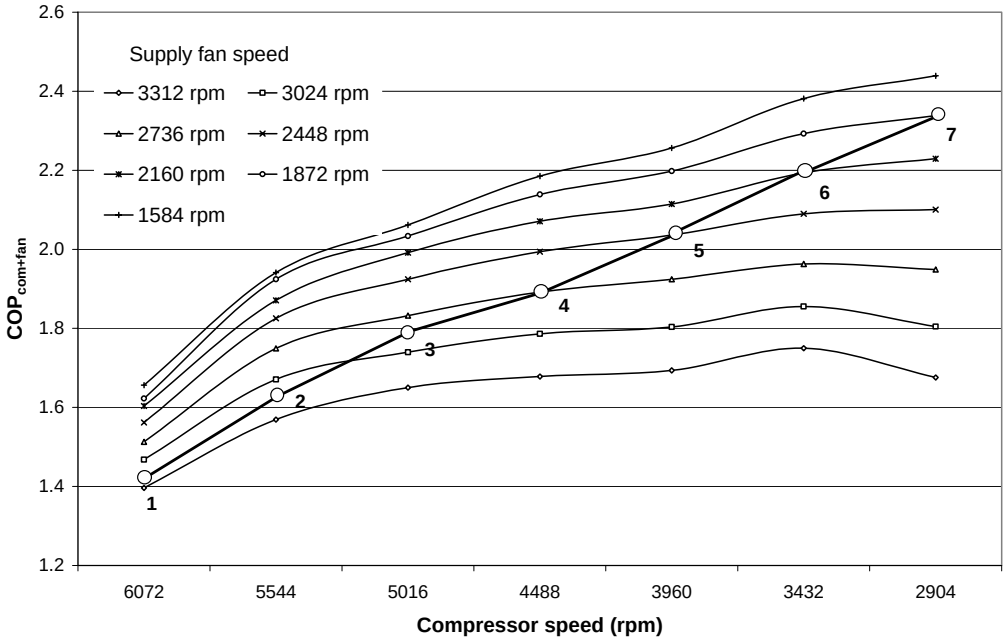

Fig. 6.16 $COP_{com+fan}$ with equipment SHR being 0.75 at different compressor and supply fan speed combinations at fixed 24ºC and 50% RH inlet air state

Based on the measured total output cooling capacity and both of its sensible and latent components at different compressor and supply fan speed combinations, as shown from Figs. 6.7 to 6.9, the following can be observed. While it was obvious that varying both speeds can lead to the varying total output cooling capacity from a DX A/C unit, it was perhaps more important for practical applications that varying both speeds can also lead to the variation of the ratios between the sensible and latent components of the total output cooling capacity. This was reflected in the variation of equipment SHRs of the DX A/C unit, as shown in Fig. 6.5. With a lower equipment SHR, the ability to dehumidify for a DX A/C unit was increased. Therefore, such operational characteristics should be fully utilized for environmental control in spaces where their cooling loads and the ratio between their sensible and latent components were highly variable. On the other hand, it must be noted that lowering the speed of supply fan or the air flow rate passing through a DX cooling coil was more effective in lowering equipment SHR than lowering compressor speed. At a fixed compressor speed or approximately a constant output cooling capacity from a DX A/C unit, the lower the supply fan speed, the lower the equipment SHR or the higher the ability to dehumidify for the DX A/C unit.

On the other hand, the practical application of varying equipment SHR by varying both compressor speed and supply fan speed was expected to be constrained by the required total output cooling capacity from a DX A/C unit. For example, if an equipment SHR of 0.75, which was chosen by reference to the equipment SHR values of 0.7 to 0.8 for standard constant-speed DX A/C units, was to be achieved, as seen from Fig. 6.5, there were at least seven known speed combinations (point 1 to 7), where the equipment SHR of 0.75 may be achieved. However, as shown in Fig.

6.15, the total output cooling capacity at point 1 was 8.6 kW at the highest compressor speed, and was reduced to 5.1 kW at point 7 at the lowest compressor speed. This represented a 41% capacity reduction. Clearly, if the required total output cooling capacity from the DX A/C unit cannot be made available at a specific speed combination, even with an appropriate equipment SHR for the application, the required space environmental control cannot be realized.

Furthermore, even when the required output cooling capacity may be provided, one further constraint would be the operating efficiency of the DX A/C unit. As seen in Fig. 6.16, for the seven points 1 to 7, the corresponding $COP_{com+fan}$ also varied significantly from 1.42 to 2.34, a 65% increase. Clearly under both an adequate output cooling capacity and a suitable equipment SHR, a higher $COP_{com+fan}$ should be preferred.

Therefore theoretically, there can be a large number of compressor and supply fan speed combinations that would result in a specific equipment SHR being suitable for a particular application, for example, 0.75 as discussed earlier, the first constraint would be that the required output cooling capacity from a DX A/C unit must be provided. This virtually narrowed down the number of speed combinations. Furthermore, the second constraint would be the operating efficiency, which further narrowed down the number of speed combinations available.

Such operational characteristics for a DX A/C unit with varying compressor speed and supply fan speed are, by their nature, inherent. Therefore these should be part of the unit's overall operational performance and should be included as part of product inventory for the DX A/C unit.

6.6 Conclusions

This Chapter presents an experimental study on the inherent operational characteristics for a DX A/C unit at a fixed inlet air state of 24ºC and 50% RH to the DX A/C unit when its compressor speed and supply fan speed were varied. Although the results presented were based on this specific air inlet state, they were considered typical and representative.

The measured inherent operational characteristics of the DX A/C unit suggested that varying both compressor speed and supply fan speed can lead to varying equipment SHR, or the varying ability to dehumidify of the unit. Therefore such an operating strategy, i.e., by varying both compressor speed and supply fan speed, may be preferably adopted for environmental control in places subjected to variable latent loads, such as the residential buildings located in hot and humid subtropical regions. Generally, lowering supply fan speed is more effective in enhancing the ability to dehumidify than increasing compressor speed. However, varying both speeds would also impact on the total output cooling capacity and the operating efficiency of a DX A/C unit. Consequently the application of changing equipment SHR for better humidity control is subject to the constraints of meeting the required total output cooling capacity from, and attaining higher operating efficiency of a DX A/C unit.

To better facilitate the design and operation of DX A/C installations in buildings for environmental control, it is necessary that inherent operational characteristics of DX A/C units, similar to those reported in this Chapter, should be provided and included as part of the units' operational performances.

Chapter 7

Experimental Study Ⅱ: Indoor Thermal Comfort Characteristics under the Control of a DX A/C Unit Having Variable-speed Compressor and Supply Fan at a Fixed Space Cooling Load Condition

7.1 Introduction

With the rapid development of HVAC industry, the use of variable-speed compressor and supply fan has become more and more prevalent and practical. In Chapter 6, an experimental investigation on the inherent operational characteristics of a DX A/C unit at fixed inlet air temperature and humidity when the speeds of its compressor and supply fan were varied has been reported. The experimental results demonstrated that varying both compressor and supply fan speeds could lead to varying equipment SHR, or the varying ability to dehumidify of the DX A/C unit. Therefore, it could be understood that simultaneously varying compressor and supply fan speeds of a DX A/C unit, would directly and indirectly affect indoor air temperature, RH, air velocity and mean radiant temperature (MRT), and consequently indoor thermal comfort level.

Previously studies by Andrade et al. [2002] and Krakow et al. [1995] only considered the indoor environmental conditions, i.e., air temperature and humidity, rather than indoor thermal comfort characteristics. On the other hand, an optimal comfort control concept for variable-speed heat pumps and air conditioners was

proposed in a simulation-based study [MacArthur and Grald 1988]. The control objective was to maximize the system's COP while simultaneously satisfying comfort requirements. A multi-dimensional search technique was employed to find the optimum compressor speed, indoor airflow rate and evaporator superheat at a given ambient condition. Simulation results indicated that although there existed an infinite number of combinations of compressor speed and indoor airflow rate that could satisfy the comfort requirements as measured by using Fanger's Predicted Mean Vote (PMV) index, only one speed combination resulted in the maximum COP. Unfortunately this study was only based on simulation and no experimental evidences were presented.

There have been recent developments in using thermal comfort index, rather than a single environmental parameter such as air temperature or humidity for controlling the operation of A/C systems. For example, there was a recently reported study [Chu et al. 2005] where the concept of thermal comfort control was integrated into a fuzzy controller for a fan-coil unit. Comfort conditions were expressed by using effective temperature (ET). The experimental results showed that such a fuzzy controller can help achieve better thermal comfort, and a higher energy efficiency and system reliability.

In this Chapter, an experimental investigation of indoor thermal comfort characteristics under the control of a DX A/C unit having variable-speed compressor and supply fan at a fixed space cooling load condition is presented. Firstly, the well-known Fanger's PMV and Predicted Percentage Dissatisfied (PPD) thermal comfort model is briefly introduced and simplified for the current experimental investigation.

This is followed by reporting the experimental results of indoor thermal comfort characteristics under the control of a DX A/C unit at a given total space cooling load, with a fixed application SHR. Finally, the potential of using thermal comfort indexes for control purpose is discussed.

7.2 Indoor thermal comfort

7.2.1 Energy exchange between a human body and its environment

According to ASHRAE Handbook Fundamentals [ASHRAE 2001], the energy balance between a human body and its environment, after combining the environmental and personal variables to produce a neutral sensation, can be expressed as follows:

$$\begin{aligned} M - W = {} & 3.96\times10^{-8} f_{cl}\left[(t_{cl}+273)^4 - (\bar{t}_r+273)^4\right] + f_{cl}h_c\left(t_{cl} - t_{adb,r}\right) \\ & + 3.05\left[5.73 - 0.007(M-W) - p_{av}\right] + 0.42\left[(M-W) - 58.15\right] \\ & + 0.0173\,M\left(5.87 - p_{av}\right) + 0.0014\,M\left(34 - t_{adb,r}\right) \end{aligned} \qquad (7.1)$$

where W is the external work done by muscles, f_{cl} clothing area factor, h_c convective heat transfer coefficient, t_{cl}, $\bar{t}_r$ and $t_{adb,r}$ the clothing temperature, MRT and indoor air dry-bulb temperature, respectively, and p_{av} water vapor pressure.

The values of h_c and f_{cl} can be estimated by using Equations (7.2) to (7.5) [ASHRAE 2001]:

$$h_c = 2.38\left(t_{cl} - t_{adb,r}\right)^{0.25} \quad \text{for } 2.38\left(t_{cl} - t_{adb,r}\right)^{0.25} > 12.1\sqrt{V} \tag{7.2}$$

$$h_c = 12.1\sqrt{V} \quad \text{for } 2.38\left(t_{cl} - t_{adb,r}\right)^{0.25} < 12.1\sqrt{V} \tag{7.3}$$

$$f_{cl} = 1.0 + 0.2I_{cl} \quad \text{for } I_{cl} < 0.5clo \tag{7.4}$$

$$f_{cl} = 1.05 + 0.1I_{cl} \quad \text{for } I_{cl} > 0.5clo \tag{7.5}$$

Where V is the air velocity, and I_{cl} the clothing insulation value.

Clothing temperature, t_{cl}, is evaluated by [ASHRAE 2001]:

$$t_{cl} = 35.7 - 0.0275\left(M - W\right) - R_{cl}J \tag{7.6}$$

where $$J = \left(M - W\right) - 3.05\left[5.73 - 0.007\left(M - W\right) - p_{av}\right] - 0.42\left[\left(M - W\right) - 58.15\right]$$
$$- 0.0173M\left(5.87 - p_{av}\right) - 0.0014M\left(34 - t_{adb,r}\right) \tag{7.7}$$

where R_{cl} is the thermal resistance of clothing.

MRT or $\bar{t}_r$, a key parameter in evaluating thermal comfort for occupants, is the temperature of an imaginary isothermal black enclosure in which an occupant would exchange the same amount of heat by radiation as in the actual nonuniform

environment. Using the actually measured results of globe temperature, t_g, indoor air dry-bulb temperature, $t_{adb,r}$, and air velocity, V, the value of $\bar{t}_r$ can be estimated. However, the accuracy of $\bar{t}_r$ determined this way would vary considerably depending on the type of environment and the accuracy of the individual measurement. The instrument most commonly used to determine t_g is a black globe thermometer because of its simplicity (see Section 7.3.3). The temperature assumed by the globe at equilibrium results from a balance between heat gained and lost by radiation and convection, and $\bar{t}_r$ can be calculated from [ASHRAE 2001]:

$$\bar{t}_r = \left[\left(t_g + 273\right)^4 + \frac{1.10 \times 10^8 V^{0.6}}{\varepsilon D^{0.4}} \left(t_g - t_{adb,r}\right) \right]^{1/4} - 273 \qquad (7.8)$$

where D is the diameter of a globe. For a standard black globe, $D = 0.15\,m$. ε is the emissivity of a globe, and for a black globe, $\varepsilon = 0.95$.

The water vapor pressure, p_{av}, can be estimated by:

$$p_{av} = RH \times p_{asw,db} \qquad (7.9)$$

where $p_{asw,db}$ is the saturated water vapor pressure which can be estimated using Equations (6.9) and (6.10) by replacing t_{awb} with $t_{adb,r}$。

Equation (7.1) can be expanded to include a range of thermal sensations by using the PMV index. Fanger [1970] related PMV to the imbalance between the actual heat

flow from a human body in a given environment and the heat flow required for optimum comfort at a specified activity by the following equation:

$$PMV = \left[0.303\exp\left(-0.036M\right)+0.028\right]L \tag{7.10}$$

where L is the thermal load on the body, defined as the difference between the internal heat production and the heat loss to the actual environment for a person hypothetically kept at comfort values of mean skin temperature and sweat rate at the actual activity level. Hence:

$$\begin{aligned} L = M - W - 3.96\times10^{-8} f_{cl}\left[\left(t_{cl}+273\right)^4 - \left(\bar{t}_r+273\right)^4\right] - f_{cl}h_c\left(t_{cl}-t_{adb,r}\right) \\ - 3.05\left[5.73-0.007\left(M-W\right)-p_{av}\right] - 0.42\left[\left(M-W\right)-58.15\right] \\ - 0.0173M\left(5.87-p_{av}\right) - 0.0014M\left(34-t_{adb,r}\right) \end{aligned} \tag{7.11}$$

After estimating the PMV using Equation (7.10), the PPD can also be estimated. Fanger [1982] related the PPD to the PMV as follows:

$$PPD = 100 - 95\exp\left[-\left(0.03353PMV^4 + 0.2179PMV^2\right)\right] \tag{7.12}$$

A PPD of 10% corresponds to the PMV range of ± 0.5, and even with PMV=0, about 5% of the people are dissatisfied. The relationship between PMV and PPD is shown in Fig. 7.1.

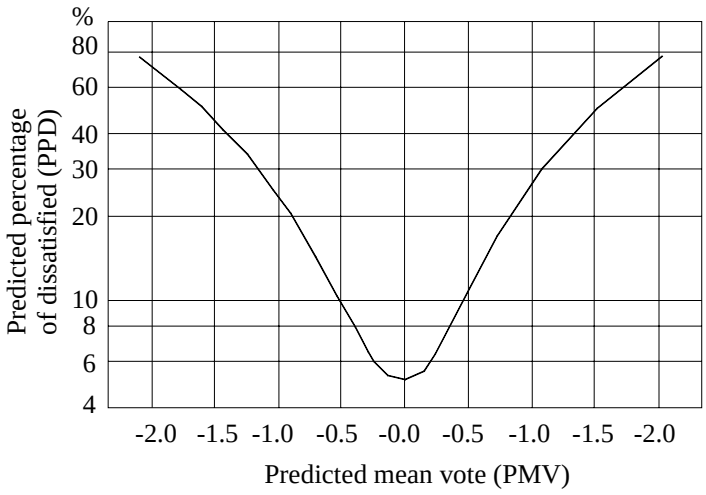

Fig. 7.1 PPD as a function of PMV [ASHRAE 2001]

Equations (7.1) to (7.12) are normally referred as Fanger's PMV-PPD model. It has been widely used and accepted for design and field assessment of thermal comfort [Yang and Su 1997]. Both ISO Standard 7730 and the new version of ANSI/ASHRAE Standard 55 [ANSI/ASHRAE 2004] include a short computer listing that facilitates the computing of PMV and PPD for a wide range of environmental and clothes resistance parameters.

Standards for maintaining comfortable indoor thermal environments have been developed by ASHRAE [ANSI/ASHRAE 2004] and ISO [ISO 1994]. ASHRAE defined three classes of acceptable thermal environment for general comfort (see Table 7.1) [ANSI/ASHRAE 2004]. Fig. 7.2 shows the comfort zone based on 90% acceptance of thermal conditions or 10% PPD (Comfort Class B), which may be applied to a space where occupants have activity levels with metabolic rates between 1.0 met and 1.3 met and where clothing is worn providing between 0.5 clo and 1.0 clo of thermal insulation.

Table 7.1 Three classes of acceptable thermal environment for general comfort defined by ASHRAE

Comfort Class	PPD (%)	PMV Range
A	< 6	-0.2 < PMV < +0.2
B	< 10	-0.5 < PMV < +0.5
C	< 15	-0.7 < PMV < +0.7

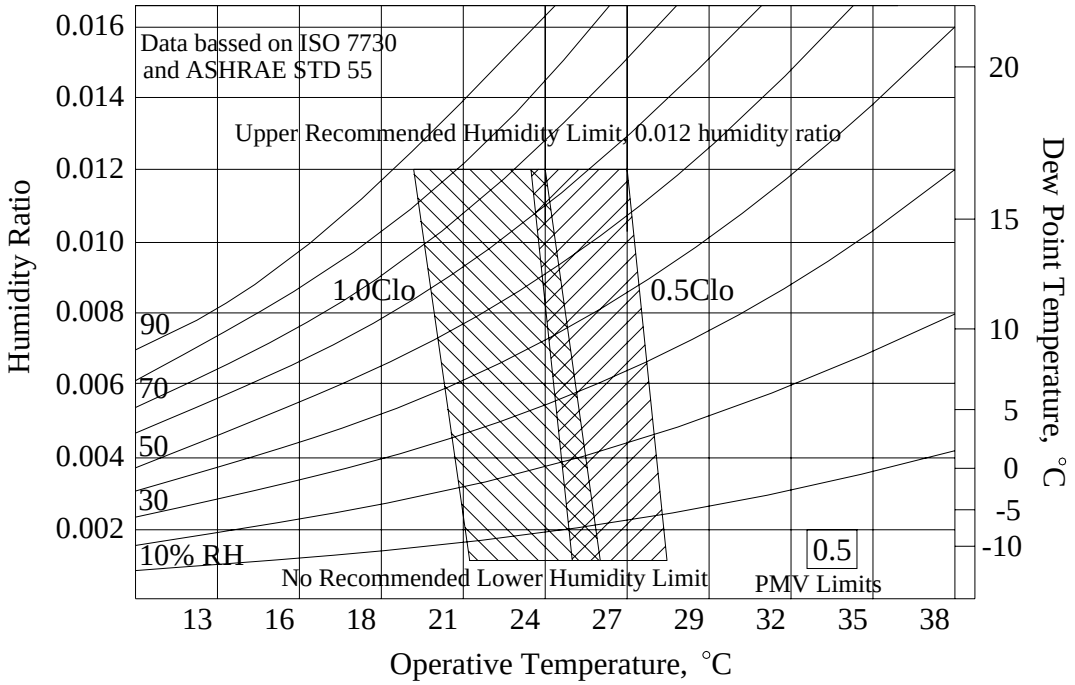

Fig. 7.2 Acceptable ranges of operative temperature and humidity for spaces corresponding to a Class B thermal environment [ANSI/ASHRAE 2004]

7.2.2 Simplifications of Fanger's PMV-PPD thermal comfort model for the experimental study

Fanger's PMV-PPD thermal comfort model is normally applicable to sedentary or near sedentary physical activity levels. In this experimental study, occupants were assumed to sit quietly or relax in an air conditioned space served by a DX A/C unit,

which could be considered as being in a sedentary physical activity level, therefore, Fanger's PMV-PPD thermal comfort model could be adopted as a base model.

The metabolic rate for quietly seated occupants was 1.0 met. It was further assumed that occupants were immobile, therefore,

$$M = 60\ W/m^2 \tag{7.13}$$

$$W = 0\ W/m^2 \tag{7.14}$$

According to ANSI/ASHRAE Standard 55, in hot and humid subtropical summer, the clothing normally wore by occupants provided a thermal insulation of 0.5 clo. This clothing value was also used in the current experimental study.

Based on the above assumptions, Equations (7.4) to (7.11) could be simplified as follows:

$$f_{cl} = 1.0 + 0.1 = 1.1 \tag{7.15}$$

$$t_{cl} = 21.324 - 0.327\,p_{av} - 6.720\times10^{-3}t_{adb,r} \tag{7.16}$$

$$\begin{aligned} L = {} & 34.078 - 4.35\times10^{-8}\left[(t_{cl}+273)^4 - (\bar{t}_r+273)^4\right] \\ & - 1.1h_c\left(t_{cl} - t_{adb,r}\right) + 4.088\,p_{av} + 0.084t_{adb,r} \end{aligned} \tag{7.17}$$

$$PMV = 0.0629L \tag{7.18}$$

There were four parameters: $\bar{t}_r$, $t_{adb,r}$, p_{av} , h_c in Equations (7.18) and (7.12) to determine the required indoor thermal comfort indexes, i.e., PMV and PPD, respectively. However, the convection heat transfer coefficient, h_c , was a function of air velocity, V ; the air vapor pressure, p_{av} , was a function of both indoor air dry-bulb temperature, $t_{adb,r}$, and air RH level, RH . These may be experimentally obtained for determining PMV and PPD indexes.

7.3 Experimentation

7.3.1 Experimental conditions

All the experiments were carried out under a given space total cooling load of 6.94 kW with a fixed application SHR of 0.69, using the heat and moisture load generating units (LGUs). This application SHR value was considered representative in residential buildings in the subtropics according to Chapter 4. On the other hand, to carry out experimental work under all possible speed combinations was neither practical nor necessary; therefore, representative discrete experimental compressor and supply fan speeds were selected. In the experimental work reported in this Chapter, the selected experimental compressor speed and supply fan speed are shown in Tables 7.2 and 7.3, respectively.

Table 7.2 Selected experimental compressor speed

	1	2	3	4	5	6
VSD Frequency (Hz)	57	66	75	84	92	101
Rotational speed (rpm)	3432	3960	4488	5016	5544	6072
% of maximum speed	40	50	60	70	80	90

Table 7.3 Selected experimental supply fan speed or airflow rate

	A	B	C	D	E	F	G
VSD Frequency (Hz)	26	31	36	41	46	50	55
Rotational speed (rpm)	1584	1872	2160	2448	2736	3024	3312
Supply airflow rate (m^3/h)	790	950	1110	1270	1420	1570	1700
% of maximum speed	30	40	50	60	70	80	90

During all experiments, the condenser cooling airflow rate was maintained constant at 3400 m^3/h, with a fixed condenser cooling air inlet temperature of 35ºC, using the existing PID controller in the experimental station. Refrigerant degree of superheat was also maintained constant at 6ºC by using the EEV and its associated PID controller in the experimental station.

An issue that needs special attention during the experimental work was the air heat gain from the supply fan. Due to the variable-speed operation of the supply fan, the air heat gain would vary with the varying supply airflow rate. Therefore, in order to maintain a constant total space cooling load and a fixed application SHR, the variation of supply fan heat gain at various supply fan speeds must be compensated by suitably adjusting the output from LGUs (see Section 7.3.4.1 for further details).

7.3.2 Measuring positions

For the four parameters to be obtained through experiments, indoor air dry-bulb temperature could be directly measured using the date acquisition system (DAS) of the experimental station, and indoor RH could be evaluated using both indoor air dry-bulb temperature, as well as wet-bulb temperature which is also directly measured using DAS. For the other two parameters, i.e., air velocity and MRT, according to ANSI/ASHRAE Standard 55 [2004], within an occupied zone, measurements should be made at locations where occupants are expected to spend their time. In this experimental station, the measuring points are shown in Fig. 7.3. There are totally 21 measuring points.

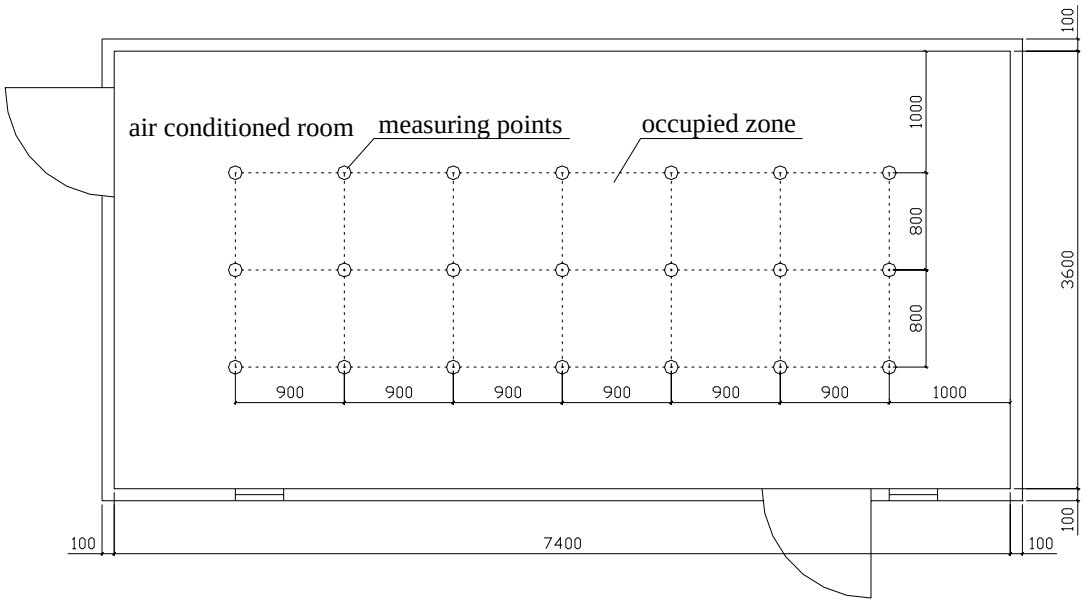

Fig. 7.3 Measuring points in the air conditioned room of the experimental station

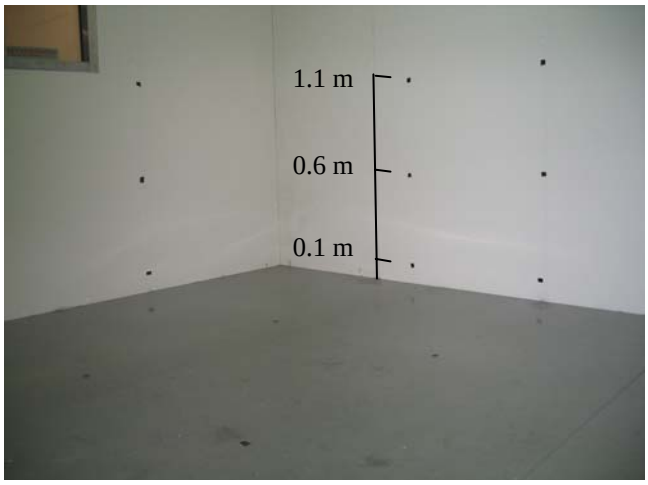

Fig. 7.4 Measuring points at three different levels (0.1, 0.6 and 1.1 m) in the air conditioned room of the experimental station

At these 21 measuring points (see Fig. 7.3), air velocity was measured at three different levels, i.e., 0.1, 0.6 and 1.1 m above floor level, corresponding to the ankle, waist and head levels of a seated occupant (see Fig. 7.4). On the other hand, globe temperature for determining MRT was measured at 0.6 m level for a seated occupant at these measuring points.

7.3.3 Measuring instruments for air velocity and MRT

Air movements in an air conditioned room are a combination of forced flow by its ventilation system and free convection flows caused by temperature differences in the room. Air movements would therefore vary in both magnitude and direction. The air velocity is of a stochastic nature and often non-stationary. According to ANSI/ASHRAE Standard 55, the air velocity should be measured free of the influence of flow direction, therefore, a 54N50 low velocity flow analyzer was used in the experimental study. The flow analyzer had a fast reacting omnidirectional

velocity sensor which is fully temperature compensated and built into the transducer housing (see Fig. 7.5). On the other hand, a black globe thermometer was used to measure globe temperature for the purpose of determining MRT [Vernon 1932, Bedford and Warmer 1935]. In each experimental condition, i.e., compressor speed and supply fan speed combination, the averaged room globe temperature, t_g, was obtained by averaging the readings at 0.6 m level from all 21 measuring points. Fig. 7.6 shows the setup of globe temperature measuring using a black globe thermometer in the air conditioned room.

(a) 54N50 low velocity flow analyzer

(b) Analyzer processor

(c) Velocity measuring point at 0.6 m height

(d) Velocity measuring point at 1.1 m height

Fig. 7.5 The 54N50 low velocity flow analyzer and its measurement setup in the air conditioned room

Fig. 7.6 A globe thermometer at 0.6 m height in the air conditioned room

7.3.4 Experimental results

7.3.4.1 Measured air heat gain from supply fan at different fan speeds and averaged indoor air velocity

At different speeds of supply fan in the experimental station, air heat gain from the supply fan, Q_{fhg}, was experimentally determined based on the difference of dry-bulb air temperatures up- and down-stream of the supply fan and the supply airflow rate:

$$Q_{fhg} = m_a C_{pa} \left(t_{adb,fi} - t_{adb,fo} \right) \tag{7.19}$$

where C_{pa} is the specific heat of air at constant pressure, m_a the supply air mass flow rate; $t_{adb,fi}$ and $t_{adb.fo}$ the dry-bulb air temperatures up- and down-stream of the supply fan, respectively.

Fig. 7.7 shows the air heat gain from supply fan at different fan speeds. As could be seen from the diagram, there are considerable differences in air heat gain at different fan speeds. In order to maintain a constant indoor cooling load and a fixed application SHR, the outputs from LGUs were correspondingly adjusted based on the heat gain characteristics shown in Fig. 7.7.

Fig. 7.8 illustrates the averaged indoor air velocity in the air conditioned room under the different supply fan speeds. It was obtained by averaging the 63 air velocity readings obtained in the 63 (21 × 3 different levels) measuring points in the air conditioned room. It might be seen that the averaged indoor air velocity has an approximately linear relationship with the supply fan speed. The maximum and minimum air velocities were 0.26 and 0.10 m/s at the supply air speed of 3312 and 1584 rpm, i.e., at 90% and 30% of the maximum supply fan speed, respectively. They both were below the recommended 0.3 m/s for residential buildings [Martin and Oughton 1995].

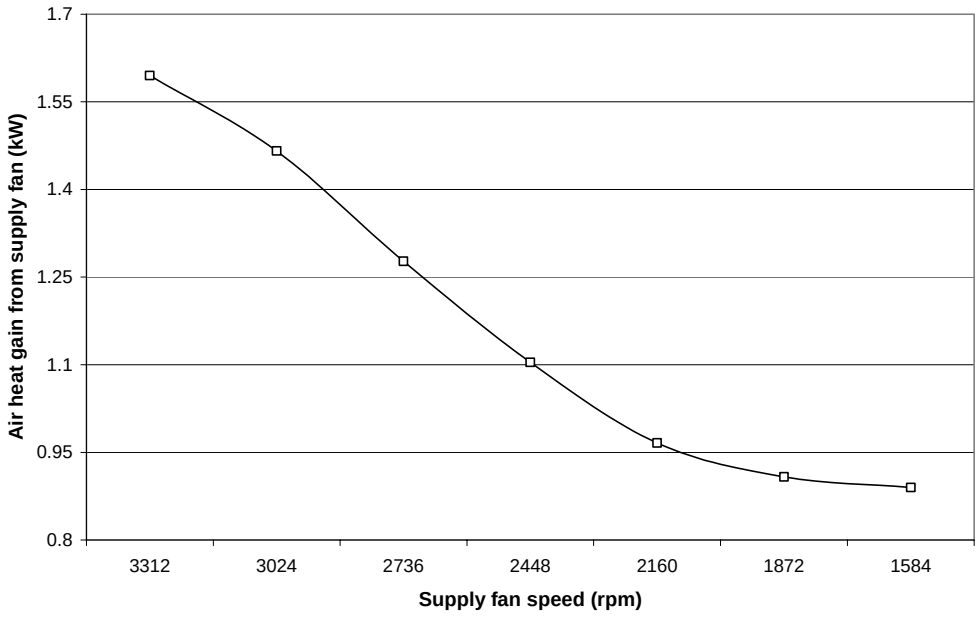

Fig. 7.7 Air heat gain from supply fan at different fan speeds

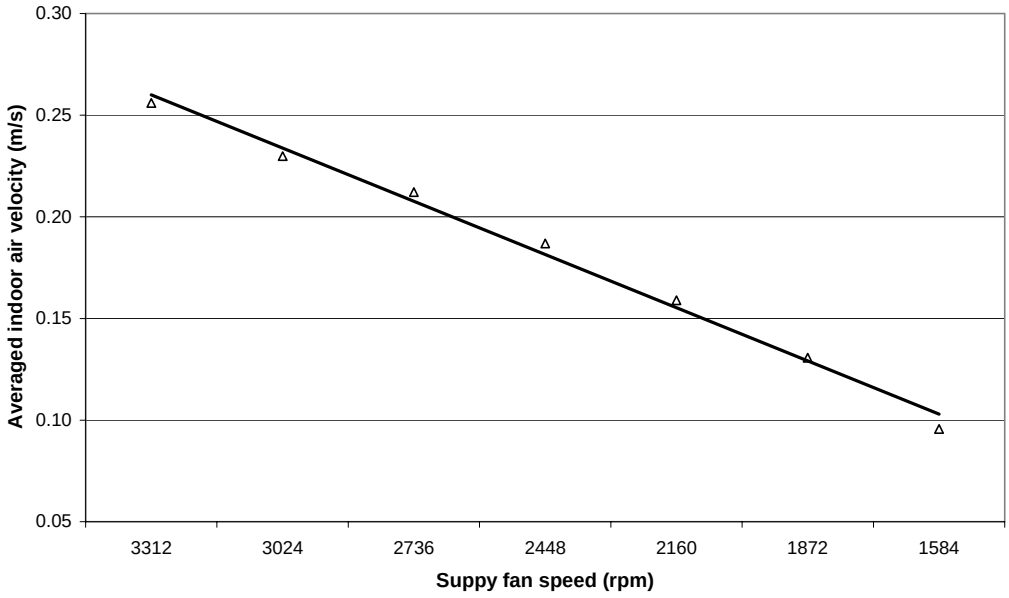

Fig. 7.8 Averaged indoor air velocity under different supply fan speeds in the air conditioned room

7.3.4.2 Measured indoor air dry-bulb temperatures and calculated RH levels

Fig. 7.9 and Fig. 7.10 show the measured indoor dry-bulb and wet-bulb air temperatures under different compressor speed and supply fan speed combinations at a fixed space cooling load condition, respectively. As seen in Fig. 7.9, for indoor dry-bulb air temperature at a fixed supply fan speed, increasing compressor speed would lead to a lower indoor dry-bulb air temperature, as more cooling was supplied to the air conditioned room via a lower supply air temperature. On the other hand, under a fixed compressor speed, reducing supply fan speed resulted in an increase, rather than a decrease of indoor dry-bulb air temperature. Similar variation patterns for indoor wet-bulb air temperature could also be observed from Fig. 7.10.

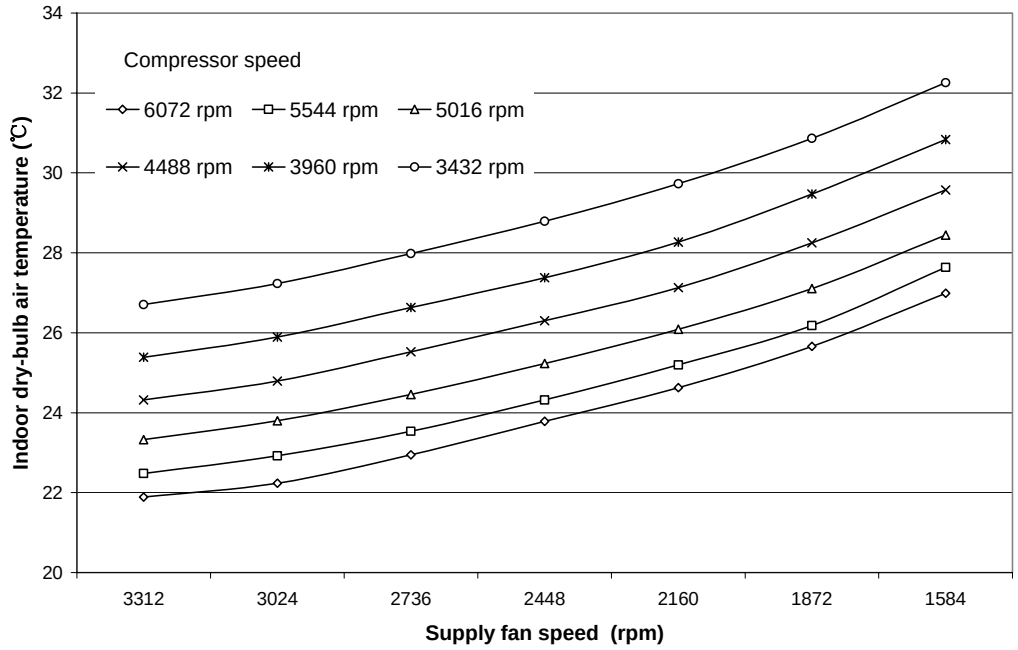

Fig. 7.9 Measured indoor dry-bulb air temperature under different compressor speed and supply fan speed combinations at a fixed space cooling load condition

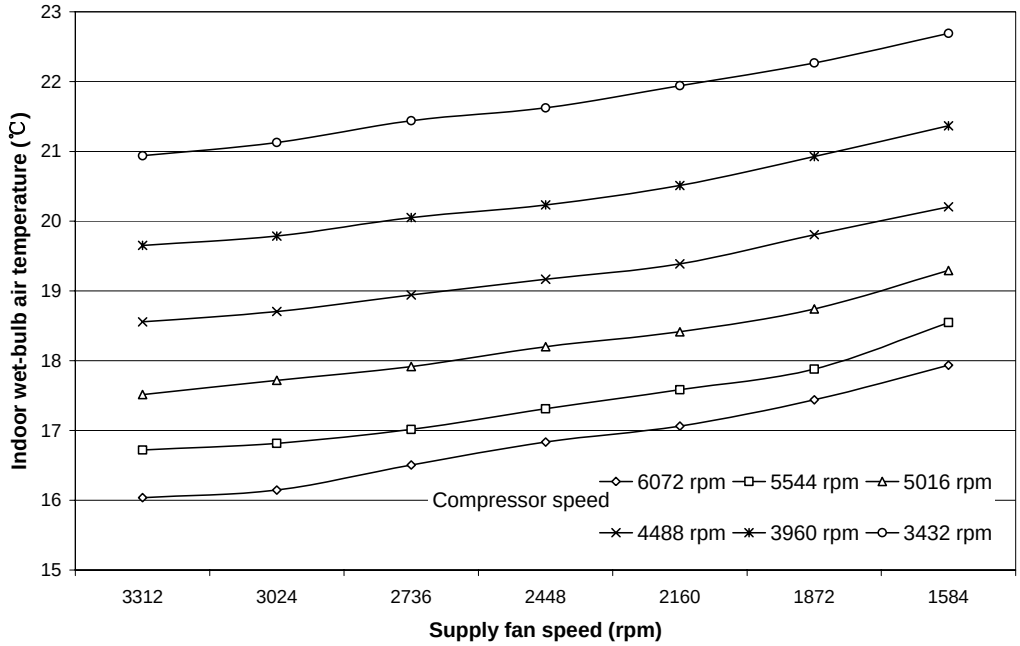

Fig. 7.10 Measured indoor wet-bulb air temperature under different compressor speed and supply fan speed combinations at a fixed space cooling load condition

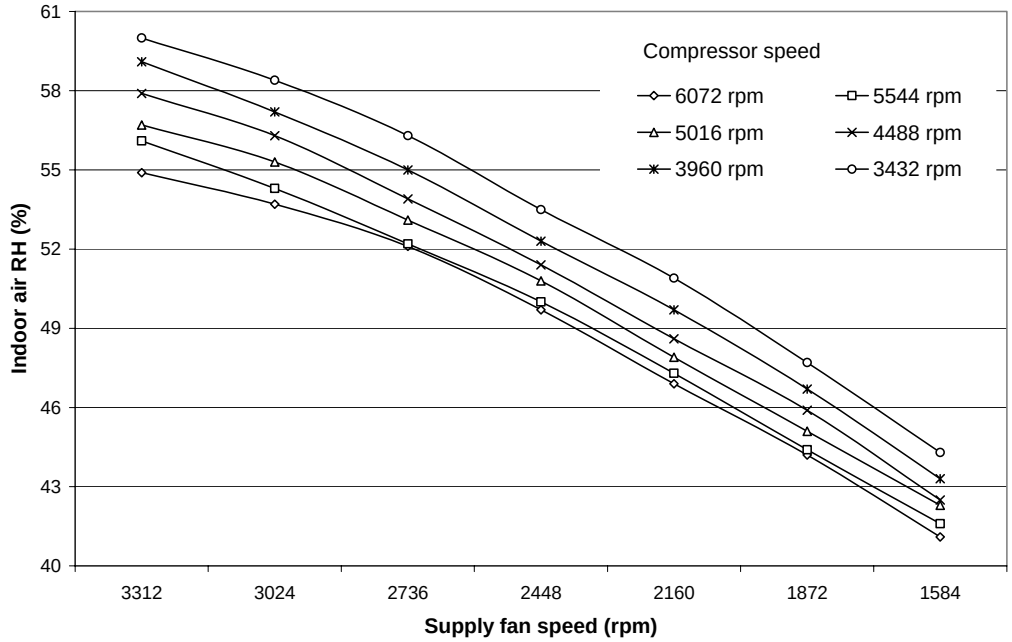

Fig. 7.11 Indoor air RH level under different compressor speed and supply fan speed combinations at a fixed space cooling load condition

With the availability of indoor dry-bulb and wet-bulb air temperatures, $t_{adb,r}$ and $t_{awb,r}$, respectively, indoor RH levels might also be evaluated. It could be seen from Fig. 7.11 that at a fixed compressor speed, RH level decreased rather quickly when the supply fan speed changed from its highest to its lowest because of a lower evaporator surface temperature that was resulted in due to that a lower face velocity across the evaporator would lead to better dehumidification. On the other hand, at a fixed fan speed, indoor RH level was rather low at higher compressor speed as more output cooling capacity was provided by the DX A/C unit for cooling and dehumidification.

7.3.4.3 Measured globe temperature and calculated MRT, PMV and PPD

Fig. 7.12 shows the averaged globe temperature in the air conditioned room under different compressor speed and supply fan speed combinations at a fixed space

cooling load condition. The variation pattern of the averaged globe temperature was very much similar to that of indoor dry-bulb air temperature shown in Fig. 7.9. Generally, under the same speed combination, the averaged globe temperature was higher than the dry-bulb air temperature by a mean value of 1.1℃.

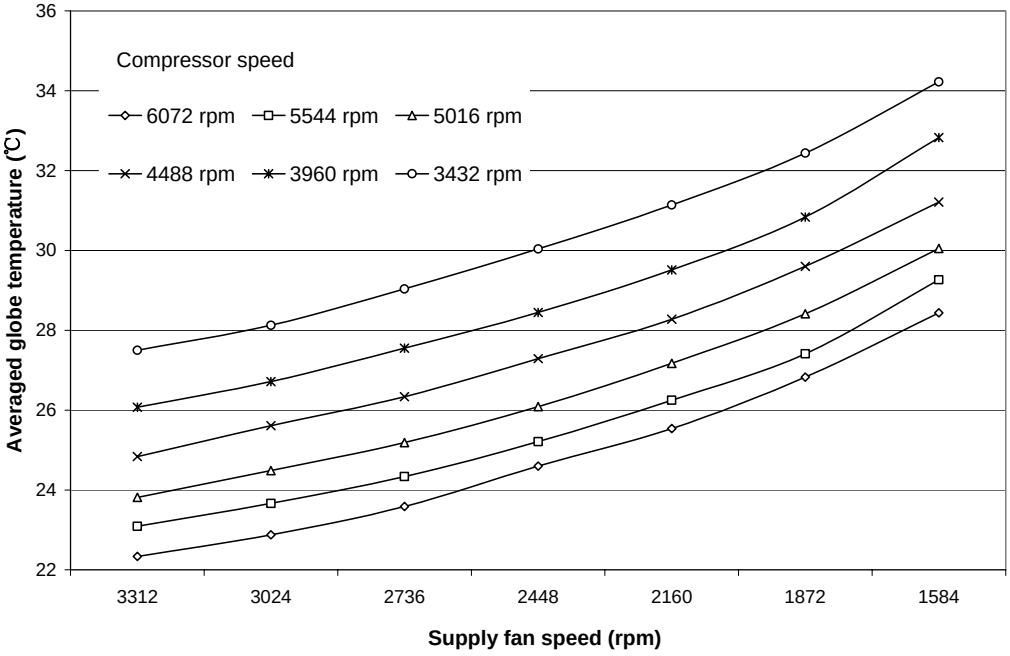

Fig. 7.12 Averaged globe temperature measured under different compressor speed and supply fan speed combinations at a fixed space cooling load condition

For each compressor and supply fan speed combination, after knowing the averaged indoor air velocity, dry-bulb air temperature and the averaged globe temperature, MRT could be evaluated. Fig. 7.13 illustrated the variation patterns of MRT in the air conditioned room under different compressor speed and supply fan speed combinations at a fixed space cooling load condition. Since MRT was determined based on largely the averaged globe temperature, its variation pattern was rather similar to that of the averaged globe temperature. Similarly, under the same speed combination, MRT was greater than indoor dry-bulb air temperature.

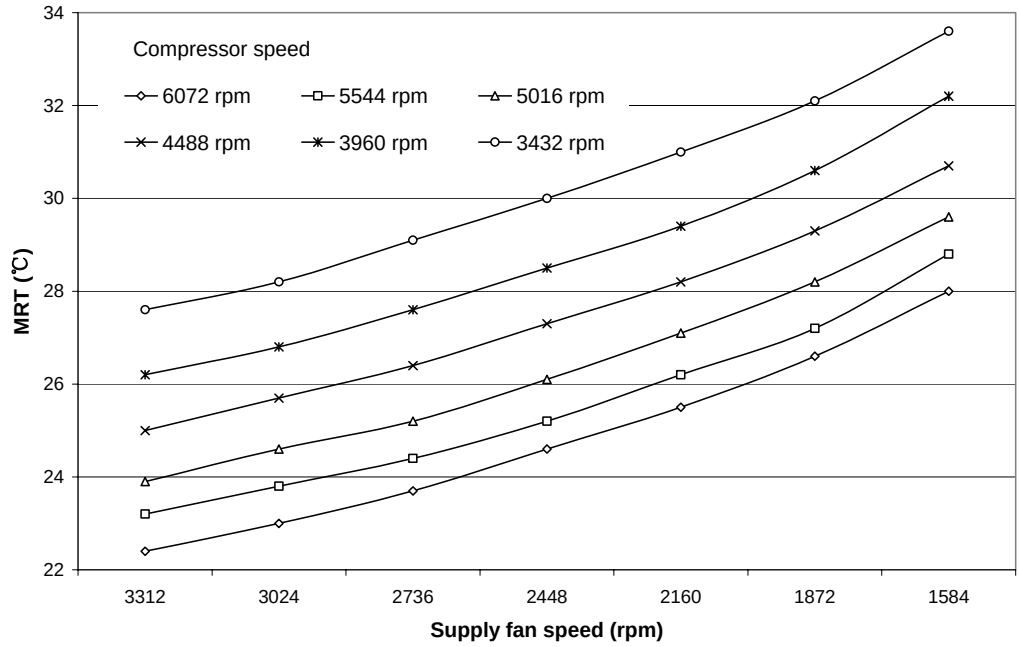

Fig. 7.13 MRT under different compressor speed and supply fan speed combinations at a fixed space cooling load condition

With the availability of all measured and calculated parameters, and using the conditions/assumptions specified in Section 7.2.2, PMV under different compressor speed and supply fan speed combinations at a fixed space cooling load condition has been evaluated using Equations (7.1) to (7.18) and illustrated in Fig. 7.14. According to Table 7.1, for comfort Class B, there were 16 experimental speed combinations that satisfied the comfort range of -0.5<PMV<0.5. Because the experimental compressor speeds and supply fan speeds were discrete, there were in fact a very large number of speed combinations within the solid bold line in Fig. 7.14 that could lead to the resulted PMV values within Class B range.

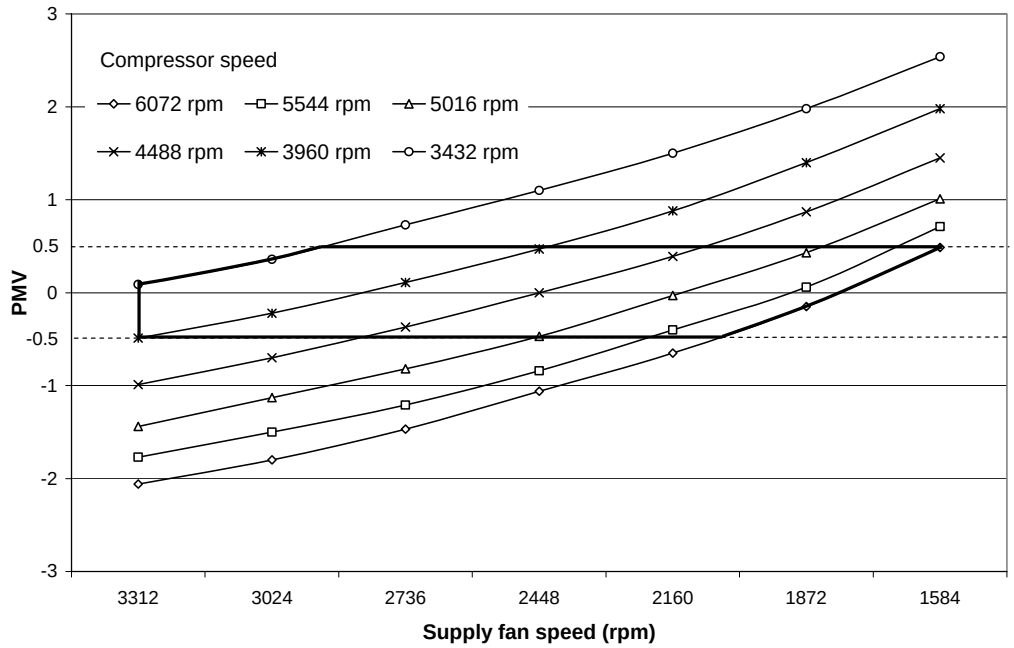

Fig. 7.14 PMV under different compressor speed and supply fan speed combinations at a fixed space cooling load condition

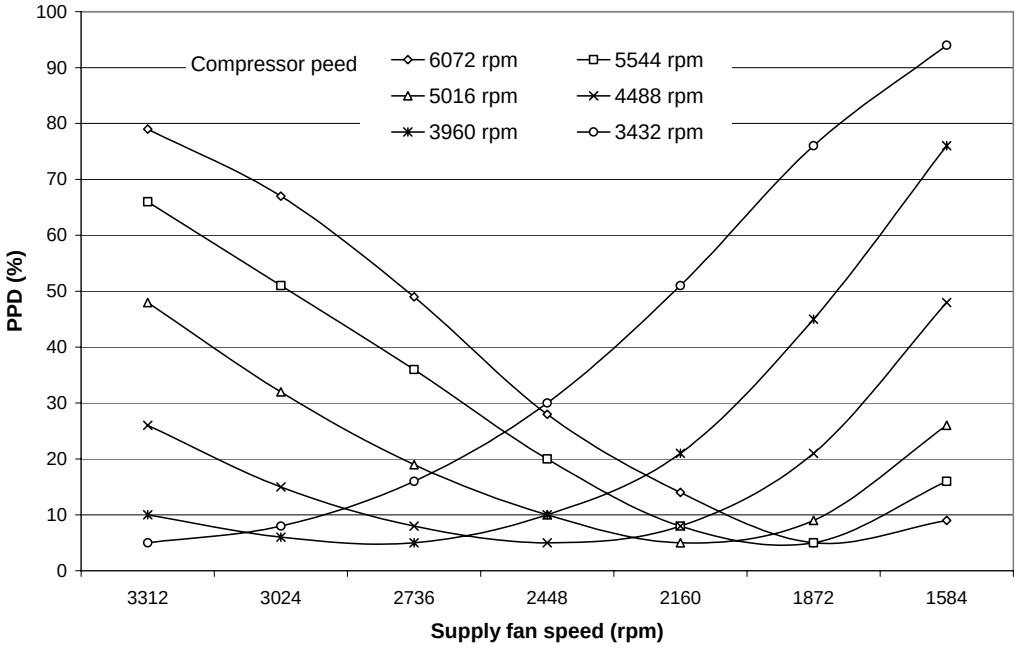

Fig. 7.15 PPD under different compressor speed and supply fan speed combinations at a fixed space cooling load condition

For all the compressor speed and supply fan speed combinations that resulted in the PMV values within the Class B range, i.e., -0.5<PMV<0.5, their corresponding PPD

values, which were calculated using Equation (7.12) and shown in Fig. 7.15, must be lower than or equal to 10%. There were also 16 discrete experimental speed combinations that could lead to PPD not greater than 10%.

7.3.4.4 The measured operating efficiency of the experimental DX A/C unit

In this experimental study, similar to that in Chapter 6, the index $COP_{com+fan}$ was used to evaluate the operating efficiency of the DX A/C unit. Fig. 7.16 shows the calculated $COP_{com+fan}$ values based on measured operating parameters of the DX A/C unit under different compressor speed and supply fan speed combinations at a fixed space cooling load condition. As seen, running the supply fan at a lower speed would make the DX A/C unit to have a higher $COP_{com+fan}$ at a fixed compressor speed. On the other hand, at a fixed supply fan speed, a lower compressor speed would lead to a higher $COP_{com+fan}$ value.

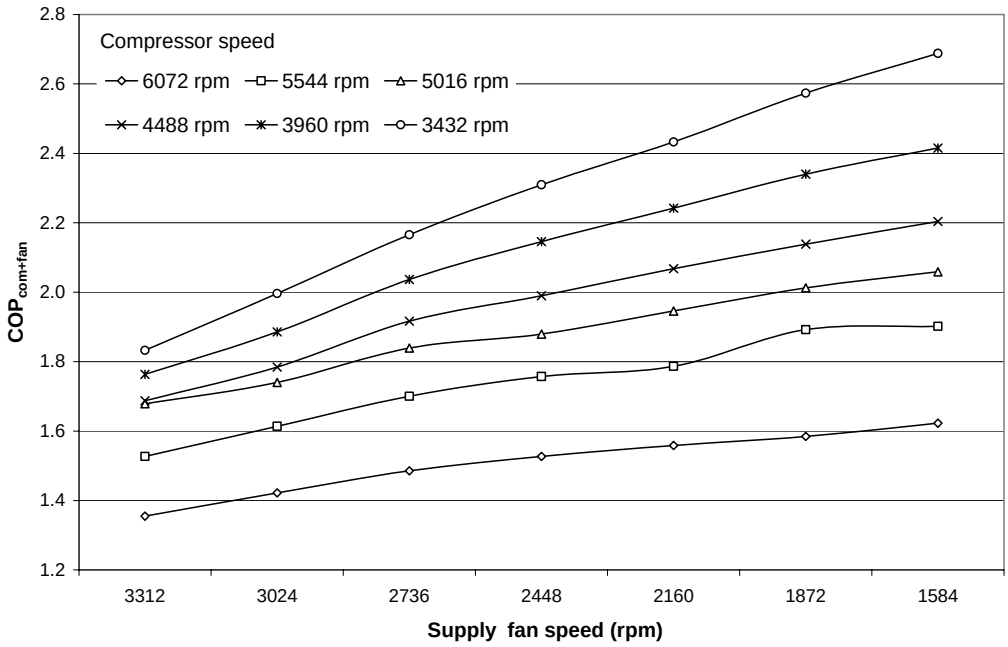

Fig. 7.16 The values of $COP_{com+fan}$ under different compressor speed and supply fan speed combinations at a fixed space cooling load condition

7.4 Discussions

The experimental results presented in Section 7.3 clearly suggested that at a fixed space load condition, for an air conditioned room served by a DX A/C unit, operating the A/C unit at different compressor speed and supply fan speed combinations would impact not only the indoor air dry-bulb temperature and RH level, but also indoor air velocity and MRT. These would, given activity level of, and clothing worn by occupants, affect indoor thermal comfort. In other words, varying compressor and supply fan speeds would directly affect indoor thermal comfort for occupants.

Table 7.4 The calculated PMV, PPD and the measured $COP_{com+fan}$

Combination	Compressor speed (rpm)	Supply fan speed (rpm)	Calculated PMV	Calculated PPD (%)	$COP_{com+fan}$
1	6072	1872	-0.15	5	1.585
2		1584	0.44	9	1.623
3	5544	2160	-0.4	8	1.786
4		1872	0.06	5	1.892
5	5016	2448	0.47	10	1.879
6		2160	-0.03	5	1.946
7		1872	0.43	9	2.012
8	4488	2736	-0.37	8	1.917
9		2448	0	5	1.99
10		2160	0.39	8	2.068
11	3960	3312	-0.49	10	1.763
12		3024	-0.22	6	1.886
13		2736	0.11	5	2.037
14		2448	0.47	10	2.146
15	3432	3312	0.09	5	1.832
16		3024	0.36	8	1.996

On the other hand, while the fundamental purpose of having A/C installations in buildings is to provide occupants with thermally comfortable environments, the operating energy efficiency of A/C installations is an important issue not to be neglected. As seen from Fig. 7.16, when its compressor speed and supply fan speed were varied, the operating efficiency of the DX A/C unit would also be varied. Hence, varying both speeds would also impact the operating efficiency of a DX A/C unit, in addition to impact indoor thermal comfort. From the experimental results shown in Figs. 7.14 to 7.16, there were 16 experimental speed combinations under which the calculated PMVs were within ± 0.5 or the calculated PPD$\leqslant$10%. The corresponding compressor speed, supply fan speed, calculated PPD and measured $COP_{com+fan}$ at these 16 combinations are shown in Table 7.4. It might therefore be clearly observed that although all the 16 speed combinations can lead to acceptable indoor thermal comfort for occupants, there were noticeable differences in the operating efficiency for the variable-speed compressor and supply fan DX A/C unit. The highest $COP_{com+fan}$ was at 2.146 and the lowest at 1.585, representing a percentage difference of 35.4%.

7.4 Conclusions

This Chapter presents an experimental study on the indoor thermal comfort characteristics under the control of a DX A/C unit having variable-speed compressor and supply fan at a fixed space cooling load condition. Although the results presented were based on a specific total space cooling load and a fixed application SHR, they were considered typical and representative.

The results of the experimental study suggested that under a given space total cooling load with a fixed application SHR, varying both compressor and supply fan speeds of a DX A/C unit would not only result in different indoor air temperatures and RH levels but also impact indoor air velocity and MRT, influencing consequently indoor thermal comfort. Experimental results showed that while appropriate indoor thermal comfort levels may be attained at different compressor speed and supply fan speed combinations, there are noticeable differences in the operating efficiency of the DX A/C unit.

The outcomes of the experimental study could possibly lead to the potential development of using indoor thermal comfort indexes, rather than indoor environmental parameters, such as indoor air dry-bulb temperature, for control purpose, with the constraint of operating a DX A/C unit at its highest possible energy efficiency.

Chapter 8

Developing a DDC-based Capacity Controller of a DX A/C Unit for Simultaneous Indoor Air Temperature and Humidity Control

8.1 Introduction

From the last two Chapters, it may be observed that the simultaneous variation of both compressor and supply fan speeds would result in changes in both the total output cooling capacity of the DX A/C unit and its equipment SHR. Therefore, when there were changes in both sensible and latent cooling loads in a space, or equivalently changes in application SHR, it was possible to simultaneously vary the speeds of compressor and supply fan, to have corresponding changes in the total output cooling capacity and equipment SHR, for simultaneous indoor temperature and humidity control.

There have been limited previously reported studies on the simultaneous control of both indoor air dry-bulb temperature and RH by varying the speeds of compressor and supply fan of a DX A/C unit as discussed in Section 2.3.7.2. The simulation results by Andrade et al. [2002] showed that the use of a variable-speed compressor and a variable-speed supply fan can help prevent short on-off cycling and improve humidity control, while possibly increasing the efficiency of a DX A/C unit by having different combinations of compressor and supply fan speeds at the expense of running the DX unit longer. It may be seen, however, that this study was also essentially for on-off cycling, not continuous, control over the condensing unit in the DX unit.

In addition, the experimental investigation by Krakow et al. [1995] indicated that to maintain indoor air temperature by varying compressor speed, and indoor RH by varying supply fan speed, separately, using PID control method, space temperature and RH may be controlled simultaneously. However, such a control strategy remained fundamentally inadequate; the transient performance of the two decoupled feedback loops (i.e., the control loop for temperature by varying compressor speed and that for RH by varying supply fan speed) was inherently poor, due to the strong cross-coupling between the two feedback loops. Nevertheless, this may be considered as an early pilot study on varying output sensible and latent cooling capacities of a DX A/C unit by altering its compressor and supply fan speeds to match the corresponding changes in space cooling loads or indoor air setpoints, so as to achieve simultaneous indoor air temperature and humidity control.

It can therefore be seen that artificially decoupling the control of two strongly coupled indoor air parameters, i.e., air temperature and RH, would only yield unsatisfactory control performance. On the other hand, it has been noted that SHR is an integrated variable relating to both sensible load and latent load, indirectly simultaneously affecting indoor air temperature and RH. Therefore, if the changes in application SHR due to changes in space cooling loads can be used as a control variable, then it is possible to take care of both indoor air temperature and humidity simultaneously, and the artificial decoupling of controlling both parameters can be eliminated.

With the rapid development of computer technology and direct digital control (DDC) technique, the computational and communication capacities of the controllers

available to HVAC industry have been greatly strengthened. A large number of operating parameters of HVAC equipment can be simultaneously real-time measured, monitored and processed. The real-time value of application SHR can then be evaluated and possibly used for control purpose.

This Chapter reports on the development of a novel DDC-based capacity controller for a DX A/C unit having variable-speed compressor and supply fan to simultaneously control indoor air temperature and RH in a conditioned space served by the DX A/C unit, using SHR as a controlled variable. Firstly, the core element of the capacity controller, a numerical calculation algorithm (NCA) based on a number of real-time measured operating parameters and the energy balance between the air side and the refrigerant side of the DX A/C unit to determine the speeds of both compressor and supply fan is introduced. This is followed by reporting the results of controllability tests of the DDC-based capacity controller at various testing conditions.

8.2 Development of the novel DDC-based capacity controller

The core element of the DDC-based capacity controller reported in this Chapter is a NCA, which consist of a psychrometirc analysis of the correlated changes between indoor air temperature and humidity, or the changes in application SHR due to the variations in space cooling loads, and uses the energy balance between the air side and the refrigerant side of a DX A/C unit. A number of real-time measured operating parameters in the DX A/C unit and the conditioned space served by the DX A/C unit

are required to be the input to the capacity controller. The NCA is detailed as follows.

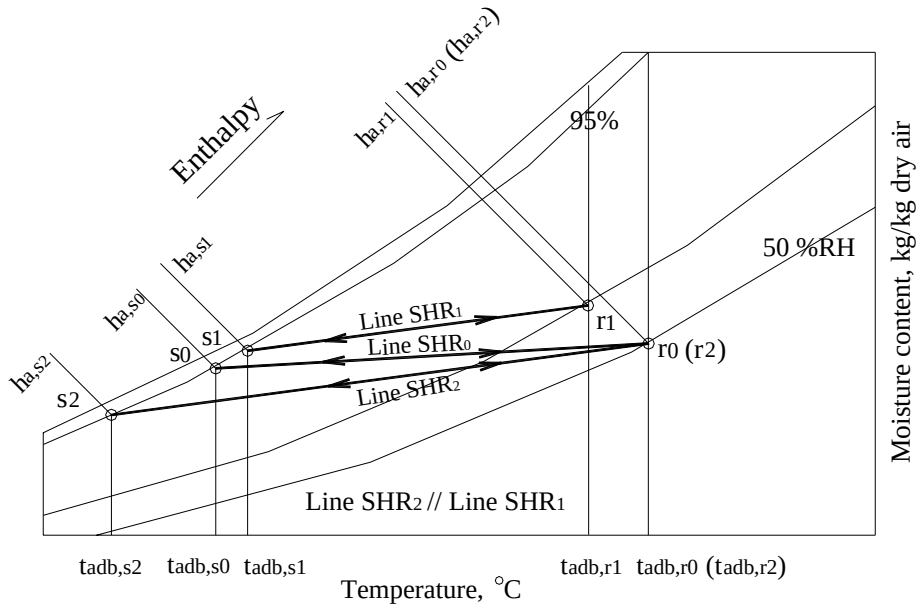

Fig. 8.1 Psychrometric analysis for realizing the NCA

Fig. 8.1 shows a psychrometric analysis for realizing the NCA. In order to simplify the development of the capacity controller, it is assumed that there is no outdoor air introduced into the DX A/C unit and the supply fan heat gain is neglected, on the basis that their contributions to the total space cooling load can be equivalently represented by other indoor cooling loads. It is also assumed that air is directly supplied from the DX A/C unit to the space without reheating at 95% saturation. In Fig. 8.1, point *r0* represents the required indoor air state. Therefore, the setpoints for indoor air dry-bulb temperature, wet-bulb temperature and enthalpy are $t_{adb,r0}$, $t_{awb,r0}$ and $h_{a,r0}$, respectively. Before any disturbance occurs to space sensible and latent cooling loads, the DX A/C unit supplies the air (at 95% saturation, point *s0*) to the conditioned space with its application SHR, SHR_{ap0}, at its dry-bulb temperature,

$t_{adb,s0}$, wet-bulb temperature, $t_{adb,s0}$, and enthalpy, $h_{a,s0}$, respectively. The supply air mass flow rate, or the airflow rate passing through the DX cooling coil is $m_{a,s0}$. All these parameters are either known (for setpoint values), or real-time measured (for temperature and air mass flow rate) and calculated (for enthalpy). On the other hand, the DX A/C unit is operated at its equipment SHR, SHR_{eq0}, with its compressor speed being n_{com0} and supply fan speed being n_{fan0}. Based on Chapter 6, at steady-state conditions, the equipment SHR is equal to application SHR, i.e., $SHR_{eq0} = SHR_{ap0}$.

When a disturbance to space sensible or/and latent cooling loads occurs, and if the speeds of both compressor and supply fan remain unchanged, SHR_{ap0} will gradually change to finally settle at a new application SHR, SHR_{ap1}. As a result, indoor air state will move from point *r0* to finally settle at point *r1* at $t_{adb,r1}$, $t_{awb,r1}$ and $h_{a,r1}$, respectively. At the same time, the supply air state would normally move to a new point, *s1*, at $t_{adb,s1}$, $t_{awb,s1}$ and $h_{a,s1}$, respectively. The move of supply air from point *s0* to point *s1* is essentially due to the changes in operating conditions of the DX A/C unit. However, points *s1* and *s0* are normally close to each other, since both compressor speed and supply fan speed are kept unchanged. At the steady-state condition, both equipment SHR and application SHR are also numerically equal to each other, i.e., $SHR_{eq1} = SHR_{ap1}$.

As can be seen in Fig. 8.1, when there are changes in both space sensible and latent cooling loads, and both the speeds of compressor and supply fan are kept unchanged,

indoor air state will depart from point *r0* to point *r1*, i.e., both indoor air temperature and RH are out of control. This is because even with $SHR_{eq1} = SHR_{ap1}$, the total output cooling capacity from the DX A/C unit remains essentially unchanged, and therefore, there can be either surplus or deficit of both sensible and latent components in the total output cooling capacity, causing the drift of indoor air state. For the example case shown in Fig. 8.1, there is a surplus in the output sensible cooling capacity, leading to a lower indoor air temperature; there is a deficit in the output latent cooling capacity, resulting in a higher indoor air moisture content. Therefore, the total output cooling capacity for the DX A/C unit will have to be adjusted to suit the new total space cooling load, with its equipment SHR to be maintained. Consequently, the DX A/C unit will output an appropriate total output cooling capacity, with a suitable ratio between its sensible and latent components to match the space sensible and latent loads, respectively, so that the required indoor air state setpoint may be maintained.

With the measured $t_{adb,r1}$, $t_{adb,s1}$ and the calculated $h_{a,r1}$, $h_{a,s1}$, SHR_{ap1} can be evaluated by:

$$SHR_{ap1} = \frac{C_{pa}(t_{adb,s1} - t_{adb,r1})}{h_{a,s1} - h_{a,r1}} \tag{8.1}$$

With the availability of SHR_{ap1}, the required new supply air point, *s2*, at $t_{adb,s2}$, $t_{awb,s2}$, and $h_{a,s2}$ can be determined by drawing a line parallel to line SHR_1 (connecting point *r1* and *s1*), line SHR_2, which starts from indoor air setpoint, *r2*(*r0*), and intersects with the 95% saturation line at point *s2*. Hence, the equipment SHR

value will be maintained after varying the total output cooling capacity from a DX A/C unit, i.e., $SHR_{eq2} = SHR_{eq1}$.

After both point *r1* and point *s1* are determined on a psychrometric chart, the new space sensible cooling load, Q_{as1}, and the new total cooling load, Q_{at1}, can be evaluated, respectively, as follows:

$$Q_{as1} = m_{a,s1} C_{pa} \left(t_{adb,r1} - t_{adb,s1} \right) \tag{8.2}$$

$$Q_{at1} = m_{a,s1} \left(h_{a,r1} - h_{a,s1} \right) \tag{8.3}$$

Where $m_{a,s1}$ is the air mass flow rate under SHR_{ap1}. Since the speed of supply fan remains unchanged, $n_{fan1} = n_{fan0}$, therefore, $m_{a,s1} = m_{a,s0}$.

In order to maintain the required indoor air settings at $t_{adb,r0}$ and $h_{a,r0}$, a new supply air mass flow rate, $m_{a,s2}$, may then be determined:

$$m_{a,s2} = \frac{Q_{as1}}{C_{pa} \left(t_{adb,r0} - t_{adb,s2} \right)} \tag{8.4}$$

or

$$m_{a,s2} = \frac{Q_{at1}}{h_{a,r0} - h_{a,s2}} \tag{8.5}$$

Therefore, a new supply fan speed, n_{fan2}, can be determined using the known supply fan operational characteristics. This completes the required change for supply fan speed.

On the other hand, the required refrigerant mass flow rate, m_{r2}, under the new space total cooling load can be determined based on the principle of energy balance between the air side and the refrigerant side in the DX A/C unit. The new total output cooling capacity from the DX cooling coil, Q_{rt1}, should be equal to the new total cooling load from the air side, i.e.,

$$Q_{rt1} = Q_{at1} \tag{8.6}$$

Therefore, the output cooling capacity can be adjusted to match the new space total cooling load by varying compressor speed.

After the occurrence of the disturbance to space cooling loads, the enthalpy of superheated refrigerant at compressor suction, $h_{r,sh1}$, can be evaluated based on the real-time measured pressure and temperature of superheated refrigerant using the R22 State Equations [Cleland 1986]. Neglecting the energy loss in the refrigerant line between DX evaporator and compressor suction owing to good thermal insulation, the enthalpy of the refrigerant leaving the DX evaporator is given by:

$$h_{r,o1} = h_{r,sh1} \tag{8.7}$$

The degree of refrigerant subcooling in a condenser with a receiver is normally rather small, and the refrigerant in the receiver can be assumed to be the saturated liquid refrigerant at condensing pressure. Therefore, after knowing the real-time measured condensing pressure, the enthalpy of refrigerant leaving the receiver, $h_{r,c1}$,

can be obtained using the R22 State Equations. Neglecting the energy loss in the refrigerant line and approximating the refrigerant throttling process in an EEV as being isenthalpic, the enthalpy of refrigerant entering the DX evaporator is given by:

$$h_{r,i1} = h_{r,c1} \tag{8.8}$$

Hence, the specific total output cooling capacity from the DX A/C unit can be evaluated by:

$$q_{rt1} = h_{r,o1} - h_{r,i1} \tag{8.9}$$

Consequently, the required refrigerant mass flow rate through the DX evaporator, to be provided by compressor, is obtained:

$$m_{r2} = \frac{Q_{rt1}}{q_{rt1}} \tag{8.10}$$

The specific volume of superheated refrigerant entering compressor, $v_{r,sh1}$, can be obtained from measured pressure and temperature of refrigerant at compressor suction using the R22 State Equations.

The swept volume of the rotor compressor, V_{com}, can be calculated based on compressor's geometric parameters, as follows:

$$V_{com} = \pi r^2 l \varepsilon (2 - \varepsilon) \tag{8.11}$$

where l is the stroke of cylinder; r the radius of rotor and ε the rotor relative eccentricity.

The compressor's overall displacement coefficient, λ_1, can be determined by:

$$\lambda_1 = \lambda_{v1}\lambda_p\lambda_{T1}\lambda_l \tag{8.12}$$

where λ_p is the pressure loss coefficient with a value approximately of 1.0; λ_l is the leakage coefficient, 0.98~0.92.

The compressor volumetric coefficient, λ_{v1}, is given by:

$$\lambda_{v1} = 1 - 0.015\left[\left(\frac{P_{r,comd1}}{P_{r,coms1}}\right)^{1/\beta} - 1\right] \tag{8.13}$$

where β is the compression index which is assumed to be constant at 1.18. $P_{r,comd1}$ and $P_{r,coms1}$ are the refrigerant pressures at both compressor discharge and suction, respectively.

λ_{T1} is the temperature coefficient and can be evaluated by [Chen 2005]:

$$\lambda_{T1} = 2.57\times10^{-3}T_{r,c1} + 1.06\times10^{-3}T_{r,sh1} \tag{8.14}$$

where $T_{r,c1}$ is the absolute refrigerant temperature at the condenser exit; $T_{r,sh1}$ the refrigerant degree of superheat at compressor suction that can be determined from measured refrigerant pressure and temperature leaving the evaporator using the R22 State Equations.

Based on the availability of m_{r2}, $v_{r,sh1}$, V_{com} and λ_1 from Equations (8.6) to (8.14), the required compressor speed can be determined by:

$$n_{com2} = \frac{m_{r2} v_{r,sh1}}{V_{com} \lambda_1} \tag{8.15}$$

This completes the required change for compressor speed.

It should be pointed out that the NCA described above is basically by reference to the configuration of the experimental station reported in Chapter 5. Therefore, for other DX A/C units with different configurations, minor modifications to the NCA may become necessary.

The following system's operating parameters of a DX A/C unit must be measured real-time so that the NCA can be completed: on-coil air dry-bulb and wet-bulb temperatures; the supply air mass flow rate; the refrigerant temperatures leaving both the evaporator and condenser; the refrigerant pressures at both compressor discharge and suction.

The flow charts for determining the speeds of both supply fan and compressor using the NCA are shown in Fig. 8.2 and Fig. 8.3, respectively.

As reported in Chapter 5, a LabVIEW logging & control (L&C) program has been developed specifically for the experimental DX A/C station. The L&C program provided an independent self-programming module (SPM) by which the novel controller developed for DX A/C units has been implemented.

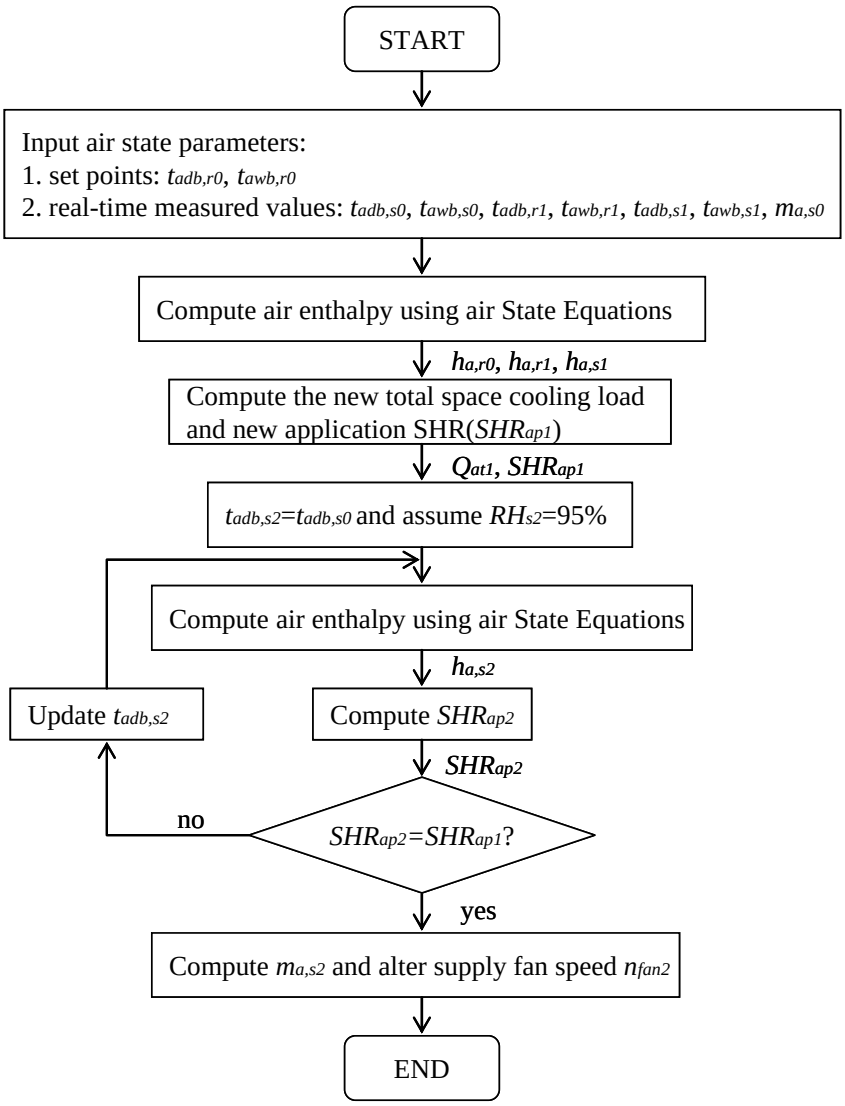

Fig. 8.2 Flow chart for determining supply fan speed using the NCA

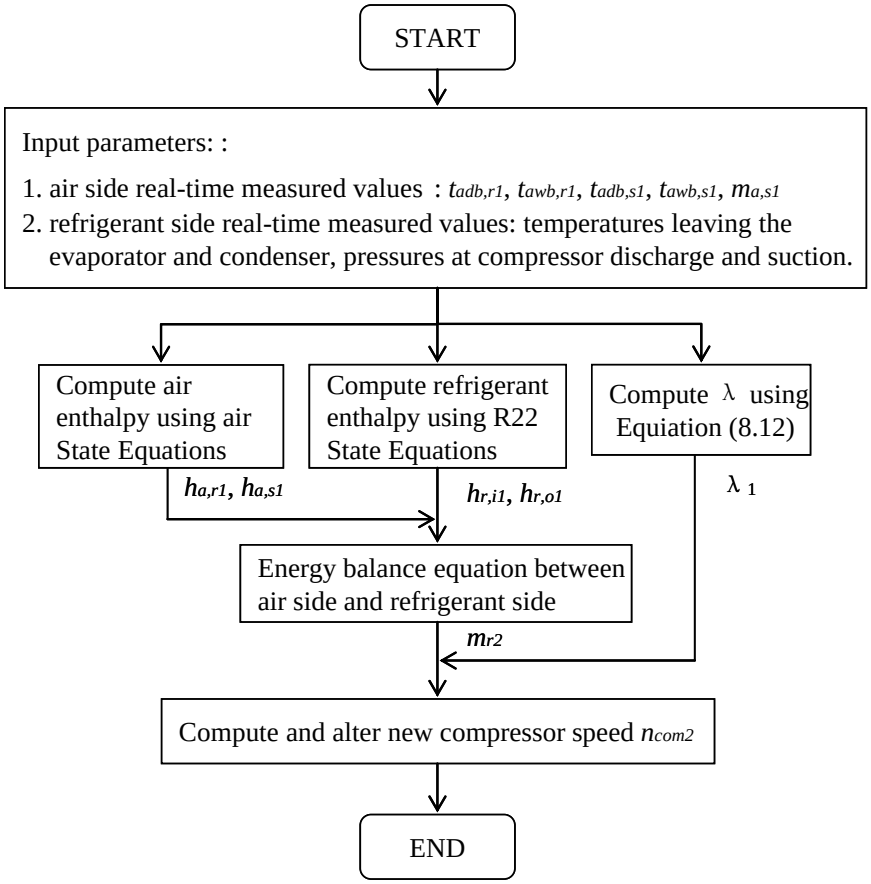

Fig. 8.3 Flow chart for determining compressor speed using the NCA

8.3 Controllability tests of the DDC-based capacity controller developed

Controllability tests of the DDC-based capacity controller developed have been carried out in the experimental DX A/C station reported in Chapter 5. For all the experimental results of the controllability tests reported in this section, the temperature and RH of air entering the DX cooling coil (or air temperature and RH inside the conditioned space in the experimental station) were fixed at 24°C and 50% RH, respectively. These were consistent with the indoor air setpoints used in Chapter 4. The total space cooling load was initially set at 7.5 kW consisting of a

sensible load of 6 kW and latent load of 1.5 kW, respectively. To maintain the required indoor air setpoints, the speeds of the compressor and supply fan were required to be set at 4488 and 3312 rpm which were 60% of the maximum compressor speed and 90% of the maximum supply fan speed, respectively. Therefore, at steady-state, based on the discussions in Chapter 6, both the application SHR and equipment SHR were 0.8, i.e., $SHR_{eq0} = SHR_{ap0} = 0.8$.

During each test, the experimental DX A/C station with the above operating parameters would have to run for an appropriate period of time, so that a steady-state operational condition arrived before the test started at *t=0 s*. At *t=600 s* (10 minutes), the internal sensible load was step-decreased by 1.6 kW to 4.4 kW, and the latent load step-increased by 1 kW to 2.5 kW, making a new space total cooling load of 6.9 kW and a new application SHR of 0.638. At steady-state, the numerical values of both equipment SHR and application SHR should be equal to each other, i.e., $SHR_{eq1} = SHR_{ap1} = 0.638$.

For all experiments reported in this Chapter, the condenser cooling airflow rate was maintained constant at 3100 m^3/h, with its inlet temperature fixed at 35ºC, using the existing PID controller in the experimental station. On the other hand, the refrigerant degree of superheat was also maintained constant at 6ºC by using the EEV and its associated PID controller in the experimental station.

The test conditions for all the controllability tests presented in this Chapter are listed in Table 8.1.

Table 8.1 Test conditions for all the controllability tests

No.	Test conditions
Test 1	No control introduced
Test 2	The DDC-based capacity controller activated at *t=3600 s*
Test 3	The DDC-based capacity controller activated at *t=1350 s*
Test 4	The DDC-based capacity controller activated at an interval of 750 seconds from *t=1350 s* to the end of test period
Test 5	The DDC-based capacity controller activated at an interval of 750 seconds from *t=1350 s*, until indoor RH was within a pre-set range, the DDC-based capacity controller was replaced by a PI controller for the supply fan speed while the compressor speed was kept unchanged

8.3.1 Results of Test 1

In this sub-section, the test results, without introducing any control after the step load changes at *t=600 s*, are presented. The purpose of the test was to provide a basis for determining when the information required for activating the DDC-based capacity controller became available.

Fig. 8.4 shows the variation profiles of various air temperatures over the entire test period of 7800 seconds. Since there was no control introduced, the speeds of compressor and supply fan remained unchanged at 4488 and 3312 rpm, respectively, during the whole test period. In the first 600 seconds from *t=0 s*, before the step load changes were introduced, indoor air temperatures entering the DX cooling coil were kept at their respective setpoints, 24ºC dry-bulb and 17.06ºC wet-bulb (with an equivalent indoor RH of 50%). After the step-changes at *t=600 s*, due to the thermal capacitance of space air, indoor dry-bulb air temperature started to drop at *t=740 s*, i.e., with a delay of 140 seconds. With the total space cooling load and sensible

cooling load reduced, air temperatures gradually decreased. Fig. 8.5 illustrates the indoor air RH variation profile over the test period. After the space latent cooling load was step-increased and the sensible cooling load step-decreased at *t=600 s*, indoor RH level began to rise. Both figures show that at the end of the test period, both indoor temperature and RH significantly deviated from the setpoints of 24°C and 50%, at 20.3°C and 64.3%, respectively. It was further noted that at the end of the test period, both indoor dry-bulb temperature and RH were not yet stabilized, which was clearly due to the thermal inertia of both the heat and moisture LGUs and indoor air.

The variation profile of application SHR is shown in Fig. 8.6. Before the load step-changes were introduced, application SHR was maintained at around 0.8. At *t=600 s*, application SHR decreased rather quickly from *t=600 s* to *t=1800 s*, fluctuating around a steady value of 0.654 towards the end of the test period. At the end of the test period (*t=7800 s*), a steady-state operation might be approximately assumed, therefore, $SHR_{eq1} = SHR_{ap1} = 0.654$. However, this was slightly higher than the new application SHR set at 0.638 after the step-changes of space cooling loads, representing a 2.5% deviation. The deviation was attributable to the increased sensible heat gain through the envelope of the conditioned space at a resultant lower indoor air dry-bulb temperature. This also explained that the total space cooling load at the end of the test period was slightly higher than the total heat output of 6.9 kW from the LGUs, as shown in Fig. 8.7.

From *t=0 s* to *t=600 s*, both indoor air temperature and RH were maintained at their respectively setpoints, therefore, the total output cooling capacity provided by the

DX A/C unit was close to the total space cooling load of 7.5 kW. At *t=600 s*, when the space step load changes was introduced, the speeds of compressor and supply fan remained virtually unchanged, and therefore, the total output cooling capacity from the DX A/C unit was approximately kept at 7.5 kW. Given the new space cooling loads and the new application SHR of 0.654 (SHR_{ap1}) after the introduction of the step-changes, there existed a notable difference between the space sensible and latent cooling loads and the corresponding output sensible and latent cooling capacities of the DX A/C unit even with the same equipment SHR value of 0.654 (SHR_{eq1}), resulting in an uncontrolled indoor air temperature and RH. For example, in Fig. 8.4, indoor air dry-bulb temperature dropped below 21ºC from its setpoint of 24ºC, because the output sensible cooling capacity from the DX A/C unit was at 4.9 kW (7.5 kW×0.654), which was greater than 4.4 kW of indoor sensible cooling load from the LGUs.

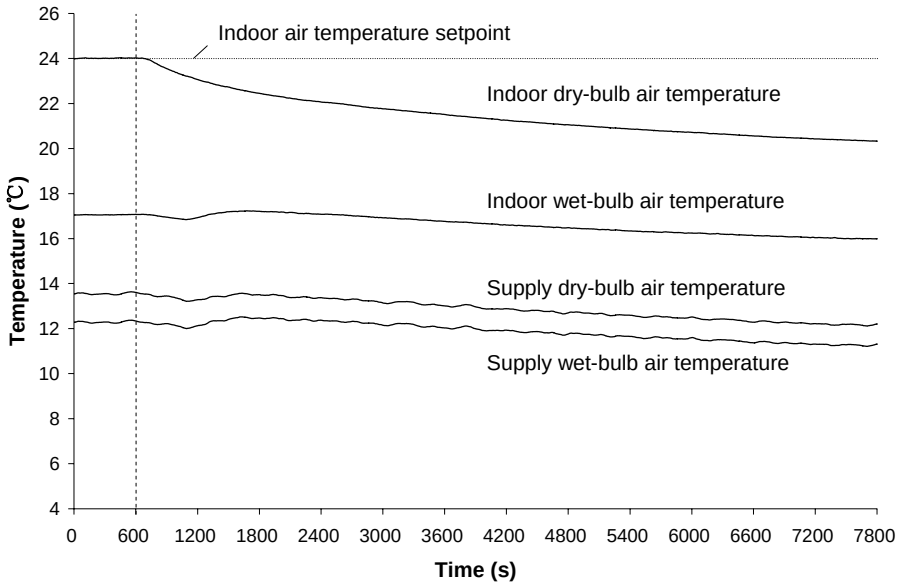

Fig. 8.4 Air temperature variation profiles (Test 1)

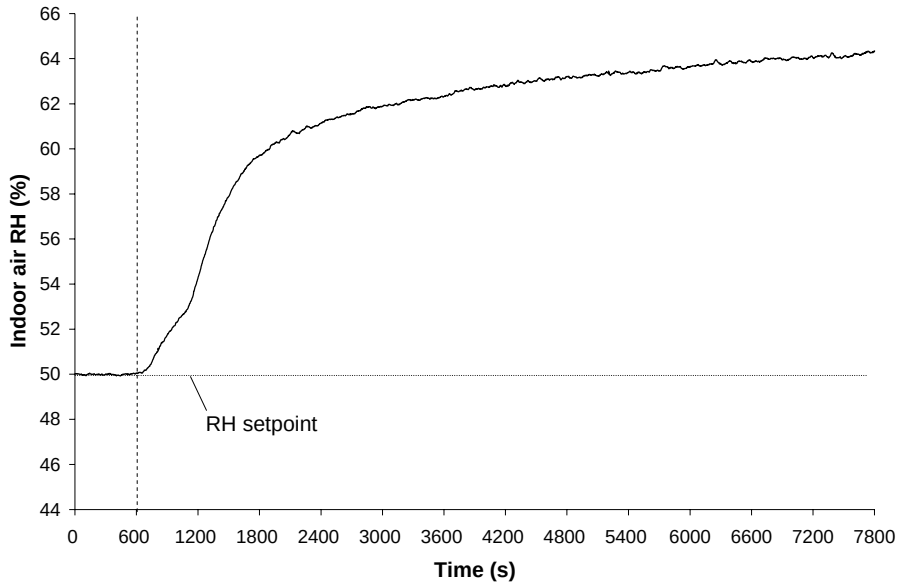

Fig. 8.5 Indoor air RH variation profile (Test 1)

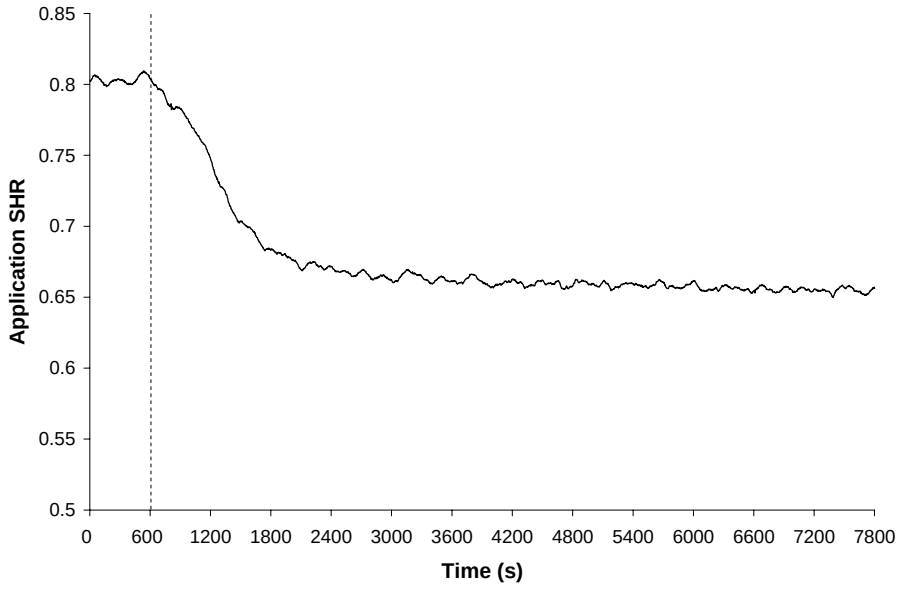

Fig. 8.6 Application SHR variation profile (Test 1)

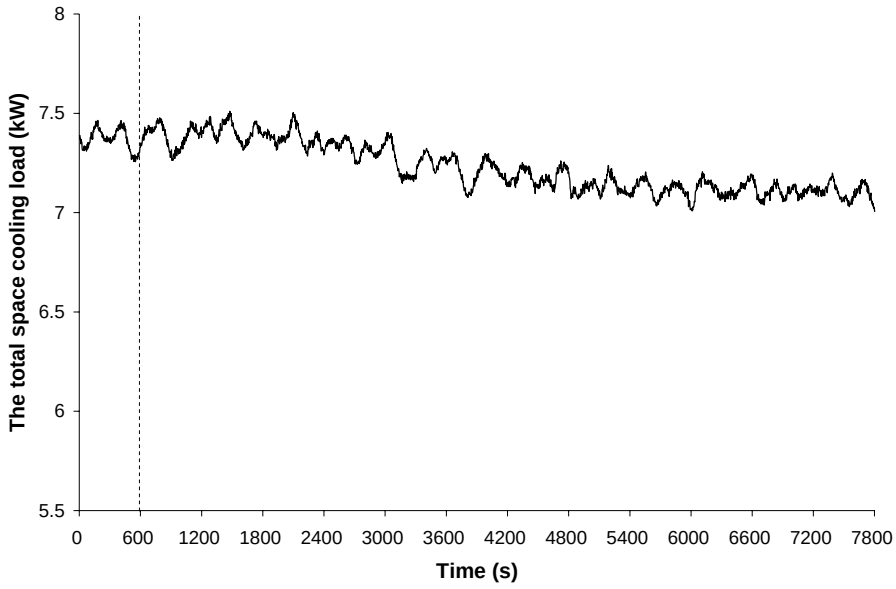

Fig. 8.7 The total space cooling load variation profile (Test 1)

8.3.2 Results of Test 2

From the results of Test 1 presented in Section 8.3.1, it was clear that it would take a pretty long time for the information of the changes of application SHR, which was required by the NCA for simultaneously controlling indoor air temperature and RH, to become available. As seen in Fig. 8.6, at the end of the period of Test 1, i.e., *t=7800 s*, or two hours after the introduction of the step-changes, the application SHR was 0.654. It was however considered unreasonable to wait for 2 hours in order to get adequate information to activate a control action. On the other hand, it was noticed that at *t=3600 s*, or 50 minutes after the step-changes, the application SHR was 0.661 (see Fig. 8.6), 1.1% greater than the application SHR of 0.654 at *t=7800 s*. Therefore, it was considered appropriate to activate the DDC-based capacity controller at *t=3600 s*, to examine its control sensitivity and accuracy.

It must be pointed out that delaying activating control due to the waiting for information required for control action to become available would yield poor control sensitivity. In this case, waiting for 2 hours, when the information required for control, i.e., the value of application SHR, would be expected to yield better control accuracy. However, this would also lead to very poor control sensitivity with such a long waiting (idling) period. Nonetheless, although shortening the waiting period may help improve control sensitivity, but at the expense of reduced control accuracy.

Therefore, in the current Test 2, at *t=3600 s*, the novel DDC-based capacity controller was activated, using the application SHR value of 0.652 at that instant (see Fig. 8.10) as an input to the NCA. In Test 2, at *t=3600 s*, the application SHR was at 0.652, which was slightly lower than 0.661 of the application SHR at *t=3600 s* in Test 1, because of different ambient conditions when carrying out both Tests. In Test 2, the compressor speed was consequently changed from 4488 to 4393 rpm and the supply fan speed from 3312 to 1647 rpm, respectively, using the NCA. Correspondingly, the supply airflow rate was reduced from 1700 to 825 m^3/h.

Fig. 8.8 shows the air temperature variation patterns of activating the controller at *t=3600 s*, after the same load step-changes at *t=600 s*. From the inherent operational characteristics of a DX A/C unit with variable-speed compressor and supply fan presented in Chapter 6, lowering compressor and supply fan speeds would lead to a lower total output cooling capacity of the DX A/C unit and a lower refrigerant evaporating temperature. Therefore, indoor dry-bulb air temperature began to increase when the controller was activated at *t=3600 s*, and returned to its setpoint of 24ºC at *t=10800 s*, i.e., 2 hours after putting the controller into action. At the same

time, supply air temperatures decreased sharply by 4.6ºC from *t=3600 s* to *t=4200 s*, primarily due to the sudden decrease of the supply airflow rate. After *t=4200 s*, supply air temperatures started to gradually increase.

Fig. 8.9 illustrates the variation pattern of indoor air RH. Again based on Chapter 6, reducing the speeds of both compressor and supply fan could help achieve the desirable dehumidification effect. It could be observed from the diagram that within the 1700 seconds after the controller was activated, i.e. from *t=3600 s* to *t=5300 s*, indoor RH decreased rather quickly from 63% to 52%, and close to the setpoint of 50% towards the end of the test period.

Fig. 8.10 shows the application SHR's variation profile over the period of Test 2. It could be seen that when the controller was put into action immediately after *t=3600 s*, the application SHR noticeably reduced to 0.565 from 0.652, and then gradually returned to the final steady value of 0.658. On the other hand, the DX A/C unit reached its steady operational state at the end of test period, its equipment SHR was numerically equal to application SHR, i.e., $SHR_{eq2} = SHR_{ap2} = 0.658$, which was 0.9% greater than 0.652, the value of application SHR, or SHR_{ap1}, input to NCA for determining the new speeds of both compressor and supply fan. Therefore, the equipment SHR of the DX A/C unit was basically maintained after the speeds of compressor and supply fan were varied.

Fig. 8.11 shows the variation profile of the total output cooling capacity of the DX A/C unit. Based on Chapter 6, lowering compressor and supply fan speeds would lead to a lower total output cooling capacity. As seen from the diagram, after the

changes of compressor and fan speed, there was a significant drop in the total output cooling capacity. Finally, it settled at 6.8 kW at the end of the test period. This demonstrated that the DDC-based capacity controller was able to regulate the output cooling capacity for the DX A/C unit to offset the changes in space cooling loads. The difference of 0.1 kW between the space cooling load of 6.9 kW and the output cooling capacity of 6.8 kW from the DX A/C unit was considered to be attributable to the fluctuating ambient temperature during the test period and uncertainty of real-time measurement for relevant operating parameters.

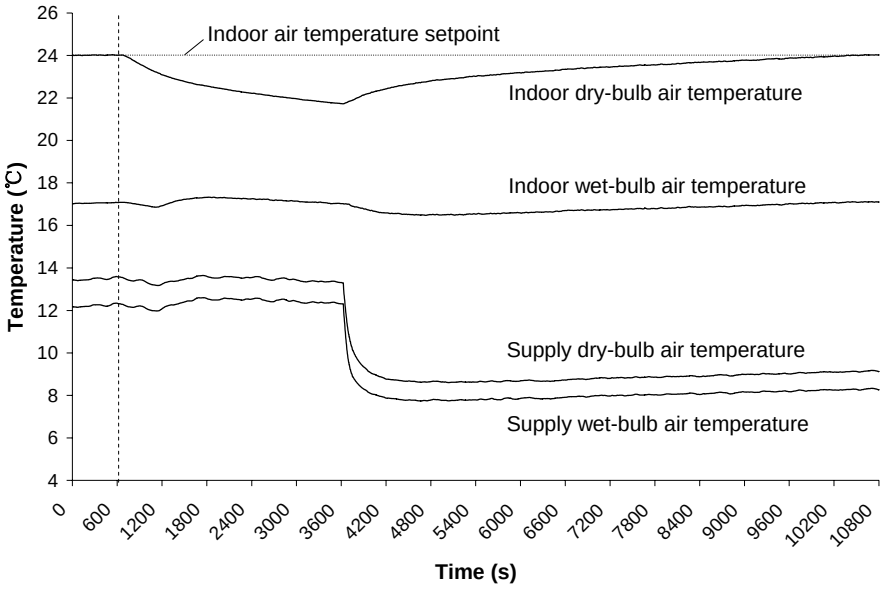

Fig. 8.8 Air temperature variation profiles (Test 2)

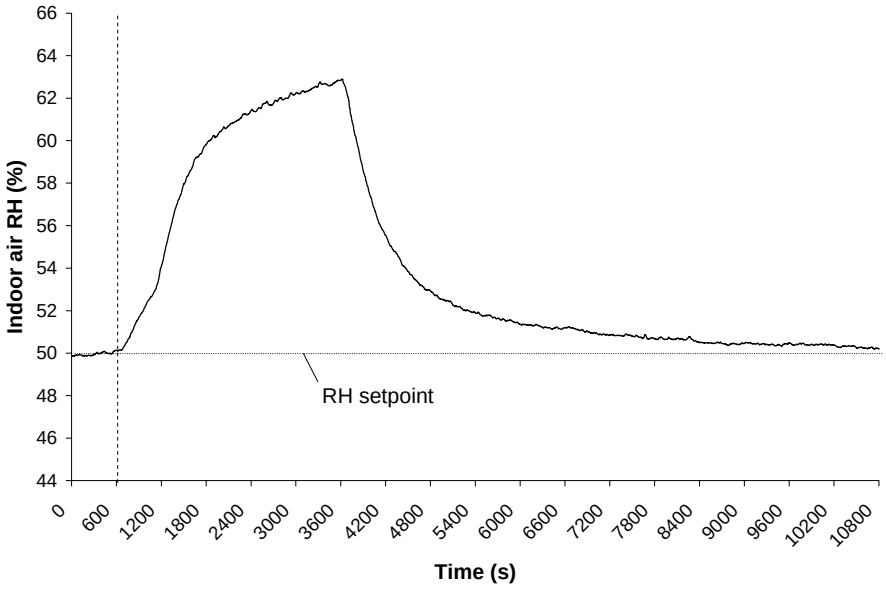

Fig. 8.9 Indoor air RH variation profile (Test 2)

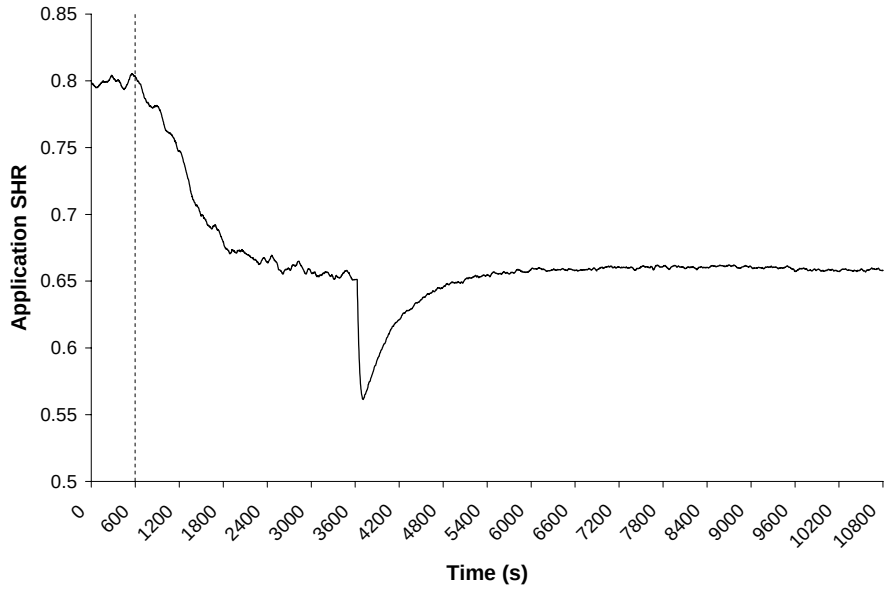

Fig. 8.10 Application SHR variation profile (Test 2)

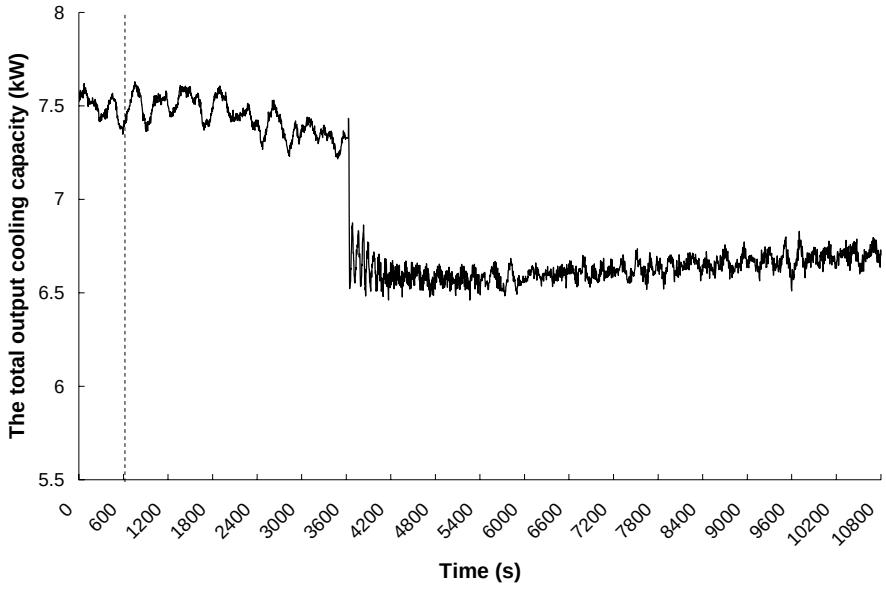

Fig. 8.11 The total output cooling capacity variation profile for the DX A/C unit (Test 2)

As can be seen from Fig. 8.10 and Fig. 8.11, the DDC-based capacity controller could not only suitably adjust the total output cooling capacity from the DX A/C unit, but also maintain an equipment SHR which was numerically equal to an application SHR. Therefore, the DX A/C unit would output appropriate sensible and latent cooling capacities to deal with space sensible and latent cooling loads, respectively. As a result, the simultaneous control for both indoor air dry-bulb temperature and RH became realistic.

8.3.3 Discussions

According to Figs. 8.8 to 8.11, the results of controllability Test 2 where the controller developed was enabled at *t=3600 s* suggested that the capacity controller developed for simultaneous indoor temperature and humidity control was

operational, with acceptable control accuracy. It was however noted that it had to wait for 3000 seconds after the load step-changes for the information required by the NCA to become available, leading to an unacceptable control sensitivity. Therefore, attempts to improve control sensitivity must be made.

On the other hand, for the specified step-changes in space cooling load, i.e., step-decrease from 6.0 kW to 4.4 kW for sensible load, and step-increase from 1.5 kW to 2.5 kW for latent load, using the DDC-based capacity controller developed, the change in compressor speed was insignificant, from 4488 down to 4393 rpm, or from 60% down to 58.2% of its maximum speed. However, the change in supply fan speed was much more significant, from 3312 down to 1647 rpm, or from 90% down to 32.2% of its maximum speed. The corresponding change airflow rate was from 1700 down to 825 m^3/h. These clearly suggested that the supply airflow rate was of primary concern as far as indoor humidity control was concerned. This agreed well with the findings from previous related studies [Khattar et al. 1987, Chuah et al. 1998, Khattar and Henderson 1999, Kurtz 2003, Hourahan 2004].

8.4 Attempts to improve the poor control sensitivity experienced by the DDC-based capacity controller

8.4.1 Results of Test 3 (Reducing the waiting time)

Attempts to improve the poor control sensitivity experienced by the capacity controller through reducing the waiting time were made, where the controller was

activated at *t=1350 s* (Test 3), or 750 seconds after the introduction of step load changes, respectively. It was expected that introducing the controller earlier may help reduce the waiting time, thus improving the control sensitivity at the expense of potentially reducing control accuracy, since the information required for accurate control action may not yet be accurately available, according to the results of Test 1.

In this Test, the DDC-based capacity controller was activated at *t=1350 s*, using the application SHR value of 0.71 at that moment. The controller increased the compressor speed from 4488 to 4573 rpm, and lowered the supply fan speed from 3312 to 2203 rpm, respectively. The corresponding airflow rate was decreased from 1700 to 1135 m^3/h. Comparing to the results in Test 2, both speeds were higher.

Figs. 8.12 to 8.15 illustrate the variation profiles of air temperatures, indoor air RH, application SHR and the total output cooling capacity in Test 3, respectively. It could be seen from Fig. 8.12 and Fig. 8.15 that both indoor air temperature and RH, at the end of test period, significantly deviated from their respective setpoints. This clearly indicated that the use of a pre-matured application SHR value would lead to poorer a control accuracy. As far as the output cooling capacity from the DX A/C unit was concerned, since the compressor was running at a higher speed, it stood at 7.1 kW at the end of Test 3.

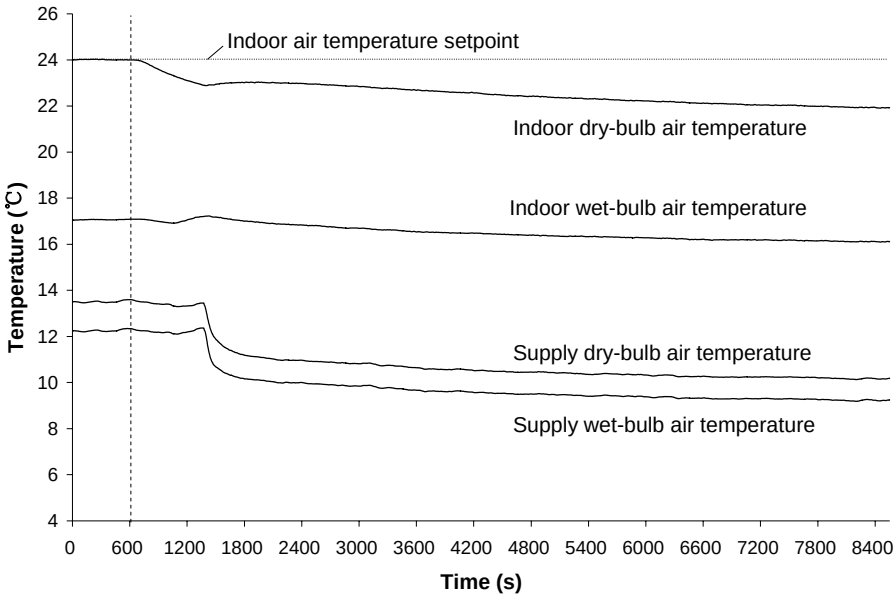

Fig. 8.12 Air temperature variation profiles (Test 3)

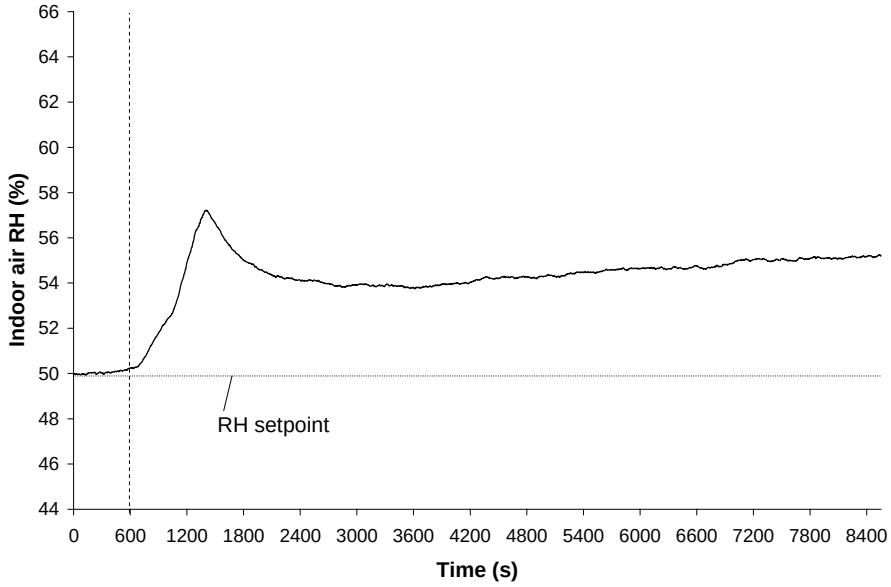

Fig. 8.13 Indoor air RH variation profile (Test 3)

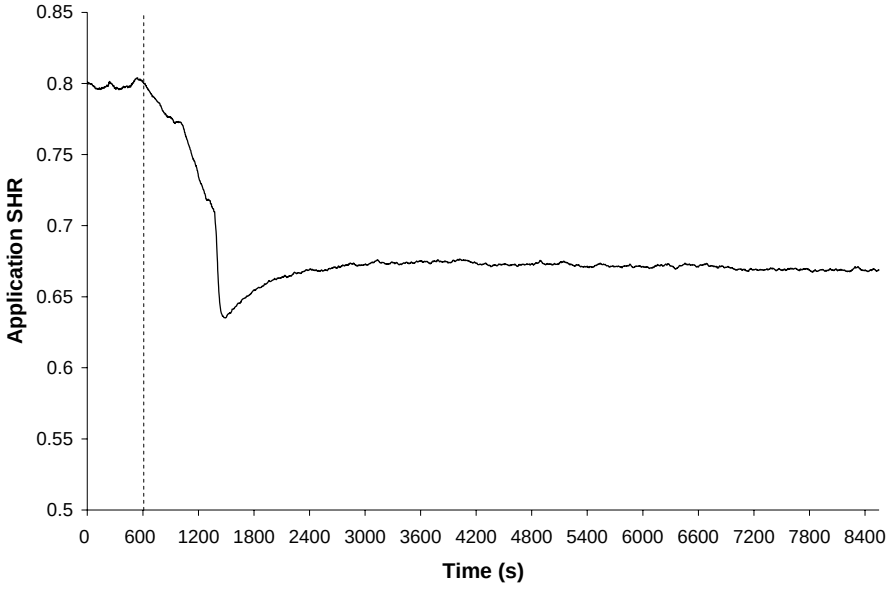

Fig. 8.14 Application SHR variation profile (Test 3)

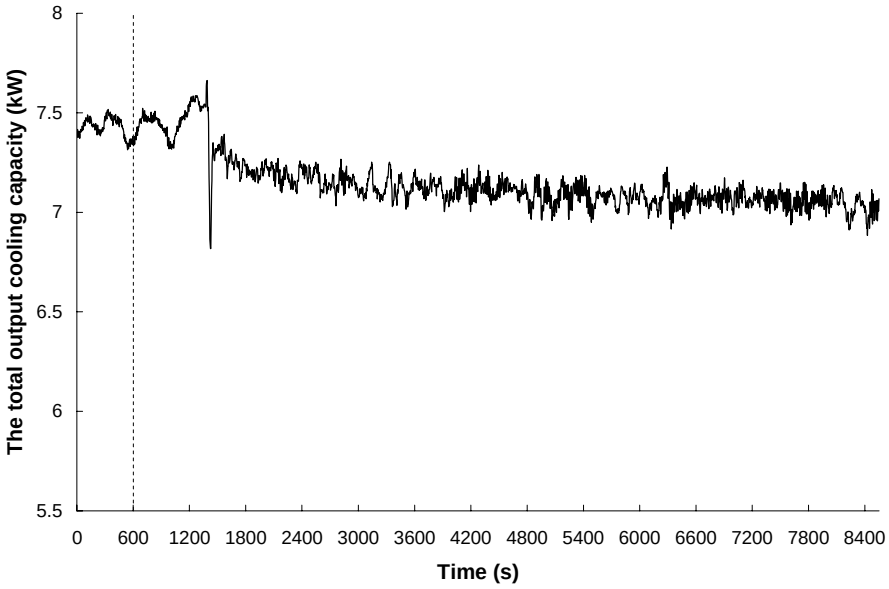

Fig. 8.15 The total output cooling capacity variation profile for the DX A/C unit (Test 3)

By looking at the results from Test 3 and comparing these with the results of Test 2, it was clear that the earlier the controller was introduced, the poorer the control accuracy, because of less information being available to the controller. This clearly illustrated that the control sensitivity might be improved at the expense of reduced

control accuracy, which was however considered unacceptable as it did not make sense to improve control sensitivity by losing control accuracy. Nonetheless, waiting for a long time in order to allow the information required by the DDC-based capacity controller to become available was neither acceptable. Therefore, further attempts at improving control sensitivity without losing control accuracy must be made.

8.4.2 Results of Test 4

The results from Test 3, i.e., introducing the controller 750 seconds after the occurrence of step load changes, provided some useful insights to the intended further attempts. It could be seen from both Fig. 8.12 and Fig. 8.13 that after the DDC-based capacity controller was activated, both indoor air temperature and RH were brought closer to their respective setpoints for a short while, and then levelled, and started to depart from their setpoints. Therefore, in Test 4, the controller was also initially activated at $t=1350$ *s*, i.e., 750 seconds after the step load changes, and was re-activated afterwards at an interval of 750 seconds, till the end of the test at 6600 seconds. Therefore, totally the controller was introduced for five times during the test. The compressor and supply fan speeds at different intervals as determined by the DDC-based capacity controller are shown in Table 8.2. Table 8.3 lists the values of application SHR, indoor air temperature and RH at the end of each interval.

Table 8.2 Compressor and supply fan speeds during different intervals (Test 4)

Time (s)	0-600	600-1350	1350-2100	2100-2850	2850-3600	3600-4350	4350-6600
Compressor speed (rpm)	4488	4488	4562	4409	4261	4177	4045
% of maximum speed	60	60	61.4	58.5	55.7	54.1	51.6
Supply fan speed (rpm)	3312	3312	2290	1745	1526	1431	1357
% of maximum speed	90	90	54.5	35.6	28.0	24.7	22.1
Supply airflow rate (m^3/h)	1700	1700	1180	880	760	705	665

Table 8.3 Application SHR, indoor air temperature and RH at the end of each interval (Test4)

Time (s)	600	1350	2100	2850	3600	4350	6600
Application SHR	0.803	0.653	0.673	0.666	0.663	0.664	0.665
Indoor air temperature (°C)	23.99	22.87	22.90	23.17	23.50	23.82	24.66
Indoor RH (%)	50.18	56.32	54.51	51.47	49.91	48.77	47.18

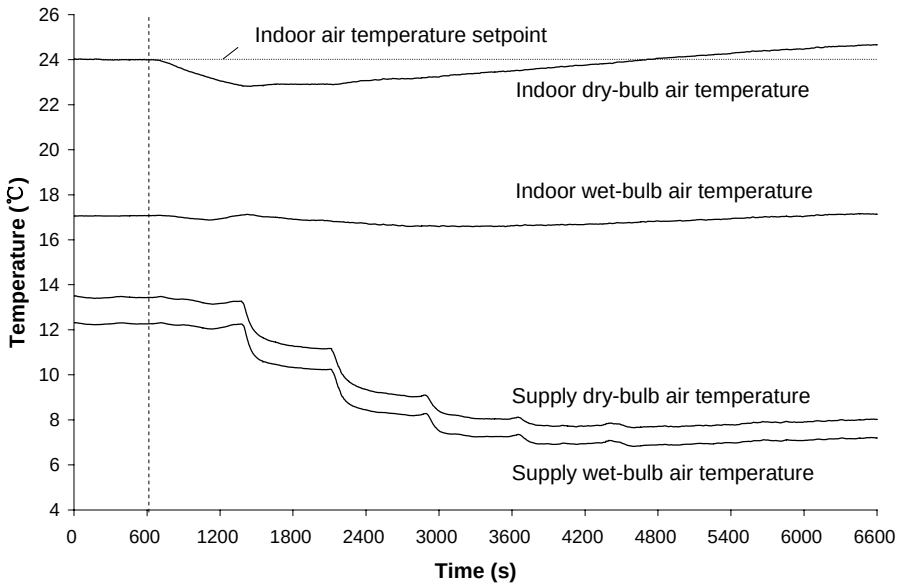

Fig. 8.16 Air temperature variation profiles (Test 4)

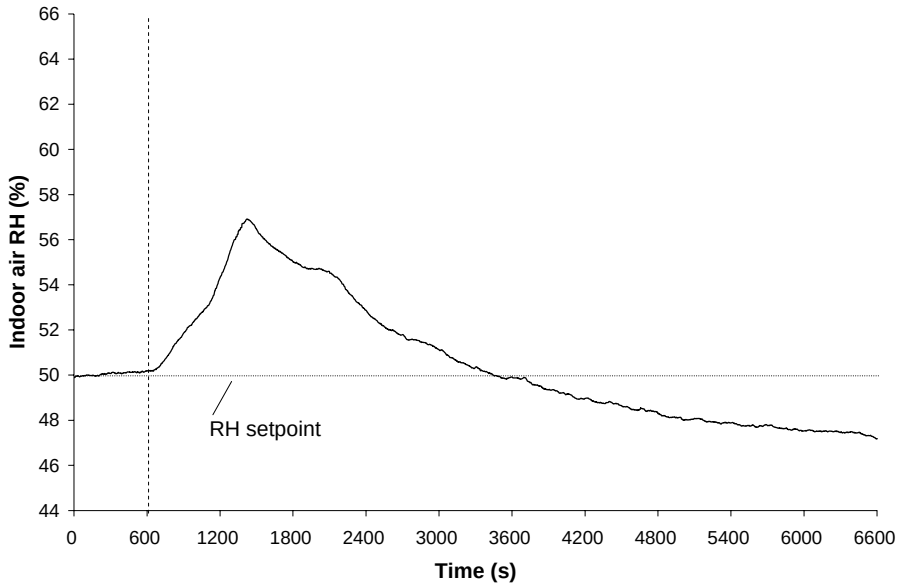

Fig. 8.17 Indoor RH level variation profile (Test 4)

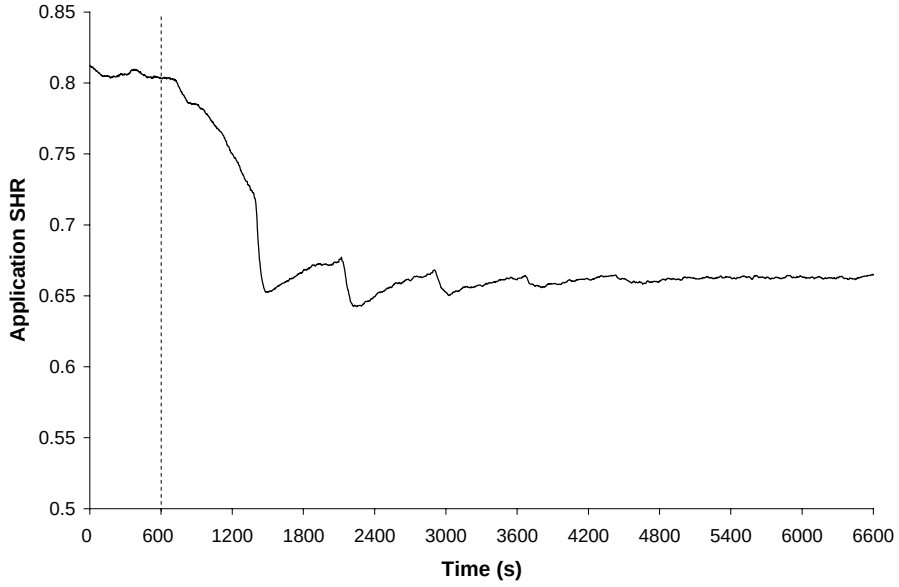

Fig. 8.18 Application SHR variation profile (Test 4)

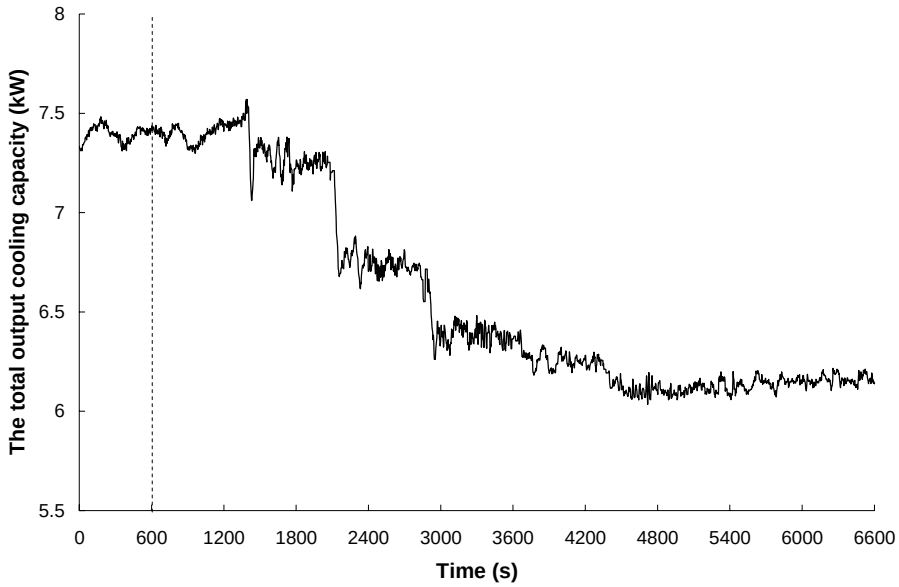

Fig. 8.19 The total output cooling capacity variation profile for the DX A/C unit (Test 4)

Results of controllability Test 4 are shown in Figs. 8.16 to 8.19. As seen in Fig. 8.16 and Fig. 8.17, indoor RH level returned to its setpoint 2100 seconds after the first activation of the controller, even after the indoor dry-bulb temperature was at 23.44ºC. However, since there was no mechanism to cease the action of the DDC-base capacity controller, when the setpoints were reached, the controller was kept to be brought in at the pre-set interval of 750 seconds, causing both indoor air temperature and RH to deviate from their respective setpoints. Although the application SHR could be finally settled at 0.662, as seen in Fig. 8.18, after the five times of the activations of the controllers, the final output cooling capacity from the DX A/C unit was only at 6.2 kW because of the lower speeds for both compressor and supply fan, as shown in Fig. 8.19. A lower output cooling capacity was considered to be the “culprit” for the poor accuracy.

8.4.3 Results of Test 5

As reported in Section 8.4.2, although the attempt to activate the DDC-based capacity controller at a fixed interval was not successful, it shed light upon the direction of further attempts to achieve both control accuracy and sensitivity by introducing a mechanism to cease the operation of the DDC-based capacity controller. The mechanism was to integrate a traditional PI controller for regulating the supply fan speed into the DDC-based capacity controller, so that when the indoor RH level was within a pre-set range of its setpoint, the compressor speed would then remain unchanged, while the supply fan speed would be controlled by the PI controller using the deviation of actual indoor RH from its setpoint as a control signal. This was because by using the DDC-based capacity controller, the change in compressor speed was of relatively small magnitude, and that in supply fan speed was much more significant.

In the current test, Test 5, the upper and lower limits of indoor RH level were fixed at 52% and 48%, respectively. At *t=1350 s*, the DDC-based capacity controller was activated for the first time, so that both indoor air temperature and RH were brought closer to their setpoints. The DDC-based capacity controller was re-activated 750 seconds later, as a result, the indoor RH level dropped to lower than 52%. Therefore, the PI controller for the supply fan speed was enabled, while the speed for compressor was kept unchanged afterwards. Table 8.4 lists the different compressor and supply fan speeds during the different intervals. The values of application SHR, indoor air temperature and RH at the end of each interval are listed in Table 8.5.

Table 8.4 Compressor and supply fan speeds during different intervals (Test 5)

Time (s)	0-600	600-1350	1350-2100	2100-2850	2850-8400
Compressor speed (rpm)	4488	4488	4557	4425	4425
% of maximum speed	60	60	61.3	58.8	58.8
Supply fan speed (rpm)	3312	3312	2298	1780	PI control
% of maximum speed	90	90	54.8	36.8	--
Supply airflow rate (m^3/h)	1700	1700	1185	900	--

Table 8.5 Application SHR, indoor air temperature and RH at the end of each interval (Test 5)

Time (s)	600	1350	2100	2850	8400
Application SHR	0.802	0.717	0.674	0.664	0.674
Indoor air temperature(℃)	24.02	22.88	22.89	23.16	23.51
Indoor RH (%)	50.10	56.89	54.29	51.44	49.98

Figs. 8.20 to 8.23 illustrate the results of Test 5. As shown in both Fig. 8.20 and Fig. 8.23, approximately 1800 seconds (30 minutes) after the first introduction of the DDC-based capacity controller, indoor air RH and temperature already arrived at 50.33 % and 23.32℃, respectively. Furthermore, these two parameters stabilized at 50±1 % and 24±0.5℃ at the end of the test period, respectively, when compared to the results in Test 2. Therefore, both indoor air temperature and RH could be maintained and the control sensitivity was significantly improved, as illustrated in both figures. The total output cooling capacity from the DX A/C unit (see Fig. 8.23) at steady-state was at 6.75 kW, which was close to that in Test 2. On the other hand, the final steady-state application SHR (see Fig. 8.22) was at 0.674, and the final equipment SHR was therefore also at 0.674. This was however slightly larger than

that (0.658) in Test 2, noting that this final equipment SHR was not derived using NCA, but based on classical PI feedback control for indoor RH.

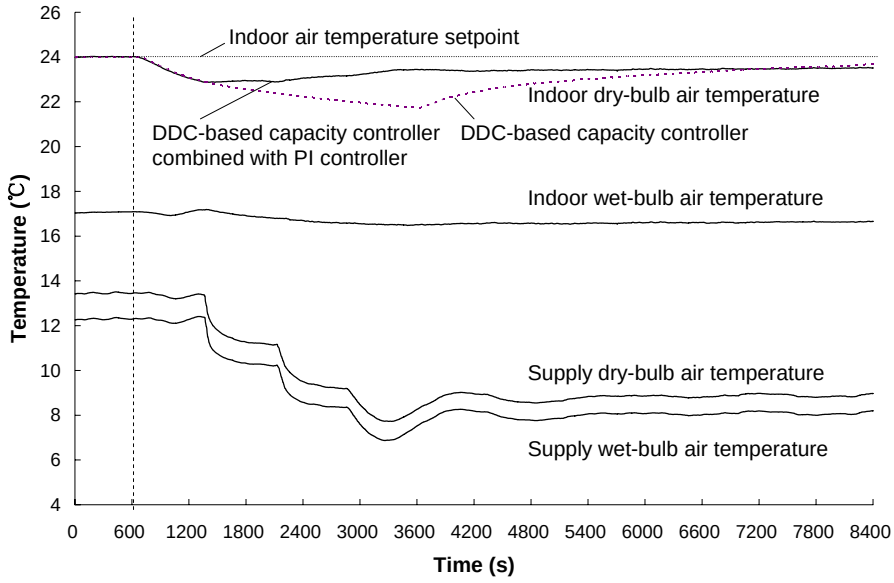

Fig. 8.20 Air temperature variation profiles (Test 5)

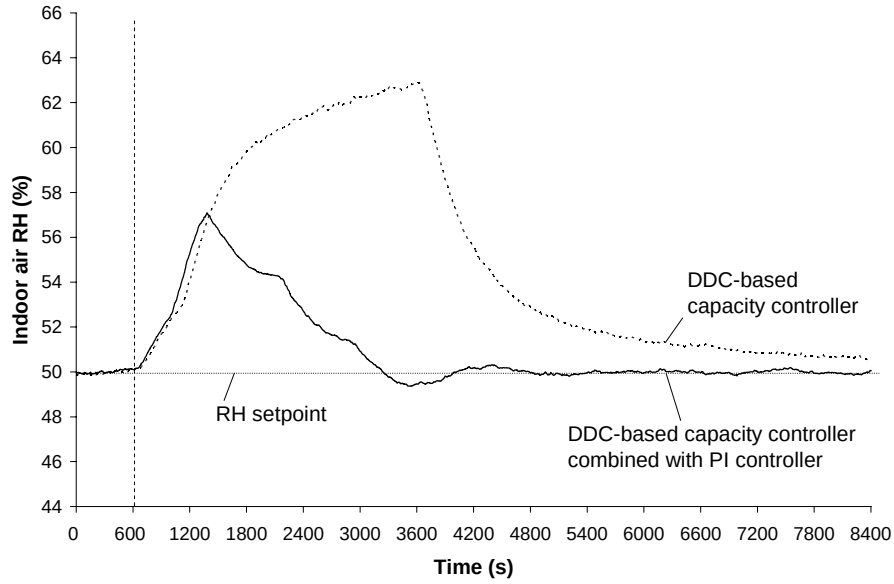

Fig. 8.21 Indoor air RH variation profiles (Test 5)

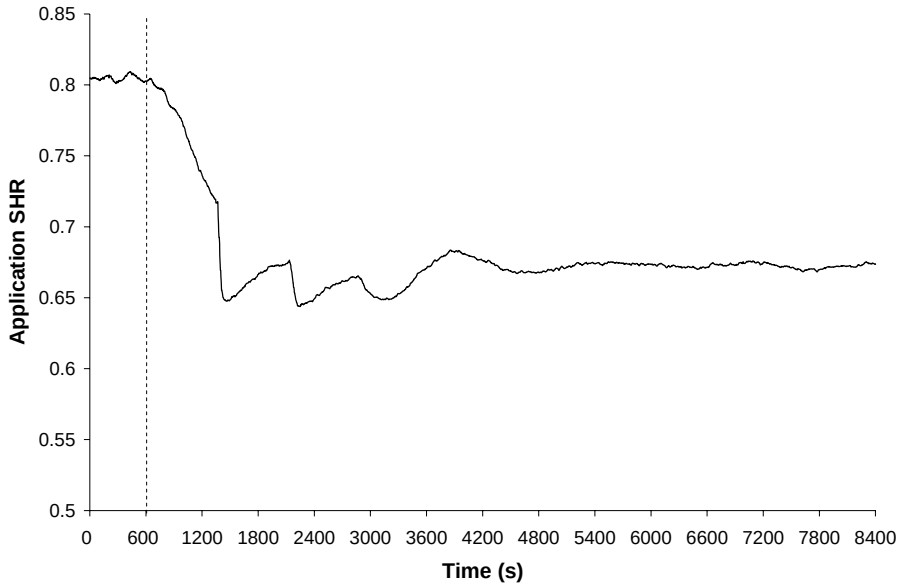

Fig. 8.22 Application SHR variation profile (Test 5)

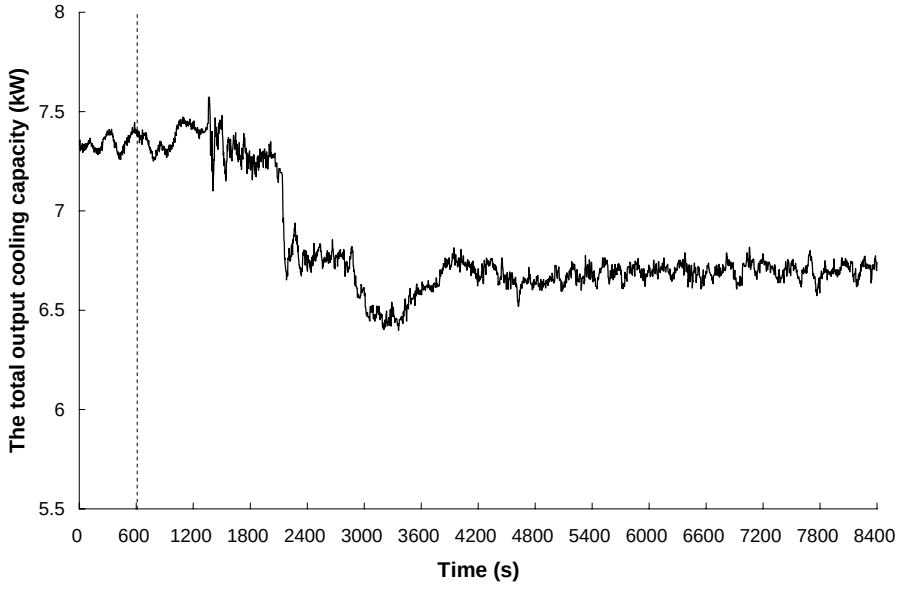

Fig. 8.23 The total output cooling capacity variation profile for the DX A/C unit (Test 5)

By integrating a traditional PI feedback controller for varying the supply fan speed, using the deviation of RH as control signal, into the DDC-based capacity controller developed, and properly switching to the use of the PI controller following pre-set

algorithms, the simultaneous control of both indoor air temperature and RH with acceptable control accuracy and sensitivity became realistic.

According to the test results shown in Figs. 8.20 to 8.23, it could be observed that the time interval of 750 seconds might be further reduced to enhance the control sensitivity. As seen in Fig. 8.22, for example, well before the DDC-based capacity controller was activated for the second time, application SHR values already stabilized. Therefore, the controller may have been enabled earlier for further improvement in control sensitivity. On the other hand, in the current attempt, only the PI controller for regulating the supply fan speed to control indoor air humidity was incorporated, resulting in a relatively poor control accuracy for air temperature, when compared to that for indoor RH. These two issues should be looked into in future investigations.

It should be pointed out that the time interval and accuracy range specified in all controllability tests were constrained by the space cooling loads and their step-changes specified at the beginning of Section 8.3. Given that there can be other cooling load situations; the numerical values of these parameters might correspondingly be different. Nonetheless, the underlying principle in developing the DDC-based capacity controller remained valid for all load situations.

8.5 Conclusions

In this Chapter, an experiment study on developing a novel DDC-based capacity controller for a DX A/C unit to simultaneously control indoor air temperature and

RH by varying the speeds of its compressor and supply fan is presented. Although the results of controllability tests were based on a specified indoor air state with specified space cooling loads and their step-changes, they were considered typical and representative.

The core element of the DDC-based capacity controller is a NCA, which uses both a number of real-time measured operating parameters and the energy balance between the air side and refrigerant side to determine both the compressor speed and supply fan speed. The results of controllability Test 1 and Test 2 for the capacity controller suggested that the controller developed was operational, with acceptable control accuracy but rooms for improvement with respect to control sensitivity.

Attempts to improve control sensitivity were made by incorporating a traditional PI controller using the deviation between the actual RH and its setpoint as a control signal into the DDC-based capacity controller. The PI controller was enabled when the indoor RH was within a pre-set range under the initial control only by the DDC-based capacity controller. The results of the controllability tests showed that such an integrated controller could achieve both control accuracy and reasonable control sensitivity.

Chapter 9

Conclusions and Future Work

9.1 Conclusions

In this thesis, a programmed research work on investigating the indoor environmental control using DX A/C units in residences in the subtropics has been successfully carried out and reported. The conclusions of the thesis are as follow:

1) The space cooling loads characteristics in the living/dining room at DOM and in the master bedroom at NOM in the summer design day in the subtropical Hong Kong have been studied using EnergyPlus. The residential space latent cooling load was basically due to ventilation and occupancy, and therefore stayed relatively steady at both DOM and NOM. However, at DOM, residential space sensible load was significantly affected by solar heat gains and indoor-outdoor air temperature difference; both varying significantly over the time. While at NOM, the space sensible cooling load was affected by both the heat stored in building envelope and accumulated over the non-air conditioning period, and the indoor-outdoor air temperature difference. Consequently, in the summer design day the resulted hourly application SHRs were also varied, at the range between 0.55 and 0.72 with a mean of 0.63 at DOM, and between 0.6 and 0.85 with a mean of 0.69 at NOM, respectively. On the other hand, the results of the simulation study quantitatively indicated that the consequences of the mismatch between the output latent cooling capacity from an on-off controlled DX A/C unit and the space latent cooling load in the summer design day and part load

operations: while an indoor dry-bulb air temperature setpoint may be maintained by on-off cycling compressor, there would be deviations in indoor RH level of varied magnitudes, depending on the magnitudes of mismatch. Finally, the simulation study included a quantitative assessment of the influences on indoor RH level due to the presence of indoor furnishings. Such influences were negligibly small at less than 2% and may therefore be neglected for practical calculation.

2) The measured inherent operational characteristics of the DX A/C unit suggested that varying both compressor speed and supply fan speed can lead to varying equipment SHR, or the unit's varying ability to dehumidify. Therefore such an operating strategy, i.e., by varying both compressor and supply fan speeds, might be preferably adopted for indoor environmental control in places subjected to variable latent cooling loads, such as the residential buildings located in hot and humid subtropical regions. Generally, lowering supply fan speed was more effective in enhancing the ability to dehumidify than increasing compressor speed. However, varying both speeds would also impact on the total output cooling capacity and the operating efficiency of a DX A/C unit. Consequently the application of changing equipment SHR for better humidity control was subject to the constraints of meeting the required total output cooling capacity from, and attaining a higher operating efficiency of a DX A/C unit.

3) The results of the experimental study on indoor thermal comfort characteristics suggested that under a given space total cooling load with a fixed application SHR, varying both compressor and supply fan speeds of a DX A/C unit would

not only result in different indoor temperatures and RH levels but also impact indoor air velocity and MRT, influencing consequently indoor thermal comfort. Experimental results showed that while appropriate indoor thermal comfort levels might be attained at different compressor speed and supply fan speed combinations, there were noticeable differences in the operating efficiency of the DX A/C unit. The results of the experimental study could possibly lead to the development of using indoor thermal comfort indexes, rather than indoor environmental parameters such as indoor air dry-bulb temperature, for control purpose, with the constraint of operating a DX A/C unit at its highest possible energy efficiency.

4) A novel DDC-based capacity controller for a DX A/C unit to simultaneously control indoor air temperature and RH by varying the speeds of its compressor and supply fan has been developed. The core element of the capacity controller was a NCA, which used both a number of real-time measured operating parameters in the DX A/C unit and the energy balance between the air side and the refrigerant side to determine both the compressor speed and supply fan speed. The results of controllability tests for the DDC-based capacity controller suggested that the controller developed was operational, with acceptable control accuracy but rooms for improvement with respect to control sensitivity. Attempts to improve control sensitivity were made by incorporating a traditional PI controller using the deviation between the actual indoor RH and its setpoint as a control signal into the DDC-based capacity controller. The PI controller was enabled when the indoor RH was within a pre-set range under the initial control only by the DDC-based capacity controller. The results of the controllability tests

showed that such an integrated controller could achieve both a control accuracy and a reasonable control sensitivity.

The project reported in this thesis has made important contributions to both DX A/C technology and its practical applications in residential buildings in hot and humid subtropics. Better indoor thermal comfort and improved IAQ for occupants, and reduced energy use for DX A/C units may be realized. The long-term significance of the project is that it will help people to better understand the important of indoor environmental control, leading to a reduction in the energy use for air conditioning, in both Hong Kong and other tropical and subtropical regions.

9.2 Proposed future work

A number of future studies following on the successful completion of the project reported in this thesis are proposed as follows:

1) The key purpose of this project is to find out an operational strategy for simultaneous indoor environmental parameters control; the costing analysis for the novel DDC-based controller developed is not considered at this stage. This might however be included as part of the future work.

2) The experimental investigation on the indoor thermal comfort characteristics under the control of a DX A/C unit having variable-speed compressor and supply fan is reported in Chapter 7. The results of the investigation could possibly lead

to the development of using indoor thermal comfort indexes, rather than indoor environmental parameters, for control purpose, with the constraint of operating a DX A/C unit at its highest possible energy efficiency. To this end, establishing a complete mathematic model of a DX A/C unit and the air conditioned space served by the DX A/C unit will be helpful, so that different indoor cooling conditions may be properly accounted for developing the control strategy.

3) Chapter 8 reported a novel DDC-based capacity controller for simultaneously controlling the indoor environmental parameters including air dry-bulb temperature and RH level. Future work in this specific aspect should be considered.

   According to the test results shown in Chapter 8, it could be observed that the time interval of 750 seconds might be further reduced to enhance the control sensitivity. As seen in Test 5, for example, well before the DDC-based capacity controller was activated for the second time, application SHR values already stabilized. Therefore, the controller may have been enabled earlier for further improvement in control sensitivity. On the other hand, in the current attempt, only the PI controller for regulating the supply fan speed to control indoor air humidity was incorporated, resulting in a relatively poor control accuracy for air dry-bulb temperature, when compared to that for indoor RH. Therefore, a PI controller for regulating the compressor speed to control indoor air temperature should also be considered.

4) In addition, in Chapter 8, the time interval and accuracy range specified in all controllability tests were based on the space cooling loads and their step-changes specified at the beginning of the Chapter. Given that there can be other cooling load situations, although the underlying principle in developing the DDC-based capacity controller remained valid for all load conditions, further similar investigations should be carried out at other load conditions.

References

1. Alpuche et al. 2005
Alpuche, M.G., Heard, C. Best, R. and Rojas, J.
Energy analysis of air cooling systems in buildings in hot humid climates. *Applied Thermal Engineering*, 2005, Vol. 25, No. 4, pp. 507-517 (2005)

2. Amrane et al. 2003
Amrane, K., Hourahan, G.C. and Potts, G.
Latent performance of unitary equipment. *ASHRAE Journal*, 2003, Vol. 45, No. 1, pp. 28-31 (2003)

3. Andersson and Lindholm 2001
Andersson, J.V. and Lindholm, T.
Desiccant cooling for Swedish office buildings. *ASHRAE Transactions*, 2001, Vol. 107, Part. 1, pp. 490-500 (2001)

4. Andrade et al. 2002
Andrade, M.A., Bullard, C.W., Hancock, S. and Lubliner, M.
Modulating blower and compressor capacities for efficient comfort control. *ASHRAE Transactions*, 2002, Vol. 108, Part. 1, pp. 631-637 (2002)

5. ANSI/ASHRAE 2001
ASHRAE
ANSI/ASHRAE Standard 62-2001, Ventilation for Acceptable Indoor Air Quality. (2001)

6. ANSI/ASHRAE 2004
ASHRAE
ANSI/ASHRAE Standard 55-2004, Thermal Environment Conditions for Human Occupancy. (2004)

7. Arens and Baughman 1996
Arens, E.A. and Baughman, A.V.
Indoor humidity and human health: part II-buildings and their systems. *ASHRAE Transactions*, 1996, Vol. 102, No. 1, pp. 212-221 (1996)

8. Armstrong and Liaw 2002
Armstrong, S. and Liaw, J.
The fundamentals of fungi. *ASHRAE Journal*, 2002, Vol. 44, No. 11, pp. 18-24 (2002)

9. ASHRAE 2000
ASHRAE
Handbook-HVAC Systems and Equipment (2000)

10. ASHRAE 2001
ASHRAE
Handbook of Fundamentals (2001)

11. Bailey et al. 1996
Bailey, D.W., Bauer, F.C., Slama, C.F., Barringer, C.G. and Flack, J.R.
Investigation of dynamic latent heat storage effects of building construction and furnishings. *ASHRAE Transactions*, 1996, Vol. 102, No. 2, pp. 133-141 (1996)

12. Barringer and McGugan 1989
Barringer, C.G. and McGugan, C.A.
Development of a dynamic model for simulating indoor air temperature and humidity. *ASHRAE Transactions*, 1989, Vol. 95, Part. 2, pp. 449-460 (1989)

13. Barringer and McGugan 1994
Barringer, C.G. and McGugan, C.A.
Effect of residential air to air heat and moisture exchangers on indoor humidity. *ASHRAE Transactions*, 1994, Vol. 100, No. 2, pp. 953-969 (1994)

14. Bedford and Warmer 1935
Bedford, T. and Warmer, C.G.
The globe thermometer in studies of heating and ventilating. J*ournal of the Institution of Heating and Ventilating Engineers* 2:544 (1935)

15. Berbari 1998
Berbari, G. J.
Fresh air treatment in hot and humid climates. *ASHRAE Journal*, 1998, Vol. 40, No. 10, pp. 64-70 (1998)

16. Berglund 1998
Berglund, L.G.
Comfort and humidity. *ASHRAE Journal*, 1998, Vol. 40, No. 8, pp. 35-41 (1998)

17. Bojic et al. 2001
Bojic, M., Yik, F. and Sat P.
Influence of thermal insulation position in building envelope on the space cooling of high-rise residential buildings in Hong Kong. *Energy and Buildings*, 2001, Vol. 33, pp. 569-581 (2001)

18. Bojic et al. 2002
Bojic, M., Yik, F., Wan, K. and Burnett, J.
Influence of envelope and partition characteristics on the space cooling of high-rise residential buildings in Hong Kong. *Building and Environment*, 2002, Vol. 37, pp. 347-355 (2002)

19. Bordick and Gilbride 2002
Bordick J. and Gilbride T.L.
Focusing on buyer's needs: DOE's engineering technology programme. *Energy Engineering*, Vol. 99, No. 6, pp. 18-38 (2002)

20. Brandemuehl and Katejanekarn 2004
Brandemuehl, M.J. and Katejanekarn, T.
Dehumidification characteristics of commercial building applications. *ASHRAE Transactions*, 2004, Vol. 114, Part. 2, pp. 65-76 (2004)

21. Capehart 2003
Capehart, B.
Air conditioning solutions for hot, humid climates. *Energy Engineering: Journal of the Association of Energy Engineering*, 2003, Vol. 100, No. 3, pp. 5-8 (2003)

22. Chen 2005
Chen, W.
Modeling and Control of a Direct Expansion (DX) Variable-air-volume (VAV) Air Conditioning (A/C) system. PhD thesis, Department of Building Services Engineering, Hong Kong Polytechnic University, 2005 (2005)

23. Chen and Chen 1998
Chen, Y.M. and Chen, Z.K.
Transfer function method to calculate moisture absorption and desorption in buildings. *Building and Environment*, 1998, Vol. 33, No. 4, pp. 201-207 (1998)

24 Chu et al. 2005
Chu, C.M., Jong, T.L. and Huang, Y.W.
Thermal comfort control on multi-room fan coil unit system using LEE-based fuzzy logic. *Energy Conversion and Management*, 2005, Vol. 46, Issues 9-10, pp. 1579-1593 (2005)

25. Chuah et al. 1998
Chuah, Y.K., Hung, C.C. and Tseng, P.C.
Experiments on the dehumidification performance of a finned tube heat exchanger. *HVAC&R Research*, 1998, Vol. 4, No. 2, pp. 167-178 (1998)

26. Cleland 1986
Cleland, A.C.
Computer sub-routines for rapid evaluation of refrigerant thermodynamic properties. *International Journal of Refrigeration*, No. 9, pp. 346-351 (1986)

27. Coad 2000
Coad, W.J.
Energy conservation is an ethic. *ASHRAE Journal*, 2000, Vol. 42, No. 7, pp. 16-21 (2000)

28. Cummings and Kamel 1988
Cummings, J.B. and Kamel, A.A.
Whole-building moisture experiments and data analysis. *FSEC-CR-199-88. Cape Canaveral: Florida Solar Energy Center*. (1988)

29. Dai et al. 2001
Dai, Y.J., Wang, R.Z., Zhang, H.F. and Yu, J.D.
Use of liquid desiccant cooling to improve the performance of vapor compression air conditioning. *Applied Thermal Engineering*, 2001, Vol. 21, No. 12, pp. 1185-1202 (2001)

30. de Dear et al. 1989
de Dear, R.J., Knudsen, H.N. and Fanger, P.O.
Impact of air humidity on thermal comfort during step-changes. *ASHRAE Transactions*, 1989, Vol. 95, No. 2, pp. 336-350 (1989)

31. Diasty et al. 1992
Diasty, R.E., Fazio, P. and Budaiwi, I.
Modelling of indoor air humidity: the dynamic behavior within an enclosure. *Energy and Buildings*, 1992, Vol. 19, pp. 61-73 (1992)

32. Dieckmann et al. 2004
Dieckmann, J., Roth, K.W. and Brodrick, J.
Liquid desiccant air conditioners. *ASHRAE Journal*, 2004, Vol. 46, No. 4, pp. 58-59 (2004)

33. Dinh 1986
Dinh, K.
High efficiency air-conditioner/dehumidifier. *U.S. Patent #4,607,498* (1986)

34. Doty 2001
Doty, S.
Applying DX equipment in humid climates. *ASHRAE Journal*, 2001, Vol. 43, No. 3, pp. 30-32 (2001)

35. Edward 1989
Edward, G.P.
Air conditioning principles and systems: An energy approach. Second edition. (1989)

36. El Diasty et al. 1993
El Diasty, R., Fazio, P. and Budaiwi, I.
Dynamic modeling of moisture absorption and desorption in buildings. *Building and Environment*, 1992, Vol. 28, No. 1, pp. 21-32 (1993)

37. Elsarrag et al. 2005
Elsarrag, E., Ali, E.E.M. and Jain, S.
Design guidelines and performance study on a structured packed liquid desiccant air-conditioning system. *HVAC and R Research*, 2005, Vol. 11, No. 2, pp. 319-337 (2005)

38. EnergyPlus Archive 2004

39. Fairey and Kerestecioglu 1985
Fairey, P.W. and Kerestecioglu, A.A.
Dynamic modeling of combined thermal and moisture transport in buildings: effects on cooling loads and space conditions. *ASHRAE Transactions*, 1985, Vol. 91, Part. 2A, pp. 461-473 (1985)

40. Fairey et al. 1986
Fairey, P., Keretecioglu, A., Vieirfa, R., Swami, M. and Chandra, S.
Latent and sensible load distributions in conventional and energy-efficient residences, final report. *Prepared by the Florida Solar Energy Center for the Gas Research Institute, FSEC Report FSEC-CR-153-86, GRI Report GRI-86/0056*, pp. 4.8-4.12 (1986)

41. Fanger 1970
Fanger, P.O.
Thermal Comfort. *Danish Technical Press*. Copenhagen 1970

42. Fanger 1982
Fanger, P.O.
Thermal comfort. *Robert E. Krieger Publishing Company*, Malabar, FL. 1982.

43. Fanger 2001
Fanger, P.O.
Human requirements in future air-conditioned environments. *International Journal of Refrigeration*, 2001, Vol. 24, pp. 148-153 (2001)

44. Fischer et al. 2002
Fischer J.C., Sand J.R., Elkin, B. and Mescher, K.
Active desiccant, total energy recovery hybrid system optimizes humidity control, IAQ, and energy efficiency in an existing dormitory facility. *ASHRAE Transactions*, 2002, Vol. 108, No. Part. 2, pp. 537-545 (2002)

45. Fountain et al. 1999
Fountain, M.E., Arens, E., Xu, T.F., Bauman, F.S. and Oguru M.
An investigation of thermal comfort at high humidities. *ASHRAE Transactions*, 1999, Vol. 105, Part. 2, pp. 94-103 (1999)

46. Gatley 1992
Gatley, D.P.
Designing for comfortable cooling season humidity in hotels. *ASHRAE Transactions*, 1992, Vol. 98, No. Part. 1, pp. 1293-1302 (1992)

47. Gawin et al. 2004
Gawin, D.J., Koniorczyk, M., Wieckowska, A. and Kossecka, E.
Effect of moisture on hygrothermal and energy performance of a building with cellular concrete walls in climatic conditions of Poland. *ASHRAE Transactions*, 2004, Vol. 110, Part. 2, pp. 795-803 (2004)

48. Green 1982
Green, G.H.
The positive and negative effects of building humidification. *ASHRAE Transactions*, 1982, Vol. 88, No. Part. 1, pp. 1049-1061 (1982)

49. Harriman Ⅲ et al. 1999
Harriman Ⅲ, L.G., Czachorski, M., Witte, M.J. and Kosar, D.R.
Evaluating active desiccant systems for ventilating commercial buildings. *ASHRAE Journal*, 1999, Vol. 40, No. 10, pp. 28-37 (1999)

50. Harriman Ⅲ et al. 2000
Harriman Ⅲ, L.G., Lstiburek, J. and Kittler, R.
Improving humidity control for commercial buildings. *ASHRAE Journal*, 2000, Vol. 42, No. 11, pp. 24-32 (2000)

51. Harriman Ⅲ et al. 2001
Harriman Ⅲ, L.G., Brundrett, G.W. and Kittler, R.
Humidity control design guide for commercial and institutional buildings. *ASHRAE engineers, Inc*. (2001)

52. Harriman Ⅲ and Judge 2002
Harriman Ⅲ, L. G. and Judge, J.

Dehumidification equipment advances. *ASHRAE Journal*, 2002, Vol. 44, No. 8, pp. 22-29 (2002)

53. Henderson 1992
Henderson, H.I.
Simulating combined thermostat, air conditioner, and building performance in a house. *ASHRAE Transactions*, 1992, Vol. 98, No. Part. 1, pp. 370-380 (1992)

54. Henderson et al. 1992
Henderson, H.I.Jr., Rengarjan, K. and Shirey, D.B.
The impact of comfort control on air conditioner energy use in humid climates. *ASHRAE Transactions*, 1992, Vol. 98, No. Part. 2, pp. 104-112 (1992)

55. Henderson and Rengarajan 1996
Henderson, H.I.Jr. and Rengarajan, K.
A model to predict the latent capacity of air conditioners and heat pumps at part-load conditions with constant fan operation. *ASHRAE Transactions*, 1996, Vol. 102, No. 1, pp. 266-274 (1996)

56. Henderson 1998
Henderson, H.I. Jr.
The impact of part-load air conditioner operation on dehumidification performance: Validating a latent capacity degradation model. *Proceeding of the 1998 ASHRAE Indoor Air Quality Conference*. (1998)

57. Hickey 2001
Hickey, D.
Focus on humidity control. *ASHRAE Journal*, 2001, Vol. 43, No. 10, pp. 10-11 (2001)

58. Hill and Jeter 1994
Hill, J.M. and Jeter, S.M.
Use of heat pipe exchangers for enhanced dehumidification. *ASHRAE Transactions*, 1994, Vol. 100, No. 1, pp. 91-102 (1994)

59. HK-BEAM 2003
HK-BEAM
An Environment Assessment for New Building Developments. 2003

60. Ho and Wijeysundera 1999
Ho, J.C. and Wijeysundera, N.E.
An unmixed-air flow model of a spiral coil cooling dehumidifying unit.

Applied Thermal Engineering, 1999, Vol. 19, No. 8, pp. 865-883 (1999)

61. Holm et al. 2004
Holm, A.H., Kunzel, H.M. and Sedlbauer, K.
Predicting indoor temperature and humidity conditions including hygrothermal interactions with the building envelope. *ASHRAE Transactions*, 2004, Vol. 110, Part. 2, pp. 820-826 (2004)

62. Hourahan 2004
Hourahan, G.C.
How to properly size unitary equipment. *ASHRAE Journal*, 2004, Vol. 46, No. 2, pp. 15-18 (2004)

63. Isetti et al. 1988
Isetti, C., Laurenti, L. and Donticiello, A.
Prediciting vapour content of the indoor air and latent loads for air-conditioned environments: effect of moisture storage capacity of the walls. *Energy and Buildings*, 1988, Vol. 12, No. 2, pp. 141-148 (1988)

64. ISO 1994
International Standard Organization
Moderate thermal environments-Determination of the PMV and PPD indices and specification of the conditions for thermal comfort. *ISO 7730*, Second edition, 1994-12-15 (1994)

65. Jalalzadeh-Azar et al. 1998
Jalalzadeh-Azar, A.A., Hodge, B.K. and Steele, W.G.
Thermodynamic assessment of desiccant systems with targeted and relaxed humidity control schemes. *ASHRAE Transactions*, 1998, Vol. 104, No. 2, pp. 313-319 (1998)

66. Karagiozis and Salonvaara 2001
Karagiozis, A. and Salonvaara, M.
Hygrothermal system-performance of a whole building. *Building and Environment*, 2001, Vol. 36, No. 5, pp. 779-787 (2001)

67. Katipamula et al. 1988
Katipamula, S., O'Neal, D.L. and Somasundaram, S.
Simulation of dehumidification characteristics of residential central air conditioners. *ASHRAE Transactions*, 1988, Vol. 88, No. 2, pp. 829-849 (1988)

68. Katipamula and O'Neal 1991
Katipamula, S. and O'Neal, D.L.
Transient dehumidification characteristics of a heat pump in cooling mode. *American Society of Mechanical Engineers, Advanced Energy Systems Division (Publication) AES*, Vol. 26, Heat Pump Design, Analysis and Application, 1991, pp. 1-9 (1991)

69. Kerestecioglue et al. 1990
Kerestecioglue, A., Swami, M. and Kamel, A.
Theoretical and computational investigation of simultaneous heat and moisture transfer in buildings: effective penetration depth theory. *ASHRAE Transactions*, 1990, Vol. 96, Part. 1, pp. 447-454 (1990)

70. Khattar 1985
Khattar, M.K.
Analysis of air reheat systems and application for heat pipes for increased dehumidification. *FSEC-PF-76-85. Cape Canaveral: Florida Solar Energy Center*. (1985)

71. Khattar et al. 1985
Khattar, M.K., Ramanan, N. and Swami, M.
Fan cycling effects on air conditioner moister removal performance in warm, humid climates. *ISA*, 1985, Vol. 24, pp. 837-842 (1985)

72. Khattar et al. 1987
Khattar, M.K., Swami, M.V. and Ramanan, N.
Another aspect of duty cycling: effects on indoor humidity. *ASHRAE Transactions*, 1987, Vol. 93, No. Pt. 1, pp. 1678-1687 (1987)

73. Khattar and Henderson 1999
Khattar, M.and Henderson, H.I.Jr.
Impact of HVAC control improvements on supermarket humidity levels. *ASHRAE Transactions*, 1999, Vol. 105, No. Part. 1, pp. 521-532 (1999)

74. Kittler 1996
Kittler, R.
Mechanical Dehumidification Control Strategies and Psychromatrics. *ASHRAE Transactions*, 1996, Vol. 102, No. 2, pp. 613-617 (1996)

75. Kohloss 1981
Kohloss, F.H.
Opportunities to save energy in tropical climates. *ASHRAE Transactions*, 1981, Vol. 87, No. 1, pp. 1415-1425 (1981)

76. Kosar et al.1998
Kosar, D.R., Witte, M.J., Shirey, D.B.III and Hedrick, R.L.
Dehumidification issues of standard 62-1989. *ASHRAE Journal*, 1998, Vol. 40, No. 3, pp. 71-75 (1998)

77. Krakow et al. 1995
Krakow, K. I., Lin S. and Zeng, Z.S.
Temperature and humidity control during cooling and dehumidifying by compressor and evaporator fan speed variation. *ASHRAE Transactions*, 1995, Vol. 101, No. 1, pp. 292-304 (1995)

78. Kurt et al. 2004
Kurt, R., Westphalen, D., Dieckmann, J. and Brodrick, J.
Modulating compressors for residential cooling. *ASHRAE Journal*, 2004, Vol. 46, No. 10, pp. 56-57 (2004)

79. Kurtz 2003
Kurtz, B.
Being size wise. *ASHRAE Journal*, 2003, Vol. 45, No. 1, pp. 17-21 (2003)

80. Kusuda 1983
Kusuda, T.
Indoor humidity calculation. *ASHRAE Transactions*, 1983, Vol. 89, Part. 2, pp. 728-738 (1983)

81. Kusuda and Miki 1985
Kusuda, T. and Miki, M.
Measurement of moisture content for building interior surfaces. *In moisture and humidity, measurement and control in Science and Industry, Proceedings of the 1985 international symposium on moisture and humidity, Washington, DC*, pp. 297-311 (1985)

82. Kuwahara 1985
Kuwahara, E.
A humidity detection method for use with a room air conditioner. *ASHRAE Transactions*, 1985, Vol. 91, Part. 2A, pp. 282-291 (1985)

83. Lam 1993
Lam, J. C.
A survey of electricity consumption and user behavior in some government staff quarters. *Building Research and Information*, 1993, Vol. 21, No. 2, pp. 109-116 (1993)

84. Lam and Hui 1995
Lam, J.C. and Hui, S.C.M.
Outdoor design conditions for HVAC system design and energy estimation for buildings in Hong Kong. *Energy and Buildings*, 1995, Vol. 22, No. 1, pp. 25-43 (1995)

85. Lam 1996
Lam, J.C.
An analysis of residential sector energy use in Hong Kong. *Energy*, 1996, Vol. 21, No. 1, pp. 1-8 (1996)

86. Lam 2000
Lam, J.C.
Residential sector air conditioning loads and electricity use in Hong Kong. *Energy Conversion & Management*, 2000, Vol. 41, pp. 1757-1768 (2000)

87. Lin 2001
Lin, J.S.
Heat transfer and internal flow characteristics of a coil-inserted rotating heat pipe. *Int. J. Heat Mass Transfer*, 2001, Vol. 44, pp. 3543–3551 (2001)

88. Lin and Deng 2004
Lin, Z.P. and Deng, S.M.
A study on the characteristics of nighttime bedroom cooling load in tropics and sub-tropics. *Building and Environment*, 2004, Vol. 39, No. 8, pp. 1101-1114 (2004)

89. Lstiburek 2001
Lstiburek, J.
Moisture, building enclosures, and mold. *HPAC Heating, Piping, AirConditioning Engineering*, 2001, Vol. 73, No. 12, pp. 22-26 (2001)

90. Lstiburek 2002
Lstiburek, J.
Residential ventilation and latent loads. *ASHRAE Journal*, 2002, Vol. 44, No. 4, pp. 18-22 (2002)

91. Lstiburek 2004
Lstiburek, J.W.
Understanding vapor barriers. *ASHRAE Journal*, 2004, Vol. 46, No. 8, pp. 40-47 (2004)

92. Lstiburek 2005
Lstiburek, J.W.

Understanding air barriers. *ASHRAE Journal*, 2005, Vol. 47, No. 7, pp. 24-30 (2005)

93. Lu 2003
Lu, X.S.
Estimation of indoor moisture generation rate from measurement in buildings. *Building and Environment*, 2003, Vol. 38, No. 5, pp. 665-675 (2003)

94. Lucas et al. 2002
Lucas, F., Adelard, L., Grade, F. and Boyer, H.
Study of moisture in buildings for hot humid climates. *Energy and Buildings*, 2002, Vol. 34, No. 4, pp. 345-355 (2002)

95. Lucas and Miranville 2004
Lucas, F. and Miranville, F.
Indoor humidity modeling and evaluation of condensation on interior surfaces. *ASHRAE Transactions*, 2004, Vol. 110, Part. 2, pp. 300-308 (2004)

96. MacArthur and Grald 1988
MacArthur, J.W. and Grald, E.W.
Optimal comfort control for variable-speed heat pumps. A*SHRAE Transactions*, 1988, Vol. 94, Pt. 2, pp. 1283-1297 (1988)

97. Marsala et al. 1989
Marsala, J., Lowenstein, A. and Ryan, W.
Liquid desiccant for residential applications. *ASHRAE Transactions*, 1989, Vol. 95, No. Part.1, pp. 828-834 (1989)

98. Martin and Oughton 1995
Martin, P.L. and Oughton, D.R.
Faber and Kell's heating and air conditioning of buildings. 1995

99. Mazzei et al. 2005
Mazzei, P., Minichiello, F. and Palma, D.
HVAC dehumidification systems for thermal comfort: a critical review. *Applied Thermal Engineering*, 2005, Vol. 25, No. 5-6, pp. 677-707 (2005)

100. McFarland et al. 1996
McFarland, J.K., Jeter, S.M. and Abdel-Khalik, S.I.
Effect of a heat pipe on dehumidification of a controlled air space. *ASHRAE Transactions*, 1996, Vol. 102, No. 1, pp. 132-139 (1996)

101. McGahey 1998
McGahey, K.
New commercial applications for desiccant-based cooling. *ASHRAE Journal*, 1998, Vol. 40, No. 7, pp. 41-45 (1998)

102. Miller 1984
Miller, J. D.
Development and validation of a moisture mass balance model for predicting residential cooling energy consumption. *ASHRAE Transactions*, 1984, Vol. 90, Part. 2B, pp. 275-293 (1984)

103. Miro 2005
Miro, C.
ASHRAE issues guidance on minimizing mold, mildew. *ASHRAE Journal*, 2005, Vol. 47, No. 3, pp. 86 (2005)

104. Murphy 2002
Murphy, J.
Dehumidification performance of HVAC systems. *ASHRAE Journal*, 2002, Vol. 44, No. 3, pp. 23-31 (2002)

105. Olesen and Brager 2004
Olesen, B.W. and Brager, G.S.
A better way to predict comfort. *ASHRAE Journal*, 2004, Vol. 46, No. 8, pp. 20-28 (2004)

106. Pasch et al. 1996
Pasch, R.M., Comins, M. and Hobbins, J.S.
Field experiences in residential humidification control with temperature-compensated automatic humidistats. *ASHRAE Transactions*, 1996, Vol. 102, No. 2, pp. 628-632 (1996)

107. Rode and Grau 2003
Rode, C. and Grau, K.
Whole-building hygrothermal simulation model. *ASHRAE Transactions*, 2003, Vol. 109, Part. 1, pp. 572-582 (2003)

108. Rode et al. 2004
Rode, C., Mendes, N. and Grau, K.
Evaluation of moisture buffer effects by performing whole-building simulations. *ASHRAE Transactions*, 2004, Vol. 110, No. 2, pp. 783-794 (2004)

109. Rowland et al. 2005
Rowland, C.A., Wendel, Jr. and Martin, J.
Dehumidification technologies. *HPAC Heating, Piping, AirConditioning Engineering*, 2005, Vol. 77, No. 3, pp. 48 (2005)

110. Sand and Fischer 2005
Sand, J.R. and Fischer, J.C.
Active desiccant integration with packaged rooftop HVAC equipment. *Applied Thermal Engineering*, 2005, Vol. 25, No. 17-18, pp. 3138-3148 (2005)

111. Scalabrin and Scaltriti 1985
Scalabrin, G. and Scaltriti, G.
A new energy saving process for air dehumidification: analysis and applications. *ASHRAE Transactions*, 1985, Vol. 91, No. Pt. 1A, pp. 426-441 (1985)

112. Shakun 1992
Shakun, W.
The causes and control of mold and mildew in hot and humid climates. *ASHRAE Transactions*, 1992, Vol. 98, No. 1, pp. 1282-1292 (1992)

113. Shariah et al. 1997
Shariah, A., Tashtoush, B. and Rousan, A.
Cooling and heating loads in residential buildings in Jordan. *Energy and Buildings*, 1997; Vol. 26, pp. 137-143 (1997)

114. Shaw and Luxton 1988
Shaw, A. and Luxton, R.E.
A comprehensive method of improving part-load air-conditioning performance. *ASHRAE Transactions*, 1988, Vol. 94, Part. 1, pp. 442-457 (1988)

115. Sherman 1999
Sherman, M.
Indoor air quality for residential buildings. *ASHRAE Journal*, 1999, Vol. 41, No. 5, pp. 26-30 (1999)

116. Shirey 1993
Shirey, D.B.III
Demonstration of efficient humidity control techniques at an art museum. *ASHRAE Transactions*, 1993, Vol. 99, No. Pt. 1, pp. 694-703 (1993)

117. Shirey and Henderson 2004
Shirey, D.B.III and Henderson, H.I.Jr.
Dehumidification at part load. *ASHRAE Journal*, 2004, Vol. 46, No. 3, pp. 42-47 (2004)

118. Soylemez 2003
Soylemez, M.S.
On the thermoeconomical optimization of heat pipe heat exchanger HPHE for waste heat recovery. *Energy Conversion and Management*, 2003, Vol. 44, No. 15, pp. 2509-2517 (2003)

119. Sterling et al. 1985
Sterling, E.M., Arundel, A. and Sterling, T.D.
Criteria for human exposure to humidity in occupied buildings. *ASHRAE Transactions*, 1985, Vol. 91, No. Part. 1B, pp. 611-622 (1985)

120. Straube 2002
Straube, J.F.
Moisture in buildings. *ASHRAE Journal*, 2002, Vol. 44, No. 1, pp. 15-19 (2002)

121. Subramanyam et al. 2004
Subramanyam, N., Maiya, M.P. and Murthy, S.S.
Application of desiccant wheel to control humidity in air-conditioning systems. *Applied Thermal Engineering*, 2004, Vol. 24, No. 17-18, pp. 2777-2788 (2004)

122. Sullivan et al. 1994
Sullivan, R., Frost, K.J., Arasteh, D.K., and Selkowitz, S.
Window U-factor effects on residential cooling load. *ASHRAE Transactions*, 1994, Vol. 100, Part. 2, pp. 50-57 (1994)

123. Tanabe et al. 1987
Tanabe, S., Kimura, K. and Hara, T.
Thermal comfort requirements during the summer season in Japan. *ASHRAE Transactions*, 1987, Vol. 93, No. Pt. 1, pp. 564-577 (1987)

124. Tanabe and Kimura 1994
Tanabe, S. and Kimura, K.
Effects of air temperature, humidity, and air movement on thermal comfort in hot and humid conditions. *ASHRAE Transactions*, 1994, Vol. 100, No. 2, pp. 953-969 (1994)

125. Taras 2004
. Taras, M.F.
Reheat: which concept is best. *ASHRAE Journal*, 2004, Vol. 46, No. 12, pp. 34-40 (2004)

126. TenWolde 1994
TenWolde, A.
Ventilation, humidity, and condensation in manufactured houses during winter. *ASHRAE Transactions*, 1994, Vol. 100, No. 1, pp. 103-115 (1994)

127. Thomas and Burch 1990
Thomas, W.C. and Burch, D.M
Experimental validation of a mathematical model for predicting water vapor sorption at interior building surface. *ASHRAE Transactions*, 1990, Vol. 96, Part. 1, pp. 487-496 (1990)

128. Toftum and Fanger 1999
Toftum, J. and Fanger, P.O.
Air humidity requirements for human comfort. *ASHRAE Transactions*, 1999, Vol. 105, Part. 2, pp. 641-647 (1999)

129. Trowbridge et al. 1994
Trowbridge, J.T., Ball, K.S., Peterson, J.L., Hunn, B.D. and Grasso, M.M.
Evaluation of strategies for controlling humidity in residences in humid climates. *ASHRAE Transactions*, 1994, Vol. 100, No. 2, pp. 59-73 (1994)

130. Vernon 1932
Vernon, H.M.
The globe thermometer. *Proceedings of the Institution of Heating and Ventilating Engineers*, 39:100 (1932)

131. Website_1 2004
http://www.eere.energy.gov/buildings/energyplus/

132. Website_2 2004
http://www.eere.energy.gov/buildings/energyplus/press_release.html

133. Westphalen 2004
Westphalen, D.
Energy savings for rooftop AC. *ASHRAE Journal*, 2004, Vol. 46, No. 3, pp. 38-46 (2004)

134. Westphalen et al. 2004
Westphalen, D., Roth, K.W., Dieckmann, J. and Brodrick, J.

Improving latent performance. *ASHRAE Journal*, 2004, Vol. 46, No. 8, pp. 73-75 (2004)

135. Wong and Wang 1990
Wong, S.P.W. and Wang, S.K.
Fundamentals of simultaneous heat and moisture transfer between the building envelope and the conditioned space air. *ASHRAE Transactions*, 1990, No. Part 2, pp. 73-83 (1990)

136. Xiao et al. 1997
Xiao, P.W., Johnson, P. and Akbarzadeh, A.
Application of heat pipe heat exchangers to humidity control in air-conditioning systems. *Applied Thermal Engineering*, 1997, Vol. 17, No. 6, pp. 561-568 (1997)

137. Yang and Lee 1991
Yang, K.H. and Lee, M.L.
Analysis of an inverter-driven air-conditioning system and its application in a hot and humid area. *International journal of energy research*, Vol. 15, pp. 357-365 (1991)

138. Yang and Su 1997
Yang, K.H. and Su, C.H
An approach to building energy savings using the PMV index. *Building and Environment*, 1997, Vol. 32, No. 1, pp. 25-30 (1997)

139. Yau 2001
Yau, Y.H.
Theoretical determination of effectiveness for heat pipe heat exchangers operating in naturally ventilated tropical buildings. *Proceedings of the Institution of Mechanical Engineers, Part A: Journal of Power and Energy*, 2001, Vol. 215, No. 3, pp. 389-398 (2001)

140. Zhang 2002
Zhang, G.Q.
China HVACR Annual Business Volume Ⅱ. *Chinese Construction Industry Press*, pp. 44-45.

Appendix

Publications Arising from the Thesis

I. Journal papers

- **Zheng Li**, Wu Chen, Shiming Deng and Zhongping Lin. The characteristics of space cooling load and indoor humidity control for residences in the subtropics. *Building and Environment*, in press (based on Chapter 4)
- **Zheng Li** and Shiming Deng. An experimental study on the inherent operational characteristics of a direct expansion (DX) air conditioning (A/C) unit. *Building and Environment*, in press (based on Chapter 6)

II. Manuscripts

- **Zheng Li** and Shiming Deng. An experimental study on the indoor thermal comfort characteristics under the control of a direct expansion (DX) air conditioning (A/C) unit. To be submitted to *Indoor Air* (based on Chapter 7)
- **Zheng Li** and Shiming Deng. A novel DDC-based capacity controller of a DX A/C unit for simultaneously indoor air temperature and humidity control. To be submitted to *International Journal of Refrigeration* (based on Chapter 8)

III. Conference papers

- **Zheng Li**, Wu Chen and Shiming Deng. Indoor humidity control with DX A/C systems in subtropical residences. *Ventilation in relation to the Energy Performance of Buildings, AIVC Conference 2005*, Brussels, Belgium, September 21-23, 2005
- Wu Chen, **Zheng Li** and Shiming Deng. Capacity control of a DX VAV

system and its modeling. *International Refrigeration and Air Conditioning Conference*, Purdue, USA, July 12-15, 2004